

Agent Based Model of  
Hyaluronic Acid-Gelatin Tissue Scaffold  
for Vocal Fold Regeneration

Caroline Shung

Master of Engineering in Biomedical Engineering

Biomedical Engineering Department

McGill University

Montreal, Quebec

December 2017

A thesis submitted to McGill University in partial fulfillment of the requirements of  
the degree of Master of Engineering in Biomedical Engineering

©Caroline Shung 2017

## ACKNOWLEDGEMENTS

I would like to thank many people for their invaluable advice and support throughout the duration of my graduate studies. Firstly, I would like to thank my supervisors, Dr. Luc Mongeau and Dr. Nicole Li-Jessen. Their patience, unwavering support and expert guidance were of immense value and comfort without which this work would undoubtedly not have been possible.

I would like to thank Dr. Joseph Jaja and Nuttiiya Seekhao for their collaboration and astute insight in model parallelization. Nuttiiya's technical knowledge as well as systematic and rigorous work was critical in advancing the project.

Thank you to Dr. Alireza Najafi Yazdi and Yvonna Li for their work in designing and developing the initial software architecture that was the cornerstone for this project. Many thanks to Kim Trickey for her extensive work establishing analysis methodologies and standardizing our model. Thank you to Samson Yuen and Harry Tao for their hard work and dedication sorting large data sets to perform sensitivity analysis and model calibration. Also, thank you to Neda Latifi and Dr. Hossein Khadivi Heris for their expertise and generously supplying cell culture and hydrogel preparation protocols integral to my research. Finally, I want to thank Annie Douillette for her assistance in cell cultures as well as testing and optimizing biochemical assays.

## ABSTRACT

Phonatory-related mechanical trauma to the vocal folds can initiate benign changes to tissue components irrevocably altering the fold vibratory function. Crosslinked hyaluronan-gelatin (HA-Gtn) scaffolds have been engineered to regenerate defected vocal folds and restore afflicted individuals communication ability. Of the many properties considered when designing engineered biomaterials, identifying parameters that yield a scaffold which mimics the natural extracellular matrix (ECM) requires the optimization of a prohibitively large number of factors. Computer simulation methods, including agent based modeling (ABM), are being used increasingly for controlled systematic studies in scaffold design to reduce empirical testing combinations, decreasing time and cost. The objectives of this study were to: model inflammatory and healing response to phonotory injury using ABMs, expand the model to simulate cellular interactions in bioactive hydrogels, perform global sensitivity analysis for parameter estimation as well as calibration and validation. The model demonstrated highly nonlinear behavior with strong therapy-dependent sensitivity of model outputs to parameter values. Cell chemsynthesis-related parameters were shown to have greatest influence. Initial calibration and validation indicate the need for more robust calibration methods and agent rules regarding biochemical signaling. Future work in optimizing the current model for a heterogeneous platform programming as well as real time visualization of large scale biologically representative environments are important steps in establishing a clinically relevant technology.

## ABRÉGÉ

Lorsque les plis vocaux vibrent, ils sont exposés à un traumatisme phonatoire. Cela peut provoquer des changements dans la structure et la fonction des tissus. L'acide hyaluronique gélatine réticulé (HA-Gtn) est un biomatériau qui peut régénérer et réparer les plis vocaux endommagés. La conception d'un biomatériau qui imite les tissus naturels est difficile. Les modèles informatiques peuvent aider réduire les coûts et le temps. L'objectif de cette étude est de développer un modèle de simulation numérique basé sur des règles d'interaction entre différents agents pour biomatériau HA-Gtn. Nous émettons une hypothèse que le ABM peut être utilisé pour prédire régénération et remodelage du plis vocal.

## TABLE OF CONTENTS

ACKNOWLEDGEMENTS . . . . .	ii
ABSTRACT . . . . .	iii
ABRÉGÉ . . . . .	iv
LIST OF TABLES . . . . .	viii
LIST OF FIGURES . . . . .	ix
1 Introduction . . . . .	2
1.1 Vocal Folds . . . . .	2
1.1.1 Vocal Fold Extracellular Matrix . . . . .	3
1.1.2 Vocal Fold Cellularity . . . . .	6
1.1.3 Phonation and Phonotrauma . . . . .	8
1.2 Inflammation and Wound Healing . . . . .	9
1.3 Vocal Fold Lesions and Scarring . . . . .	10
1.4 Current Treatment and Therapy for Vocal Fold Scars . . . . .	11
1.4.1 Behavioral Therapy . . . . .	12
1.4.2 Bioactive Injectable Tissue Scaffolds . . . . .	13
1.4.3 Crosslinked Hyaluronan-Gelatin Hydrogel . . . . .	14
1.5 Translational Systems Biology . . . . .	16
1.5.1 Inflammation Models . . . . .	17
1.5.2 Agent Based Models . . . . .	18
1.5.3 Agent Based Model of Vocal Fold Inflammation and Healing	19
1.5.4 Current Challenges and Limitations of Agent Based Models	20
1.6 Research Objectives . . . . .	21
1.7 Original Contributions . . . . .	22
2 Computational Methods . . . . .	26
2.1 Vocal Fold Acute Phonotrauma Agent Based Model . . . . .	26
2.1.1 Purpose . . . . .	26

2.1.2	Programming Environment . . . . .	27
2.1.3	Scale and Environment . . . . .	27
2.1.4	Entities and State Variables . . . . .	27
2.1.5	Process Overview and Scheduling . . . . .	30
2.1.6	Design Concepts . . . . .	30
2.1.7	Initialization . . . . .	33
2.1.8	Input Data . . . . .	33
2.1.9	Submodels . . . . .	33
2.2	Hyaluronic Acid-Gelatin Tissue Scaffold Agent Based Model . . .	40
2.2.1	Purpose . . . . .	40
2.2.2	Programming Environment . . . . .	40
2.2.3	Scale and Environment . . . . .	40
2.2.4	Entities, State Variables and Scales . . . . .	41
2.2.5	Process Overview and Scheduling . . . . .	41
2.2.6	Design Concepts . . . . .	41
2.2.7	Initialization . . . . .	43
2.2.8	Input Data . . . . .	43
2.2.9	Submodels . . . . .	43
2.3	Agent Based Model Analysis for Verification and Validation . . .	54
2.3.1	Morris Parameter Screening . . . . .	55
2.3.2	Sobol Sensitivity Analysis . . . . .	57
2.3.3	Sensitivity Index for Correlated Factors . . . . .	59
2.4	Model Calibration and Validation . . . . .	61
2.4.1	Multivariate Calibration . . . . .	61
2.4.2	Predictive Validation . . . . .	63
3	Experimental Methods . . . . .	69
3.1	Materials . . . . .	69
3.2	Human Vocal Fold Fibroblast Cell Culture . . . . .	70
3.3	HA-Gtn Fabrication and and Cell Encapsulation . . . . .	70
3.4	Biochemical Analyses . . . . .	71
3.4.1	Total Protein Assay . . . . .	71
3.4.2	Soluble Collagen Assay . . . . .	71
3.4.3	Cell Proliferation Assay . . . . .	72
3.4.4	Viability Assay . . . . .	73

4	Results . . . . .	74
4.1	Vocal Fold Agent Based Model . . . . .	74
4.1.1	Morris Screening Plots . . . . .	74
4.1.2	System Dynamics for Model Outputs across Treatment Groups . . . . .	75
4.1.3	Parameter Classification . . . . .	76
4.1.4	Sobol Sensitivity Analysis . . . . .	77
4.1.5	Figure of Merit as Sensitivity metric . . . . .	78
4.2	HA-Gtn Scaffold Agent Based Model . . . . .	79
4.2.1	Overview . . . . .	79
4.2.2	Event Validation . . . . .	79
4.2.3	Face Verification . . . . .	80
4.2.4	Model Calibration . . . . .	81
5	Discussion . . . . .	94
5.1	Vocal Fold ABM . . . . .	94
5.1.1	Sensitivity Analysis . . . . .	94
5.1.2	Figure of Merit . . . . .	95
5.1.3	Model Limitations . . . . .	96
5.1.4	Model Significance . . . . .	97
5.2	HA-Gtn Scaffold Agent Based Model . . . . .	97
5.2.1	Validation and Verification . . . . .	97
5.2.2	Model Limitations . . . . .	98
5.2.3	Model Significance . . . . .	99
6	Conclusions . . . . .	100
6.1	Future Work . . . . .	101
	Appendix A: Vocal Fold Agent Based Model Agent Rules . . . . .	102
	Appendix B: Vocal Fold Agent Based Model Chemsynthesis Agent Rules and Parameters . . . . .	103
	Appendix C: Hyaluronic Acid-Gelatin Agent Based Model Agent Rules . . . . .	108
	Appendix D: Vocal Fold Agent Based Model Morris Screening Results . . . . .	110
	References . . . . .	113

LIST OF TABLES

<u>Table</u>	<u>page</u>
2-1 Vocal Fold ABM and HA-Gtn ABM agents and state variables. . . . .	45
2-2 Vocal Fold and HA-Gtn ABM agent sensing abilities. . . . .	48
2-3 Vocal Fold ABM and HA-Gtn ABM initialization. . . . .	49
2-4 Overview of chemical agent rules. . . . .	50
2-5 Overview of HA-Gtn Agent Based Model agent rules. . . . .	52
2-6 Overview of Vocal Fold Agent Based Model parameters. . . . .	64
2-7 Evaluation of sensitivity analysis methods with respect to analysis aims.	66
2-8 Morris and Sobol sensitivity analysis applicability. . . . .	67
2-9 First ( $S_i$ ) and Total ( $S_{Ti}$ ) sensitivity index equations for variance-based Sobol methods. . . . .	68
4-1 Top ranked influential parameters according to Figure of Merit. . . . .	87
4-2 Comparison of Sobol Jansen and Figure of Merit sensitivity rankings for pro-inflammatory model output. . . . .	88
4-3 Comparison of Sobol Jansen and Figure of Merit sensitivity rankings for anti-inflammatory model output. . . . .	89
6-1 Vocal Fold Agent Based Model parameters nomenclature and default value. . . . .	105

## LIST OF FIGURES

<u>Figure</u>	<u>page</u>
1.1 Coronal section of the vocal fold layered structure. . . . .	23
1.2 Phases of the wound healing cascade. . . . .	24
1.3 Cell population profile during wound healing. . . . .	25
2.1 Three dimensional rendering of (a) vocal fold (b) Vocal Fold Agent Based Model. . . . .	44
2.2 Flowchart of Vocal Fold Agent Based Model. . . . .	47
2.3 Flowchart of cell function. . . . .	51
2.4 Flowchart of HA-Gtn Agent Based Model. . . . .	53
2.5 Complexity and applicability of sensitivity analysis methods. . . . .	65
4.1 Vocal Fold Agent Based Model parameters sensitivity indices for TNF model output in the voice rest case. . . . .	82
4.2 Average Morris sensitivity indices (A-B) absolute mean and (C-D) coefficient of variation for pro- and anti-inflammatory chemical populations. . . . .	83
4.3 Identification of influential parameters for voice rest (VR), resonant voice (RV) and spontaneous speech (SS) using Morris screening methods. . . . .	84
4.4 Sobol-Jansen first and total order sensitivity indices for TNF model output for the voice rest case. . . . .	85
4.5 Sobol-Jansen total order sensitivity indices (A) ranked in descending order (B) compared to Figure of Merit sensitivity indices. . . . .	86
4.6 Vocal Fold Agent Based Model cell population profiles. . . . .	90

4.7	Hyaluronic-Acid Gelatin Agent Based Model time-varying mechanical properties (A) elastic modulus, (B) swelling ratio, (C) mass loss for different scaffold compositions. . . . .	91
4.8	Black box validation of calibrated Hyaluronic Acid-Gelatin Agent Based Model outputs (A) fibroblast, (B) collagen, (C) total protein. . . . .	92
4.9	Calibrated Hyaluronic Acid-Gelatin Agent Based Model population response prediction. . . . .	93
A1	Vocal Fold Agent Based Model agent rules. . . . .	102
B1	Vocal Fold Agent Based Model chemical synthesis agent rules. . . . .	104
C1	HA-Gtn Agent Based Model agent rules. . . . .	109
D1	Morris parameter screening with respect to output (A) TNF, (B) TGF, (C) FGF, (D) MMP8, (E) IL1, (F) IL6, (G) IL8, (H) IL10 for voice rest case. . . . .	110
D2	Morris parameter screening with respect to output (A) TNF, (B) TGF, (C) FGF, (D) MMP8, (E) IL1, (F) IL6, (G) IL8, (H) IL10 for spontaneous speech case. . . . .	111
D3	Morris parameter screening with respect to output (A) TNF, (B) TGF, (C) FGF, (D) MMP8, (E) IL1, (F) IL6, (G) IL8, (H) IL10 for resonant voice case. . . . .	112

## NOMENCLATURE

### Acronyms

<i>2D</i>	2-dimensional
<i>3D</i>	3-dimensional
<i>ABM</i>	Agent Based Model
<i>AU</i>	Arbitrary Units
<i>COL</i>	Collagen
<i>CPU</i>	Central Processing Unit
<i>CUDA</i>	Compute Unified Device Architecture
<i>DLP</i>	Deep Lamina Propria
<i>ECM</i>	Extracellular Matrix
<i>ELA</i>	Elastin
<i>FGF</i>	Fibroblast Growth Factor
<i>GAG</i>	Glycosaminoglycans
<i>GPU</i>	Graphics Processing Unit
<i>Gtn</i>	Gelatin
<i>HA</i>	Hyaluronic Acid
<i>HGABM</i>	HA-Gtn Tissue Scaffold Agent Based Model
<i>IL1</i>	Interleukin-1 $\beta$
<i>IL10</i>	Interleukin-10

<i>IL6</i>	Interleukin-6
<i>IL8</i>	Interleukin-8
<i>ILP</i>	Intermediate Lamina Propria
<i>LP</i>	Lamina Propria
<i>MMP8</i>	Matrix Metalloproteinase-8
<i>RVIS</i>	Resonant Voice Impact Stress
<i>RVVS</i>	Resonant Voice Vibratory Stress
<i>sECM</i>	Synthetic Extracellular Matrix
<i>SLP</i>	Superficial Lamina Propria
<i>SSIS</i>	Spontaneous Speech Impact Stress
<i>SSVS</i>	Spontaneous Speech Vibratory Stress
<i>TGF</i>	Tumor Growth Factor
<i>TNF</i>	Tumor Necrosis Factor- $\alpha$
<i>VF</i>	Vocal Fold
<i>VFABM</i>	Vocal Fold Agent Based Model
<i>VFF</i>	Vocal Fold Fibroblast
<i>VFI</i>	Vocal Fold Injectable

**Chemical Agents (v, w)**

<i>FGF</i>	Fibroblast Growth Factor
<i>IL1</i>	Interleukin-1 $\beta$
<i>IL10</i>	Interleukin-10
<i>IL6</i>	Interleukin-6
<i>IL8</i>	Interleukin-8

*MMP8* Matrix Metalloproteinase-8

*TGF* Tumor Growth Factor

*TNF* Tumor Necrosis Factor  $\alpha$

**Extracellular Matrix Agents (x)**

*COL* Collagen

*ELA* Elastin

*HA* Hyaluronic Acid

**Cellular Agents (y)**

*F* Fibroblast

*M* Macrophage

*N* Neutrophil

*P* Platelet

**Patch Agents (z)**

*cap* Capillary

*HG* HA-Gtn

*tiss* Tissue

**Agent Based Model Parameters**

$a_v^{y+}$  Probability of *cell y* activation for local concentration of *chemical v*

$a_v^{y-}$  Probability of *cell y* deactivation

$d^y$  Probability of *cell y* death

$e^x$  Fibroblast synthesis rate of *extracellular matrix x*

$F_v^w$  Fibroblast secretion of *chemical w* in response to local concentrations of *chemical v*

$h_v$	Half life of <i>chemical v</i>
$i_z^y$	Number of <i>cell y</i> recruited to <i>patch z</i>
$M_v^w$	Macrophage secretion of <i>chemical w</i> in response to local concentrations of <i>chemical v</i>
$N_v^w$	Neutrophil secretion of <i>chemical w</i> in response to local concentrations of <i>chemical v</i>
$p^y$	<i>Cell y</i> proliferation rate
$P_v^w$	Platelet secretion of <i>chemical w</i> in response to local concentrations of <i>chemical v</i>
$r_z^y$	Time interval of <i>cell y</i> recruitment to <i>patch z</i>
$t_v$	Threshold level of <i>chemical v</i>

## CHAPTER 1

### Introduction

Voice disorders are among the most common communication disorders across a lifespan, with an estimated 3 - 9% of the population exhibiting some form of voice dysfunction [13]. Although the precise pathophysiology of voice disorders remains largely unknown, the majority of voice disorder cases follows injurious mechanical, chemical or phonatony-related stimuli resulting in lesions or scars. The associated injuries can inhibit the production of a normal mucosal wave and significantly impair vocal fold oscillatory function, decrease voice quality, reduce vocal stamina and create physical discomfort. In an attempt to better understand the highly diverse and unpredictable formation as well as treatment response of vocal fold scars, an agent based computation-model (ABM) characterizing the inflammatory and healing response to vocal fold injury is being developed with the ultimate application being a clinical tool to prescribe and optimize patient-specific treatment.

This chapter provides background information from the literature. A review of acute phonotrauma-related inflammation, wound healing and current biotechnological treatments as well as associated computational models is presented in addition to objectives and hypothesis of this research project.

#### 1.1 Vocal Folds

Vocal folds (VF) are a mucous membrane stretched across the larynx, consisting of an epithelium, connective tissue or lamina propria and vocalis fibers of the

thyroarytenoid muscle [86]. The vocal folds can be anatomically classified into different layers going from superficial to deep: epithelium, superficial lamina propria (SLP), intermediate lamina propria (ILP), deep lamina propria (DLP) and the thyroarytenoid muscle (Figure 1.1). Lamina propria (LP) tissue is composed of various proteins and cells. Together the cells and their secreted extracellular matrix form a histological framework, providing the vocal folds' unique tissue-level vibratory function [57, 121, 64].

### 1.1.1 Vocal Fold Extracellular Matrix

Vocal fold tissue components can be classified as either cellular or extracellular. The extracellular matrix (ECM) is an organized network of structural and regulatory proteins which together provide structural and biochemical support to surrounding cells. These proteins can be classified as either fibrous (collagen, elastin), interstitial (proteoglycans, glycoproteins) or other molecules (lipids, carbohydrates). Cell-ECM interactions play a fundamental role in cell adhesion, migration, growth, differentiation, death, chemokine secretion and protein synthesis, all of which are important in determining the spatial and temporal ECM turnover. Imprecise, unregulated or interrupted ECM remodelling can have detrimental effects on tissue structure and function. Researchers have explored the role of collagen [136, 78, 82, 63, 66, 38], hyaluronic acid (HA) [62], elastin [65, 78, 62] in animal models and human LP. The following sections summarize the current understanding of the biological and biomechanical function of each of these key proteins as it pertains to vocal folds.

**Hyaluronic Acid.** Hyaluronic acid (HA) is polyanionic glycosaminoglycan (GAG) consisting of repeating disaccharide units of  $\beta$  - 1,4-D-glucuronic acid and  $\beta$

- 1,3, N-acetyl-D-glucosamine [90]. Like most interstitial GAG proteins, its major biochemical property is its ability to attract cations and water with its negatively charged units. They are primarily interspersed between fibrous structural proteins and aid in resisting mechanical stress during deformation. As such, HA lends to viscous dissipation of stress and tissue-level structural integrity [54, 47]. Additionally it acts as space-filling molecules as well as a means for controlling hydration, tissue flow resistance, osmosis, and nutrition diffusion [53, 47]. In addition to its role in determining tissue mechanics, HA also has been shown to act as a signaling molecule. Its effect on cell-cell and cell-matrix interactions is critical in the stabilization and organization of ECM [50, 47, 40], the regulation of cell adhesion and motility [40, 27] as well as the mediation of cell proliferation and differentiation [43, 108] in angiogenesis and wound healing. In vocal folds, although its concentration and spatial distribution is fairly uniform across LP layers, HA has a significant influence on viscoelastic and biomechanical properties [23]. It has frequently been hypothesized to play a role in energy dissipation in response to impact and compressive stresses [95]. It has been shown to regulate the effectiveness of growth factors such as TGF- $\beta$ 1 as well as elastin, collagen and versican synthesis by fibroblast cells [37]. Hyaluronic acid is one of the first macromolecules to appear in VF ECM during wound healing [2], an indication of its critical role in the initiation of the inflammation cascade and the coordination of tissue repair [25].

**Elastin.** Elastin fibers are a lysine-mediated cross-linked polymer of tropoelastin monomers [3]. Elastin fibers within the ECM help it retain shape and resist stress. Often intertwined and/or collocated with inelastic collagen fibrils, together

collagen and elastin prevent tissue damage and enable compressive-tension cycles [3]. Following crosslinking, elastin is insoluble and is metabolized by proteolytic elastase enzymes including serine, aspartic, cysteine and metalloproteinases (MMPs). The homeostatic function of the ECM requires a balance between elastin monomer synthesis and MMPs to regulate matrix degradation and turnover. In vocal folds, elastin constitutes 9% of tissue total protein compared to 2 - 4% in the skin, 30% in the lungs and 70% in large arteries [62]. The density and organization of elastic fibers regulate tissue pliability and resilience [87] and as such have been found to vary in concentration within the LP layers according to biomechanical needs. Quantitative analysis of elastin distribution has demonstrated how high concentrations of mature elastic fibers in deep layers decrease towards the epithelial layer where they are found in their less elastic form [62, 55]. Elastin has a natural half-life on the order of years. While the turnover in healthy native tissue is slow, changes in metabolism following aging or disorders can result in excessive degradation and altered function [45].

**Collagen.** Collagen is an abundant fibrous protein consisting of triple  $\alpha$ -helix tropocollagen units of repeating amino acid sequence Glycine-X-Y, where X and Y are proline or hydroxyproline. These tropocollagen units facilitate high order fibril assembly into various fibrils, sheets or cross-link, each of which lend different tissue properties. Considered a load bearing protein, in soft tissue these collagen structures lend tensile and compressive strength [48]. Additionally, collagen has been shown to modulate cell function, encouraging cell adhesion and consequently controlling cell morphology, migration, and in some cases differentiation. In vocal folds, collagens' complex fibrillar assembly varies throughout the different layers of

the LP [53]. While non-fibrillar collagen types associated with ECM stabilization and angiogenesis have been found in the basement membrane zone [118], structural fibrillar collagen types I, II and III have been identified in the LP [56]. Delicate reticular collagen (type III) fibers in SLP are highly branched with empty space filled with GAGs and elastic fibers to provide a support network [135]. Thicker fibers such as type I and III are generally aligned in a direction parallel to the anterior-posterior free margin of vocal fold and are more abundant in DLP [56, 53, 67]. These non-elastic collagen fibers form a basket-like woven network to guarantee tensile strength, permitting deformation and elongation during frequency modulation to maintain tissue structure, especially important during VF phonation [38].

### **1.1.2 Vocal Fold Cellularity**

The major cellular components of vocal fold lamina propria (VFLP) include: fibroblasts, myofibroblasts and macrophage cells [53]. Fibroblasts were originally believed to be the only cells to produce proteoglycans (aggrecan, versican, decorin, fibromodulin, heparin sulfate) [121]. Since then, macrophage and myofibroblasts have been shown to be involved in their synthesis [121], highlighting the importance of several different cell types, not solely fibroblast cells, in the manufacturing and maintenance of VFLP.

**Vocal Fold Fibroblasts and Myofibroblasts.** Human vocal fold fibroblasts (VFFs) are an abundant and predominant cellular component of VFLP [21], and are present with uniform population density in all layers of the vocal folds [53]. They contribute to the general maintenance of connective tissues through the deposition, degradation and rearrangement of ECM [21, 53]. In vocal folds, they have been

shown to enter an active state where they produce collagenous and elastin fibers [68]. Additionally, as mature mesenchymal cells VFFs can differentiate into myofibroblasts following injury or damage [36, 21]. These myofibroblast cells provide periodic or continuous reorganization of actin and fibronexus to repair collagenous and elastic connective tissues [53]. They also regulate the intensity and duration of inflammatory response by secreting cytokines [3]. Their population density is highest in the superficial layer of LP and decreases with depth within the LP. Increased proliferation following injury and high population in areas of high stress are indicative of the importance of their role in the reparative process.

**Macrophages.** Macrophages are a specialized cell type formed and recruited in response to infection or damage. They populate a fraction of native human vocal folds in moderate concentration below the basement membrane zone and in the SLP [53, 21] in response to the greater presence of mucosal irritants and mechanical stress. When exposed to specific chemical signalling molecules, macrophages enter an activated state. These activated cells function as antigen-presenting cells that respond to and combat inflammatory response through the secretion of both pro- and anti-inflammatory cytokines [21, 53] in addition to polyamines and proline [33]. These secreted inflammatory mediators play a role in immunoregulating fibroblast behavior and ECM protein secretion [89].

**Neutrophils.** Neutrocytes or neutrophils are granulocyte cells. An essential part of the innate immune system, they accumulate in large numbers at tissue damage sites and act as scavengers to remove irritants and damaged or excess extracellular deposits. Found in low density in native vocal fold tissue relative to other cell

types, they are recruited following injury during inflammation but disappear prior to active fibroblast-mediated mucosa remodeling [105]. When exposed to chemotactic agonists, neutrophils migrate into extravascular space and enter an activated state where they change shape, adherence, enzyme secretion and display directed movement [9].

### **1.1.3 Phonation and Phonotrauma**

Vocalization is a result of air flow-excited oscillations of the vocal folds. Air expelled from the lungs creates a pressure difference yielding a inferior to superior high frequency (100 - 1000 Hz) vertical shear wave [158]. This small amplitude vibration primarily occurs in the vocal fold cover (epithelium and SLP) with the vocal fold body (DLP and muscle) remaining largely stationary. During phonation, areas of the vocal fold undergoing oscillations are under various stresses including tensile, shear, contractile, inertial, aerodynamic (pressure) and impact [157]. Prolonged phonatory-related and/or nonphonatory stress without sufficient rest periods can result in vocal fold injury, triggering a host tissue wound healing response [128]. Injury in vocal folds can be classified into four broad categories based on the source and chronicity: nonphonatory (mechanical or chemical) injury, acute phonotrauma and chronic phonotrauma [128].

Nonphonatory trauma can occur following mechanically or chemically traumatic events including endotracheal intubation, phonomicrosurgery, external laryngeal trauma or inhalation of chemical irritants. These are generally characterized by disruption of epithelium, basement membrane and underlying LP requiring full host

repair response [155, 154, 138]. On the other hand, phonatory-related or phonotrauma occurs as a direct result of voice use. Acute phonotrauma is associated with temporary vocal abuse yielding in the disruption of vascular network, basement membrane zone and ECM components [17]. Chronic phonotrauma on the other hand is classified as extended and/or focal regions of acute phonotrauma resulting in a relatively permanent state of inflammation. The VFLP microstructure has a high reparative capacity that enables it to accommodate a limited amounts of acute phonotrauma-related microstructural damage without requiring a full scale wound healing response [17]. Long term or heightened inflammation however is believed to contribute to the development of benign tissue changes such as vocal fold lesions or scars. One of the major remaining challenges treating vocal fold lesions include understanding complex wound healing processes and large variations in individual inflammation response to phonotrauma.

## **1.2 Inflammation and Wound Healing**

Wound healing is a common mechanism to maintain homeostatic conditions consisting of three major overlapping phases: (1) inflammation, (2) ECM deposition/epithelialization and (3) remodeling [128, 17, 32] (Figure 1.2). Inflammation refers to response of living tissue to local injury through containment, neutralization or dilution of injurious agents. In vocal folds, inflammatory response is typically initiated by injury disrupting local vasculature. Leakage of blood from disrupted blood vessels fill tissue deficits and provide a provisional matrix to signal cells to migrate to the site of the injury. Recruited inflammatory cells enzymatically clear contaminants and promote recruitment of fibroblast cells for reconstitution of ECM through the

secretion of collagen, elastin, and HA. The final stage of the wound healing cascade is a dynamic remodeling process in which further deposition and reorganization of matrix components occurs. In proper healing of vocal folds, the total collagen content is highly controlled and stable after inflammatory stages followed by increased degradation and deposition along lines of mechanical stress [113]. Meanwhile pathological healing following premature stasis or arrest of healing processes, elevated levels of procollagen production in early wound healing followed by remodeling of thick disorganized collagen bundles and fragmented elastin fibers in late stages are observed [17]. These histological changes are associated with the formation of benign vocal fold lesions or scars.

### **1.3 Vocal Fold Lesions and Scarring**

Vocal fold lesions and scars manifest as benign tissue changes resulting in different biomechanical properties, mass and/or irregularly shaped vocal fold edge. This can impair neuromuscular control and disrupt vocal fold vibratory function resulting in dysphonia [11]. There are four general vocal fold structural abnormalities: nodules, polyps, cysts and scars. Nodules are believed to arise from trauma disrupting the basement membrane and separating epithelial layer from underlying tissue [52] resulting in stiffening of the vocal folds [91]. Polyps are associated with acute vascular injury with less severe basement membrane disruption [35]. Vocal fold cysts follow high impact stress [17], resulting in basement membrane thickening between that found in polyps and nodules [35]. Vocal fold scars are a stiff fibrous segment replacing normal vocal fold tissue. They often are formed following a large disruption of the epithelium beyond a critical size requiring secondary healing or ulceration

whereby fibrin deposition by inflammatory cells is followed by excessive fibrous collagen deposition [12].

The inflammatory response to high-effort vibration or phonotrauma is a common factor associated with the formation of midmembranous benign vocal fold lesions [130, 163]. Although this study focuses on the treatment of vocal folds scars, it has been hypothesized that scars and lesions are simply a continuum of vocal fold injury, with differences arising from the chronicity of phonotrauma, diffuse nature of injury and/or premature arrest of acute inflammatory or wound healing [157, 130, 163, 91, 159, 83]. Currently, precise inflammatory mechanisms responsible for regulating fibroblast gene expression governing ECM component synthesis and scar formation remain unclear. While specific biochemical marker levels in laryngeal secretions following phonotrauma can reflect an acute inflammatory process [164] providing insights into the nature of the development of vocal fold scars, a better understanding of underlying mechanisms is needed. This can then be used to improve current clinical techniques and therapeutic targets used to minimize vocal fold scar formation.

#### **1.4 Current Treatment and Therapy for Vocal Fold Scars**

Currently, there exist few effective treatment options for vocal fold scarring. Behavioral voice therapy is used as a conservative first-line approach. It focuses on ceasing injurious activity and modulating natural wound healing reparative processes to restore biomechanical function. Occasionally more invasive treatments are used to treat resistant lesions. These treatments include growth factor therapies [93, 71, 69],

cell therapies [93, 71, 28, 22, 84] and injectable augmentation substances [112, 81, 30] which attempt to re-establish mucosal pliability through LP replacement [172].

#### **1.4.1 Behavioral Therapy**

The purpose of behavioral therapy is to restore vocal function by adapting voice production to produce the best possible sound while preventing further phonotraumatic injury. This is typically accomplished through a series of voice rest and voice production exercises in varying combinations. Classical approaches encourage voice rest facilitated recovery which minimizes impact stresses normal to the epithelial surface [20]. Absolute voice rest on the range of days to weeks is recommended for acute phonotrauma while partial voice rest is prescribed for vocal fatigue resulting from chronic abuse. This is hypothesized to enhance tissue healing phenotype, allowing time for the tissue to heal while minimizing the aggravation or introduction of any new injury [60]. Despite voice rest being prescribed more widely clinically, a second theory has been proposed that argues large-amplitude low impact vocal fold vibratory exercises can promote active mucosal healing by stimulating the production of anti-inflammatory mediators reducing chronic inflammation [1]. Despite the practice of both theories, behavioral therapy remains a preventative measure for the development of vocal fold lesions. Behavioral therapy alone rarely yields substantial improvement or resolution of fully formed lesion or scars arising from chronic phonotrauma [73]. Most patients must either live with unresolved conditions or undergo surgery. As such, there remains an unmet clinical need for vocal fold restoration. Current research in tissue engineering attempts to fulfill this unmet need through

injectable bioactive biomaterials to promote long-term repair and tissue regeneration for the treatment of tissue defects.

#### **1.4.2 Bioactive Injectable Tissue Scaffolds**

Phonosurgery uses vocal fold injections (VFIs) of biomaterials to augment tissue biochemical and mechanical properties in two ways. The first is used as a filler substance in the lateral aspect of thyroarytenoid/lateral cricoarytenoid muscle. These treat glottal insufficiency by displacing the free edge of the vocal fold cover [112]. The second are used for LP replacement or regeneration to correct vibratory defects from mid-to-moderate severity vocal fold lesions in the superficial subepithelial space [112]. This work focuses on the latter VFI for vocal fold augmentation. Current injectables for vocal fold regeneration still require great advancements in delivery method, instrumentation, rheological/biomechanical properties and incorporation of bioactive agents for long-term ECM turnover and regeneration [112]. This section will focus on the unmet need of a bioactive hydrogel-based injectables in cases of vocal fold scarring.

Cell therapy relies on the introduction of autologous or genetically engineered cells with division and differentiation potential to facilitate long term tissue remodeling without immunorejection. In vocal folds, the introduction of autologous mesenchymal stem cells (MSCs) [85] and autologous fibroblasts [29] has shown to yield favourable morphological and histologic changes in the regeneration of injured vocal folds. Many are now exploring the local release of bioactive molecules in conjunction with cell therapy to manipulate temporal and spatial variations in cell activity. Modulation of VFF activity has been shown through administration of hepatocyte growth

factor (HGF), epidermal growth factor (EGF), basic fibroblast growth factor (bFGF) and transforming growth factor-beta-1 (TGF- $\beta$ 1) [110, 37, 72]. Growth factors (GFs) are bioactive proteins expressed by cells for cell-cell signaling. They can be used as a regulatory factor to increase VFF ECM production [42]. Repeated administration of HGF has shown to be antifibrotic decreasing fibroblast production of collagen type I while administration of TGF $\beta$ 1 increased both collagen I and fibronectin production [70]. Extended administration using time-controlled release of heparin bound GFs in injectable hydrogels has been explored *in vivo* [123]. Controlled spatiotemporal release has been reported to yield more organized cellular angiogenic response. As such, injectable therapies ideally use a combination of cells and growth factors in a matrix scaffold for controlled long term tissue regeneration and remodelling. Natural, synthetic, or mixed materials have been applied as synthetic extracellular matrix (sECM) scaffold to support three-dimensional (3D) tissue regeneration [128, 96, 8]. Various materials have been applied for vocal fold regeneration and augmentation including teflon [116], collagen [46], autologous fat [144] and HA-based materials [81]. These scaffolds must provide appropriate mechanical and viscoelastic support as well as biochemical, physical and cellular stimuli to guide the proliferation, differentiation and migration of cells. Of the materials investigated, HA-based materials remain among the most promising for their excellent biocompatibility, biodegradability, tunable mechanical and viscoelastic properties [61, 143, 160, 173].

### **1.4.3 Crosslinked Hyaluronan-Gelatin Hydrogel**

Hyaluronan or hyaluronic acid (HA) and its derivatives have been widely used in clinical medicine [10, 18, 19, 109, 119, 122, 125, 162, 147, 150, 124] as implants for

surgical repair of ECM defects in soft tissues [149, 170, 34]. Hydrogels derived from chemically modified HA have been shown to provide cells with a microenvironment that promotes cell-guided tissue remodeling and regeneration. Hyaluronic acid-based scaffolds have been shown to be biocompatible and nontoxic to VFFs *in vitro* as well as shown to enhance healing and regeneration in *in vitro* 2D environments and *in vivo* animal models [26, 42, 41, 142]. Fibroblasts encapsulated in crosslinked thiol-modified-HA have remain viable for over 4 weeks while retaining a proliferative and synthesis phenotype, actively secreting new ECM [149]. There remain significant limitations in HA-based hydrogels as negatively charged glucuronic acid residues impart highly poly-anionic behavior at physiological pH, hampering cell attachment and adequate ECM synthesis necessary for formation of new tissue [120, 148]. Many have explored the addition of biomolecules through *in situ* crosslinking for additional functionalization [149, 146]. In an effort to introduce cell adhesion functionalization, researchers have developed hybrid scaffolds by combining HA with biomolecules containing the Arg-Gly-Asp (RGD) peptide sequence such as collagen [88, 99], chitosan [170], silk fibroin [49], directly covalently binding RGD peptides [127, 51] and gelatin [98, 74, 6]. Addition of RGD tripeptide sequences promotes integrin receptor binding and cellular attachment to aid in regulating cell growth and differentiation. These hybrid scaffolds have been used to successfully fabricate 3D scaffolds for skin [31], cartilage [24], liver [94] and bone [106].

Gelatin (Gtn) is a denatured form of collagen and a major component of natural ECM. In addition to being low-anitgenic, it has been shown to retain RGD sequence of native collagen [104]. Crosslinked HA-Gtn sponges seeded with human tracheal

scar fibroblasts and implanted into the flanks of nude mice have been shown to grow healthy new human fibrous tissue at 4, 8, and 12 weeks [107], proving non-toxic to cells *in vitro*. Other injectable forms of HA-Gtn sECM when seeded with NIH 3T3 fibroblast cells have grown 1-cm diameter healthy fibrous tissue 8 weeks following subcutaneous implantation in nude mice [145].

The design of tissue scaffolds must consider the complex heterogeneous hierarchical structure of the host tissue. These include factors such as porosity, pore size and compliant mechanical properties. Recent research focuses on developing biomaterials with microenvironments that closely approximate the biomechanical, biochemical and viscoelastic properties of native tissue. Many groups have demonstrated how varying HA-Gtn hydrogel composition can yield a wide range of tunable rheological, biochemical and mechanical properties [161, 173]. However, the systematic assessment of the optimal material composition for vocal fold augmentation is costly. It often requires the optimization of a prohibitively large number of biochemical and biomechanical factors. Additionally, scaffold parameters and properties are often not independent and decoupling them experimentally is time and cost expensive.

## 1.5 Translational Systems Biology

Recent improvements in computer technology have enabled the use of high-performance computing for developing models of complex biological systems. Translational Systems Biology (TSB) is a multidisciplinary approach to apply predictive computational and dynamic *in silico* simulation methods to improve understanding of molecular, cellular, tissue and clinical-level behavior [166]. These numerical

simulations often incorporate the structure, organization and behavior of *in vivo* biological systems including their various interacting components, control feedback loops, multiple levels and non-linear dynamics. In the current study, TSB principles were employed to numerically simulate the biological response of vocal folds following phonotrauma and biomaterial injection as a complex biological system with the intention of coupling mechanism with tissue function to aid in improving clinical practice.

### 1.5.1 Inflammation Models

There are two general approaches to modeling inflammation as a complex system. These include: data-driven methods and mechanistic methods. Examples of data driven models include regression based, principal component analysis or hierarchical clustering. These methods infer the molecular network interactions and organizational dynamics by modeling abstract features of system response [111, 79]. In addition to lacking mechanistic insight, data-driven models are generally linear within training data, making model outputs difficult extrapolate and apply to wider data sets.

Mechanistic models focus on individual parts and their coupled interactions. Examples of these models include partial differential equations (PDEs), ordinary differential equations (ODEs), rule-based and agent based models (ABM) [4, 5]. While straightforward, numerically inexpensive ODEs do not allow for modeling spatial variability. Although methods for numerical and analytical solutions of PDEs are well developed, computational time are longer than that for ODEs and differential functions break down at small length scales. Agent based models (ABMs) do not

have these limitations allowing for modular and scalable architecture. ABMs are a rule based discrete event modeling technique where cell-as-agent resolution allows for integration of basic cellular level mechanistic knowledge. These yield emergent system properties not obvious from encoded interactions. The major benefit is that outputs are theoretically predictive outside of conditions and time points in which they were trained. However this is assuming the model is correct, used within its intended context and free parameters are appropriately selected. These assumptions are non-trivial and if are not met, the model is not generalizable. In the current project, mechanistic models of agent-based simulation were used. A review of ABMS in modeling complex biological systems are reviewed below.

### **1.5.2 Agent Based Models**

Agent based models (ABM) are a bottom-up approach to modeling. The three primary components of an ABM include: (1) autonomous agents at varying scales, (2) decision-making heuristics agent rules, (3) virtual environment. Low level components (agents) and their interactions (agent rules) are specified, while high-level behaviors arising from local mechanisms are observed at different spatial and temporal scales. Agent based models have been applied in disciplines involving complex systems of autonomous entities including social sciences, economics, geography and political sciences. In biology ABMs have been used to simulate various inflammatory diseases such as diabetes, spinal cord injuries and sepsis.

Agent based models are advantageous when modeling cellular-level biological systems for a number of reasons. Firstly, elements of a system can be represented

as discrete autonomous agents that move and interact according to a series of deterministic and/or stochastic rules based on their state and environment. This is generally advantageous for complex systems where deterministic and stochastic events occur with spatial or temporal heterogeneity, such as biological systems. Secondly, given their non-analytical nature ABMs can directly incorporate low level knowledge or hypotheses about components not easily expressed mathematically. This is particularly important in cases where it is difficult or unfeasible to isolate and directly measure all biologically relevant parameters. Additionally, critical underlying molecular properties can be incorporated explicitly or implicitly to capture poorly understood cell-matrix interactions. Thirdly, emergent properties arising from low level entities and their low level states may reflect behavior not apparent by simple aggregation. These emergent properties may be essential in coupling dynamics occurring at different time and length scales to better understand cellular mechanisms. Finally, statistical simulations with different initial conditions can be used to explore the distribution of possible outcomes. Additionally, the high modularity of agent populations and agent rules allow the disabling of specific mechanisms, relative contribution adjustments and sensitivity analysis of parameters to identify connections between intracellular descriptions and multicellular dynamics.

### **1.5.3 Agent Based Model of Vocal Fold Inflammation and Healing**

An ABM of inflammation and tissue healing in skin was previously developed[115] and later adapted for the vocal folds [101, 102]. The preliminary model was built using freeware *Netlogo* (Center for Connected Learning and Computer-Based Modeling, Northwestern University, Evanston, IL) representing a two-dimensional (2D)

1.8 mm  $\times$  1.8 mm grid populated by 110 resting cells (macrophage, neutrophil, fibroblast) within tissue and blood, ECM protein (collagen) and chemical mediators (tumor necrosis factor- $\alpha$  (TNF- $\alpha$ ), interleukin-1 $\beta$  (IL-1 $\beta$ ), interleukin-10 (IL-10), TGF- $\beta$ 1). Simulations were shown to qualitatively reflect relevant generally-accepted mechanisms of wound healing. These were validated against relevant changes in cell population and effector cytokines during normal wound healing (Fig. 1.3). Experimental measures of inflammatory mediators in laryngeal secretions were used to adapt the model for inflammation in response to acute phonotrauma [103] and surgical injury [102]. This required extending the previous model with additional inflammatory mediators (interleukin-6 (IL-6), interleukin-8 (IL-8), bFGF, MMP-8) as well as ECM components (elastin, HA). Population- and individual-based “Leave-One-Out-Cross-Validation” calibration used for iterative parameter estimation and model calibration [103]. Simulation levels within a 95% confidence interval of empirical results were used for model validation. Model simulations agreed qualitatively with known aspects of inflammation and healing with individual based calibration yielding improved model prediction than compared to population based calibration [165]. The biosimulation was shown to reproduce trajectories of experimental inflammation biomarkers in laryngeal secretions of individuals subjected to phonotrauma 24h post-injury [165].

#### **1.5.4 Current Challenges and Limitations of Agent Based Models**

Despite initial efforts, various problems and limitations remain in modeling biological systems using ABMs. Firstly, the freeware agent-based toolkit NetLogo not designed for extensive simulations, limiting its performance and application. For

large number of agents, there are significant drops in execution speeds. Secondly, the analysis of complex dynamics of ABMs require sophisticated high-dimensional analytical approaches. ABMs use behavior of individually encoded micro-level rules and dynamic interactions to observe macroscopic phenomena. These often yield complex non-linear interactions with non-normal output distributions and high-order effects. Comprehensive and compelling statistical analysis of ABM outputs is fundamental to the model design, implementation and the understanding of dynamic properties and model structures. Given the stochastic property of the ABM, repeated random sampling such as Monte Carlo sampling is required to attain pseudo random samples of parameter settings to adequately achieve statistical robustness. Most ABMs only apply simple visual analysis, or classic local techniques that assume linear or monotonic relationships between model factors (input, parameters) and model outputs, while neglecting the interaction effects. More recently, researchers have begun to adopt more robust statistical analysis methods to explore the sampling space of uncertain model factors. Sensitivity analysis and parameter estimation are two types of statistical analyses which have become critical steps for proper calibration and validation of computational models (Section 2.3).

## **1.6 Research Objectives**

In this thesis project, a computer-aided tissue engineering approach was hypothesized to capture and predict cellular behavior using agent based modeling in an attempt to simplify behavioral clinical treatment and injectable biomaterial optimization for vocal fold augmentation. The specific aims of the present study were to (1) integrate the current understanding of HA-Gtn hydrogels on cell behavior into the

existing vocal fold ABM (2) apply variance-based analysis methods for global sensitivity analysis to examine model dynamics and identify key influential parameters for model calibration as well as (3)conduct first pass attempts at model calibration and black box validation.

## 1.7 Original Contributions

To achieve the research objectives outlined above, several original contributions were made including: model implementation using a low-level programming language, expanding the model to include assumed effects of scaffold composition on cell activity and ECM productions as well as performing and interpreting model sensitivity analysis. The above contributions create a complete and functional implementation of *in vivo* and *in vitro* model of inflammation and tissue remodeling in vocal fold. These contributions are unique and have never before been presented to our knowledge. Implementation using a low-level lightweight programming platform ensures a fast, efficient simulation. This establishes a base model necessary for model parallelization and speedups on heterogeneous computing platforms [140] as well as large scale 3D simulations and real time visualization [139]. Results from the sensitivity analysis are important steps in reducing model complexity and simplifying model calibration which are both important steps for patient specific calibration. As such, this work served a critical milestone in creating a clinically relevant computational technology for patient-specific vocal fold augmentation.

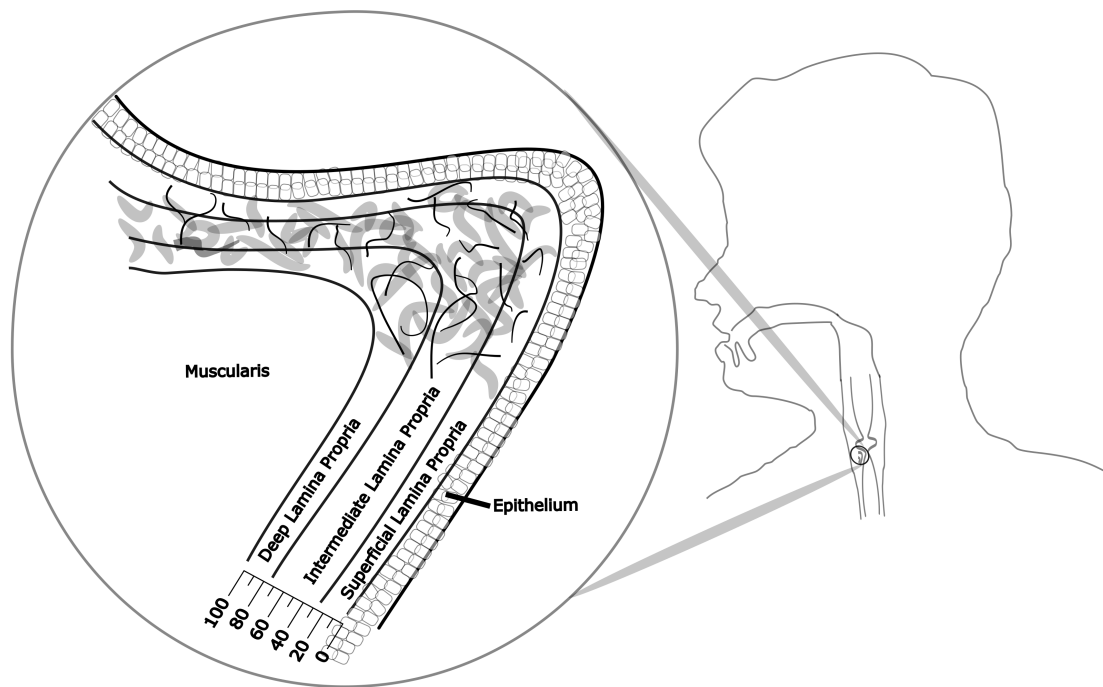


**Figure 1.1:** Coronal section of the vocal fold layered structure.

Numbers refer to % of total depth of lamina propria. Modified from [53].

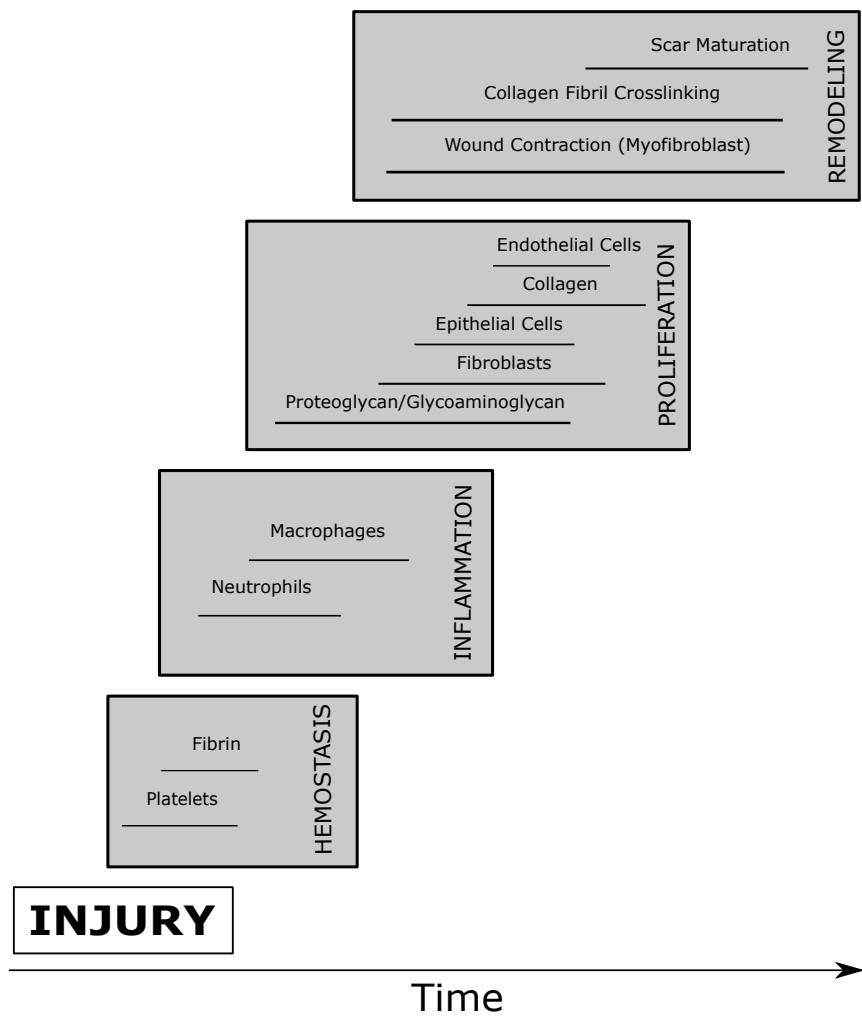


**Figure 1.2:** Phases of the wound healing cascade.

Modified from [131].

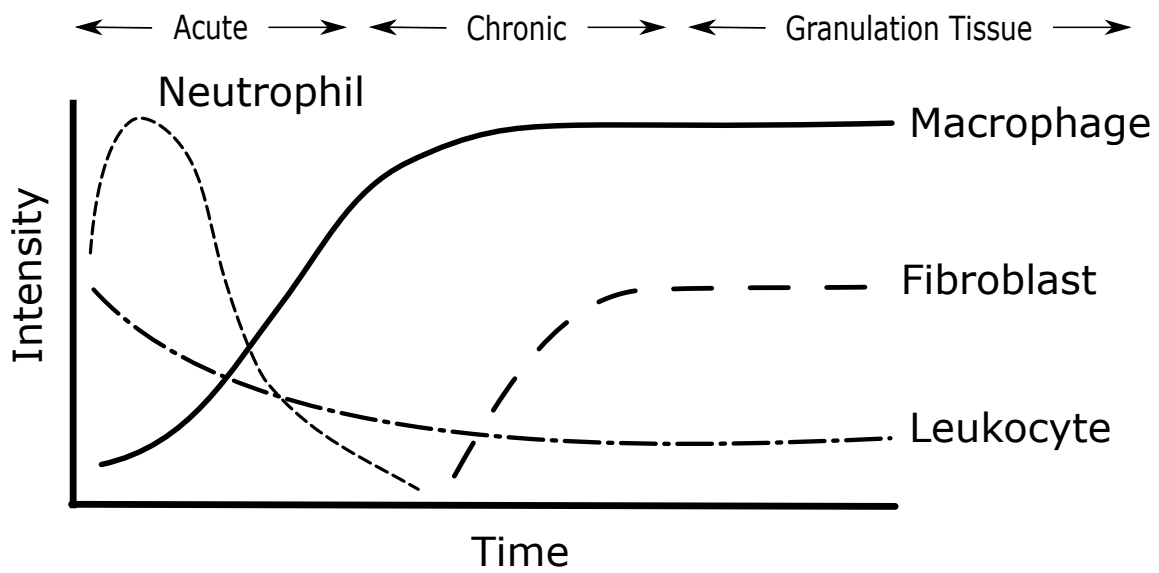


**Figure 1.3:** Cell population profile during wound healing.

Modified from [129].

## **CHAPTER 2**

### **Computational Methods**

This chapter aims at providing an overview of the proposed agent based models. It will be divided into two separate models: the base ABM of inflammation and wound healing following acute phonotrauma in vocal folds and the extended ABM simulating vocal fold fibroblast tissue remodeling when seeded in hyaluronic acid-gelatin tissue scaffold constructs. The proposed ABMs will be described following the Overview, Design concepts and Details (ODD) standard protocol for describing agent based models components, general logic flow and simulation conditions [58, 59]. As the ODD protocol was originally developed to describe ecological models of social systems, a modified version of ODD is used herein.

#### **2.1 Vocal Fold Acute Phonotrauma Agent Based Model**

##### **2.1.1 Purpose**

The vocal fold acute phonotrauma ABM (VFABM) is used to dynamically represent molecular, cellular and organ level dynamics of inflammation and repair processes in vocal fold tissue following acute phonatory damage. The VFABM aims to couple molecular mechanisms with tissue-level response for three different behavioral therapy exercises: (1) voice rest, (2) resonant voice, and (3) spontaneous speech. The goal is to predict healing response and help prescribe behavioral treatment.

### 2.1.2 Programming Environment

The model was previously implemented on the ABM toolkit, *Netlogo* (Center for Connected Learning and Computer-Based Modeling, Northwestern University, Evanston, IL) [101, 102]. Given the need for larger simulations with a greater number of agents, the Netlogo VFABM was re-architected. The model was implemented on a computer processing unit (CPU) platform using object-oriented C++. It was later extended with Open Multi-Processing (OpenMP) to enable concurrent operation executions on multi-core Graphics Processing Units (GPUs) [141].

### 2.1.3 Scale and Environment

The VFABM is a 3D representation of the lamina propria of an average adult human (Fig. 2.1A). For simplicity, the LP is mapped onto a Cartesian coordinate system with the x-y plane representing a coronal plane of the VF (Fig. 2.1B). The virtual environment or *world* represents a  $24.9\text{ mm} \times 1.6\text{ mm} \times 17.4\text{ mm}$  space discretized into  $0.015\text{ mm} \times 0.015\text{ mm} \times 0.015\text{ mm}$  spatial grid cells or *patches*. For our purposes, given constraints in computational complexity and execution time, the *world* structure was limited to a 2D domain (x-y plane). As ABMs iteratively execute rules and commands, a time step or *tick* of 30 minutes was chosen as the time scale for agents to perform actions in agent rules. With intentions of modeling injurious, therapeutic and inflammatory processes following acute phonotrauma, a time course of 24 hours was chosen.

### 2.1.4 Entities and State Variables

Entities refer to individual agents, attributes describing agents or collections of agents. Each agent has a set of attributes or state variables that define its current

state. This set of state variables are consistent for a given agent type, although values of these state variables may vary across individuals of the same type and/or vary for an individual over time.

The VFABM contains five agent classes: *world* (environment), *patches* (spatial unit), *chemicals* (spatial unit), *ECM* (spatial unit), *cell* (individual) and *agent populations* (collective). A summary of agent classes and their corresponding state variables are shown in Table 2–1. Note, it was chosen to use “encapsulated complexity” to form aggregated descriptive variables abstracting several molecular species into one state variable. For example collagen types I, II, III are abstracted under “collagen”. This was chosen as the VFABM does not take into account specific molecular interactions but instead consequences of the interactions of cell and chemical populations behavior.

**World.** A *world* represents the high-level environment that drives the behavior of agents and grid units within it. A *world* is characterized by the state variables: *length*, *width*, *height*, *clock*, *wound* and behavioral therapy *treatment*. *Clock* represents the current time in ticks. The “*wound*” is a set of patches flagged as having phonatory-related tissue damage while “*treatment*” is either *voice rest* (no tissue mobilization), *resonant voice* (high vibratory stress, low impact stress) or *spontaneous speech* (high vibratory stress, high impact stress).

**Patches.** *Patches* are discrete spatial grid units in the vocal fold *world*. They can represent different biological tissue types (*epithelium*, *SLP*, *ILP*, *DLP* or *capillary*). In addition to tissue *type*, each *patch* is characterized by the state variables: *spatial coordinates*, *cell occupancy* and *damage*. *Cell occupancy* is a boolean variable

representing the presence or absence of a cell on a given patch. The volume of a single *patch* matches the approximate dimensions of a single biological cell to simplify coordination of *patch* occupancy. All alarm or danger biochemical signals arising from necrosed tissue or fragmented ECM proteins following phonatory-related mechanical stress is abstracted under an arbitrary “*damage*” variable. *Patches* with *damage* act as a pseudo inflammatory mediators to attract and induce cellular inflammatory response.

**Chemicals.** A total of eight pro- and anti-inflammatory cytokines, growth factors and collagenases are considered in the model (*tumor necrosis factor (TNF)*, *transforming growth factor (TGF)*, *fibroblast growth factor (FGF)*, *matrix metalloproteinase - 8 (MMP8)*, *interleukin-1 beta(IL-1 $\beta$ )*, *interleukin-6 (IL-6)*, *interleukin-8(IL-8)*, *interleukin - 10(IL-10)*). Collectively they will be referred to as *chemicals*. *Chemicals* are modeled as discrete spatial grid units undifferentiated from patches, with state variables characterizing the *diffusivity constant* and local patch *concentration* of each chemical.

**ECM.** *ECM* managers are discrete spatial grid units undifferentiated from a patch which contain information regarding major ECM components on a given patch(*collagen*, *elastin*, *HA*). They are characterized by the state variables *spatial coordinates* as well as protein content(*tropocollagen*, *fibril collagen*, *fragmented collagen*, *tropoelastin*, *elastin fibers*, *fragmented elastin*, *HA* and *fragmented HA*).

**Cells.** A world is occupied by a group of biological cell types involved in inflammation and wound healing processes (*platelet*, *neutrophil*, *macrophage*, *fibroblast*). They are characterized by a set of state variables: remaining *life*, *spatial*

*coordinates* and *activation* state. *Cells* are created with a lifespan on the order of either hours, days or months according to the average lifespan of their given cell type. The remaining natural lifespan is stored in units of ticks. *Activation* state is a boolean variable establishing cell phenotype and/or activity level. *Macrophages* have the additional attribute denoting if they *originate from blood or tissue*.

### 2.1.5 Process Overview and Scheduling

Within each tick or time step, several submodels are processed in the following order: chemical diffusion, cell function, ECM function, synchronous attribute update (Algorithm 1, Figure 2.2). Details of these modules are described in Section 2.1.9. Within each submodel, individual agents are processed serially in a stochastic manner. Any changes to state variables values are stored until all agents have executed all processes whereupon the state of all agents are updated at once. This synchronous updating ensures the model output is independent of order in which individual agent are processed.

### 2.1.6 Design Concepts

**Basic Principles.** Inflammation and wound healing is a multi-scale complex biological system that involves a series of interacting cascades of signaling events (Section 1.2). This includes coordinated signaling network of cell responses as well as production of inflammatory signaling molecules (chemicals and ECM proteins). This model abstracts all signaling cascades as interactions between autonomous agents using agent rules (Section 2.1.9). Patient-specific calibration and validation may provide insights about how inflammation and wound healing varies between individuals.

**Emergence.** In literature collective cell populations reflect events within the wound healing signaling cascade (Figure 1.3). In the VFABM, collective cell and ECM protein populations are similarly used as emerging outputs reflecting the assembly of agents, their states and consequential interactions. Collective chemical populations dynamics are similar to that of laryngeal secretions in reflecting average cell response and wound healing events, however are more tightly imposed by model rules and boundary conditions and are thus more-so built in rather than emergent.

**Adaptation.** Cells have adaptive traits that change in response to changes in their own states or their environment. These include chemical/ECM synthesis rate, proliferation rate and activation probability, which change in response to the presence of damage as well as number of chemical and ECM protein agents. These adaptive traits cause individuals to reproduce observed behaviors that implicitly reflect different phenotypic states cells undergo throughout the wound healing process.

**Learning, Objectives and Prediction.** Currently, individual agents do not change their adaptive traits or learn as a consequence of experience in an attempt to maximize some predictive objective.

**Sensing.** Sensing refers to state variables of other individuals and entities that an agent can perceive and consider in decisions. In the VFABM, different agents classes have the ability to sense different state variables as summarized in Table 2–2. All sensing is local and limited to agents on the same or immediate neighboring patches.

**Interaction.** Cell-ECM and cell-chemical interactions in which individuals encounter and affect others are assumed to be direct. The interactions involve communication through sensing the presence and/or state variables corresponding to local agents. Cell-cell interactions are indirect via production and subsequent diffusion of chemotactic chemicals.

**Stochasticity.** A few processes within cell submodel are modeled assuming they are partly random: activation, deactivation, death, proliferation, ECM synthesis. This stochasticity is introduced to natural variability of these processes.

**Collectives.** Collectives are aggregation of individuals agents and represent intermediate levels of organization. In the VFABM, collective populations are defined as a set of chemical, ECM and cell individuals with the same agent class and type. These collective populations are used to indicate emergent property of individuals assembling and interacting.

**Observation.** Two types of data were collected from the ABM for testing and validation. Collective cell and ECM population outputs were collected at each time point or tick. This was to be compared to widely accepted population dynamics in the wound healing literature [129]. Collective chemical populations were sampled at 4 time points: baseline, immediately following phonatory loading, 4-hr following treatment and 24 hours post baseline. This sampled data was compared to laryngeal secretions collected in an empirical study following the same initial, loading and treatment conditions [1].

### 2.1.7 Initialization

The VFABM initialization reflects the number and spatial distribution of cells and ECM proteins of average healthy adult VFLP tissue in the absence of phonotraumatic perturbation (Table 2–3). State variables of cells, ECM and patches are set according to user inputs. Chemicals are uniformly distributed with collective population reflecting baseline laryngeal secretions (no loading). Unlike cell and ECM protein initialization, this may vary among simulations and are chosen to reflect patient-specific baseline measurements. Tick 0 represents time immediately following an acute phonotraumatic event. This includes injury-related ECM catabolism (conversion of *collagen*, *elastin*, *HA* to their *fragmented* form), exudation of *platelets* to and accrue of *damage* on *patch* entities within the wound site. System trajectories following tick 0 correspond to subsequent treatment, inflammation and wound healing response.

### 2.1.8 Input Data

The model uses input from data files for model initialization. This input data includes patient-specific collective chemical levels (*TNF- $\alpha$* , *TGF*, *FGF*, *MMP8*, *IL-1 $\beta$* , *IL-6*, *IL-8*, *IL-10*), wound dimensions (*length*, *depth*, *severity*) and prescribed behavioral treatment (*voice rest*, *resonant voice*, *spontaneous speech*) from laryngeal secretions of individuals subjected to experimental phonotrauma up to 4 hrs post-injury [101].

### 2.1.9 Submodels

Three modules are constructed in the VFABM, including chemical diffusion, cell function, ECM function. As mentioned in section 2.1.4, there are four cell types

involved in inflammation and wound healing processes: *fibroblasts*, *macrophages*, *neutrophils* and *platelets*. The rules for each of these processes as well as cell agent subtypes constitute a sub-model in the VFABM. Details of these sub-models are presented in this section. A summary of the agent rules directing and flow chart illustrating the cellular sub-models can be found in Table 2–4 and Figure 2.3, respectively.

**Platelets.** In native tissue, *platelets* circulate through capillaries and blood vessels. Upon injury, *platelets* are rapidly deployed to the damage site whereby they modulate inflammatory processes through secretion of *cytokines* ( $IL-1\beta$ ,  $TGF$ ) and other *inflammatory mediators* ( $MMP8$ ). Platelets have a lifespan between 12 and 24 hours. This *life* state variable decreases with time until it reaches 0, at which time the *platelet* dies and is removed.

**Neutrophils.** Similar to platelets, in native vocal fold tissue *neutrophils* move randomly through blood capillaries where upon injury are recruited to the damage site. *Neutrophils* respond to pro-inflammatory stimuli by turning on their activation state variable. *Activated neutrophils* migrate along pro-inflammatory signal gradients, which triggers the pro-inflammatory kinase cascade which results in release of *pro-inflammatory cytokines* ( $TNF-\alpha$ ,  $MMP8$ ). *Neutrophils* have a lifespan between 12 to 20 hours. Like *platelets* this is represented with a *life* state variable. This rate of aging can change in response to mechanisms (removal of tissue debridement, high IL-10 levels) that can speed up apoptosis.

**Macrophages.** In native healthy tissue, *macrophages* move randomly through LP tissue and through capillaries. *Macrophages* represent both pro-inflammatory and

anti-inflammatory state signaling pathways (receptors, kinases, genes and transcription) that drive response to and release of chemicals during inflammation. Patch and chemical state variables contain information regarding pro-inflammatory stimuli sensed by *macrophages*. In the presence of pro-inflammatory stimuli (*damage*, *TNF- $\alpha$* , *IL-1 $\beta$* , *IL-6*, *IL-8*), *macrophages* migrate towards the site of inflammation whereby they enter an activated state and release both pro-inflammatory and anti-inflammatory mediators (*TGF- $\beta$* , *IL-10*). High pro-inflammatory stimuli activate negative and positive feedback control systems resulting in increased production of anti-inflammatory cytokines and inhibiting production of pro-inflammatory cytokines. *Macrophages* originating in blood have a life span between 8 and 70 hours while those originating in tissue have one from 60 to 120 days.

**Fibroblast.** *Fibroblasts* are located throughout the LP, predominantly within the superficial layer or in regions withstanding high mechanical stress. In the absence of damage or inflammatory signal they move following a Brownian motion and maintain natural ECM turnover. In the presence of necrosed or damaged tissue, they enter a proliferative state where, based on the local environment (*TNF*, *TGF*, *FGF*, *IL-1 $\beta$* , fragmented HA on surrounding neighbor patches), they have an increased probability of proliferating. If they are within close proximity to the *wound*, *fibroblast* cells will migrate along any *TGF* gradients as opposed to Brownian motion. Low *TGF- $\beta$*  promotes the probability of fibroblasts entering an *activated state*. *Activated fibroblast* are responsible for maintaining the distribution of protein and interstitial molecules. In addition to making tropocollagen, tropoelastin and HA molecules,

fibroblasts synthesis pro-inflammatory(*TNF- $\alpha$* , *IL-6*, *IL-8*) and anti-inflammatory chemicals (*TGF- $\beta$* , *IL-10*).

**Extracellular Matrix.** *Extracellular matrix*(ECM) individuals represent all structural and regulatory proteins that makeup a cells microenvironment. These include *monomer*, *polymer and fragmented* forms of each *collagen and elastin* as well as polymer and fragmented forms of *HA*. Activated fibroblasts make monomers of the proteins or *tropocollagen*, *tropoelastin and HA*. Above a given threshold tropocollagen and tropoelastin monomeric units form collagen and elastin polymers respectively.

*Collagen, elastin and HA* can undergo accelerated catabolism to form fragmented form following high impact stress or high local TNF concentration. Additionally, collagen catabolism can be further accelerated for high local MMP8 concentrations.

**Chemical Diffusion.** In the VFABM, cells act as a source of cytokines and growth factors. These chemicals diffuse from their source creating chemical gradients to attract and facilitate directed migration of inflammatory cells to site of phonatory damage. Through the development of the VFABM, different numerical methods were explored to model diffusion in an attempt to increase accuracy and reduce computational load.

A generalized partial differential equation (PDE) for diffusion in 2-dimension (2D) is stated as

$$\frac{\partial \rho(x, y, t)}{\partial t} = D \left( \frac{\partial^2 \rho(x, y, t)}{\partial x^2} + \frac{\partial^2 \rho(x, y, t)}{\partial y^2} \right), \quad (x, y, t) \in [a, b] \times [c, d] \times [0, T]. \quad (2.1)$$

with initial conditions

$$\rho(x, 0) = \rho_0(x) \tag{2.2}$$

and boundary conditions

$$\rho(a, t) = g_a(t), \tag{2.3}$$

$$\rho(b, t) = g_b(t) \tag{2.4}$$

where  $t$  is a time variable,  $x$  and  $y$  are state variables,  $\rho(x, t)$  is an function satisfying the equation,  $D$  is the diffusion coefficient and  $u_0, g_a, g_b$  are continuous functions. With the imposed initial conditions (equation 2.2) and boundary conditions (equation 2.3, 2.4) there exists a unique solution to equation 2.1. A numerical solution can be found using finite difference schemes to approximate solutions to the PDE. There are three basic classes of schemes for approximating  $\rho_x$ : forward, backward and central difference approximation.

Previous versions of the VFABM on the software system Netlogo [168], used its built in diffusion library to simulate transient and steady-state distribution of chemicals [167]. Simply, for each call of the NetLogo diffusion model every patches diffuse 50% of its chemicals equally to its 4 neighbouring patches. This method is advantageous in its simplicity and being not computationally intensive. Additionally, this scheme can simulate high spatial resolution with no restriction on time-step. This scheme is however limited in terms of its accuracy. Computational speed ups achieved using lower level programming language (C++) and parallelization (OpenMP), provided an opportunity to implement a more computationally intensive but more accurate scheme of chemical diffusion.

An explicit FTCS (forward in time, central in space) finite difference discretization was chosen. For a set of grid points in the domain  $S(x,y,t) = [a, b] \times [c, d] \times [0, T]$  are defined as having a state step size  $\Delta x = \frac{b-a}{N}$  and  $\Delta y = \frac{d-c}{N}$  where a set of horizontal and vertical lines across S yield intersection points  $(x_i, y_j, t_n)$ . A time step size is chosen  $\Delta t = \frac{T}{M}$  or  $t_n = n\Delta t, n = 0, \dots, M$ . The FTCS of equation 2.1 is

$$\frac{\rho_{i,j}^{n+1} - \rho_{i,j}^n}{\Delta t} = D \left( \frac{\rho_{i+1,j}^n - 2\rho_{i,j}^n + \rho_{i-1,j}^n}{\Delta x^2} + \frac{\rho_{i,j+1}^n - 2\rho_{i,j}^n + \rho_{i,j-1}^n}{\Delta y^2} \right), \quad (2.5)$$

where  $\rho(i, j, n) = \rho_{i,j}^n$ . For  $\alpha = D\Delta t/\Delta x^2$  and  $\beta = D\Delta t/\Delta y^2$ , a harmonic ansatz  $\epsilon_{i,j}^n = g^n e^{i(k_x x_i + k_y y_j)}$  can be used to analyze the diffusion equation, giving an amplification factor  $g(k)$ :

$$g(k) = 1 - 4\alpha \sin^2 \frac{k_x \Delta x}{2} - 4\beta \sin^2 \frac{k_y \Delta y}{2}. \quad (2.6)$$

A stable solutions holds true for

$$\alpha + \beta \leq \frac{1}{2}, \quad (2.7)$$

whereby the stability condition on time step is

$$\Delta t \leq \frac{\Delta x^2 \Delta y^2}{2D(\Delta x^2 + \Delta y^2)}. \quad (2.8)$$

For the case  $\Delta x = \Delta y$ , the stability condition reads:

$$\Delta t \leq \frac{\Delta x^2}{4D\Delta x^2}. \quad (2.9)$$

An explicit FTCS finite difference is relatively simple, computationally fast and is first-order accurate in time and second-order in space with its main drawback being that it must satisfy stability conditions which limit time step size. Alternative schemes, second order accurate in time and space, such as Crank-Nicholson are significantly more computationally and time intensive. Given diffusion is already one of the computational bottlenecks, these schemes are not ideal. Similarly, implicit schemes such as FTBS (forward in time, backward in space) while having no restrictions on time steps, are only first-order accurate in time and space where larger time steps generate inaccurate solutions. Alternative numerical methods to further decrease work complexity using a FFT-based convolution diffusion on a graphics processing unit (GPU) concurrently with central processing unit (CPU) threads are currently being explored [141].

## 2.2 Hyaluronic Acid-Gelatin Tissue Scaffold Agent Based Model

The Hyaluronic Acid-Gelatin Tissue Scaffold ABM (HGABM) is an extended version of the VFABM with additional agent rules. This section will provide an overview of difference in work flow and logic than that of the VFABM outlined in Section 2.1.

### 2.2.1 Purpose

The HGABM is used to simulate cellular level dynamics of new tissue formation and remodeling processes in a PEGDA crosslinked thiol-modified HA-Gtn hydrogel for vocal fold reconstruction. The HGABM aims to couple hydrogel parameters with viscoelastic, biochemical properties and cellular proliferative/synthesis response. The goal is to predict cellular phenotype over time to help identify the most significant hydrogel parameters for design optimization.

### 2.2.2 Programming Environment

The model was implemented on the same platform and programming languages as described in section 2.1.2.

### 2.2.3 Scale and Environment

The HGABM represents a 3D HA-Gtn hydrogel construct seeded with vocal fold fibroblasts (Table 2-3). Similar to the VFABM, the space is discretized into  $0.015\text{ mm} \times 0.015\text{ mm} \times 0.015\text{ mm}$  patches. The dimensions of the *world* is  $3\text{ mm} \times 3\text{ mm} \times 3\text{ mm}$ . However, given constraints in computational complexity and execution time the *world* structure was limited to a subset of the entire world, representing  $0.6\text{ mm} \times 0.6\text{ mm} \times 0.6\text{ mm}$ . Each *tick* or time step represented 30 minutes while the entire time course of the simulation was set at 9 days.

## 2.2.4 Entities, State Variables and Scales

As mentioned previously, the HGABM is an extension of the VFABM. Many of its entities and state variables are a subset of those in the VFABM (Section 2.1). The HGABM contains five different agent classes: *world*(environment), *patches* (spatial unit), *chemicals* (spatial unit), *ECM* (spatial unit), *cell* (individual) and *agent populations* (collective). Although a large number of state variables are the same as those in the VFABM, there are some differences (Table 2–1). Variables related to behavioral treatment, wound and capillary are no longer applicable. Attributes related to macrophage, neutrophil or platelet cell agent type are not included while additional patch attribute type HA-Gtn and associated mechanical and biochemical properties were added.

## 2.2.5 Process Overview and Scheduling

The HGABM follows the same process and scheduling as the VFABM (Section 2.1.5) as outlined in Algorithm 1. Additional agent rules integrating cell signalling from scaffold viscoelastic and biochemical properties are summarized in Table 2–5 and illustrated in Figure 2.4.

## 2.2.6 Design Concepts

**Basic Principles.** Tissue scaffolds mimic the ECM of native tissue encouraging cell attachment, migration, delivery/diffusion of biochemical factors and exert mechanical and biological influences to direct cell behavior for 3D tissue formation. Similar to inflammation and wound healing *in vivo*, this requires a signaling network of cell response to HA-Gtn and production of inflammatory signaling molecules

(chemical, ECM proteins). Empirical calibration and validation may provide insights how variations in scaffold composition can influence tissue formation *in vitro*.

**Emergence.** Similar to the VFABM, collective agent populations emerge from traits and behaviors of individuals. Cell and ECM proteins populations are expected to vary in complex and unpredictable ways in response to changes in individual characteristics or environment to reflect formation of new functional tissue. Collective chemical populations are more tightly imposed to reflect changing culture media and less dependent on individual behaviors.

**Adaptation.** Cells have similar adaptive traits outlined as outlined in the previous section. These traits reflect different phenotypic states fibroblasts can enter.

**Learning, Objectives and Prediction.** Individual agents do not learn from experience nor change adaptive traits over time.

**Sensing.** Agents' ability to sense state variables of nearby agents is the same as those in the VFABM (Table 2–2).

**Interaction.** Cell-ECM and cell-chemical interactions are assumed direct and achieved through sensing while cell-cell interactions are indirect via production of chemical mediators.

**Stochasticity.** Activation, deactivation, death, proliferation and ECM synthesis processes within the cell submodel are modeled as partly random to introduce variability.

**Collectives.** Collagen and fibroblast cell agents form collective aggregation indicating assembly and interaction of individuals during new tissue formation.

### 2.2.7 Initialization

The initial state of the model world represents a fibroblast seeded 3D HA-Gtn scaffold submerged in culture media for 24 hours (Table 2–3). The initialization remains the same among simulations although initial patch state variables corresponding to scaffold composition may vary among simulations according to input data.

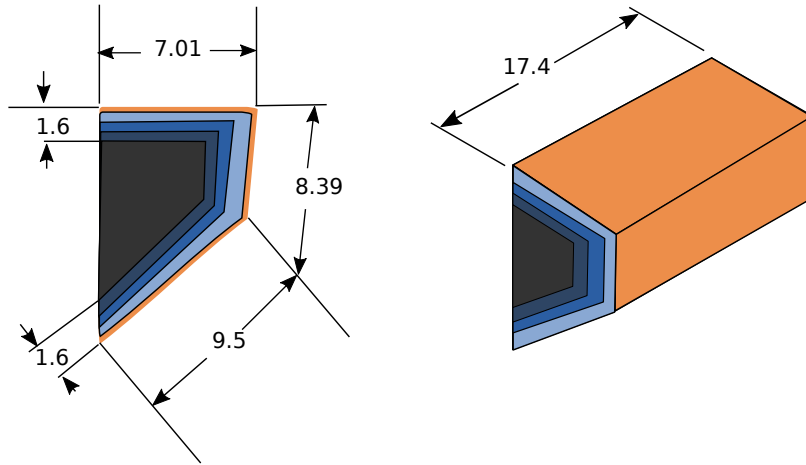
### 2.2.8 Input Data

The model uses input from external data files to direct model initialization. The input data include culture media collective levels, half lifes and diffusivity constants of chemical agents ( $TNF-\alpha$ ,  $TGF$ ,  $FGF$ ,  $MMP8$ ,  $IL-1\beta$ ,  $IL-6$ ,  $IL-8$ ,  $IL-10$ ), number of immortalized cells (*fibroblast*), volume of 1% (w/v) HA, volume of 1% (w/v) Gtn, volume of 1.67% (w/v) PEGDA.

### 2.2.9 Submodels

The fibroblast, ECM and diffusion submodels outlined in Section 2.1.9 in the VFABM remain the same in the HGABM.

**A**



**B**

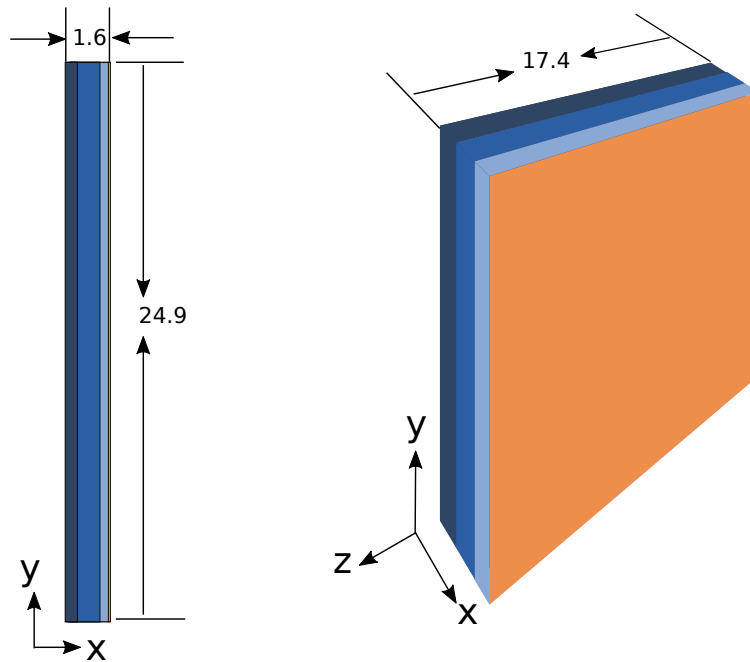


**Figure 2.1:** Three dimensional rendering of (a) vocal fold (b) Vocal Fold Agent Based Model.

All units in millimeters.

**Table 2–1** Vocal Fold ABM and HA-Gtn ABM agents and state variables.

	<b>Vocal Fold ABM</b>	<b>HA-Gtn ABM</b>
<b>Agent</b>	<i>State Variables</i>	<i>State Variables</i>
<b>World</b>	Length	Length
	Width	Width
	Height	Height
	Clock	Clock
	Treatment (Voice Rest, Resonant Voice, Spontaneous Speech)	-
	Wound (Length, Depth, Severity)	-
<b>Patch</b>	Health	Health
	Type (Tissue, Epithelium, Capillary)	Type (HA-Gtn, Tissue)
	Spatial Coordinates	Spatial Coordinates
	Occupancy (None, Fibroblast Macrophage, Neutrophil, Platelet)	Occupancy (None, Fibroblast)
	Damage	Damage
	-	Composition(PEGDA, HA, Gtn conc)
	-	Elastic Modulus
	-	Crosslink Density
	-	Swelling Ratio
	-	Mass Loss
-	Pore Width	
<b>Chemical</b>	Chemical concentration(TNF, TGF, FGF, MMP8, IL1 $\beta$ , IL6, IL8, IL10)	Chemical concentration(TNF, TGF, FGF, MMP8, IL1 $\beta$ , IL6, IL8, IL10)
	Chemical Diffusion coefficient	Chemical Diffusion coefficient
	Fibroblast chemogradient (TGF)	Fibroblast chemogradient (TGF)
	Macrophage chemogradient (IL1 $\beta$ , TNF, TGF, FGF, IL6, IL8, frag. collagen)	-
	Neutrophil chemogradient (IL1 $\beta$ , TNF, TGF, FGF, frag. elastin)	-
<b>ECM</b>	tropocollagen content	tropocollagen content
	Collagen content	Collagen content
	Frag. collagen content	Frag. collagen content
	tropoelastin content	tropoelastin content
	Elastin content	Elastin content
	Frag. elastin content	Frag. elastin content
	HA content	HA content
	Frag. HA content	Frag. HA content
<b>Cell</b>	Age	Age
	Type (Fibroblast, Macrophage, Neutrophil, Platelet)	Type (Fibroblast)
	Location	Location
	Activation State	Activation State
	Origins (Blood or tissue)	-
	-	Migration Speed

---

**Algorithm 1** Overview of Vocal Fold Acute Phonotrauma ABM.

---

```
1: procedure VFABM
2:   Initialization of patches
3:   Initialization of chemicals
4:   Initialization of cells
5:   Initialization of ECM
6:   Initialization of damage
7:   while  $time \leq 1day$  do
8:     Diffuse Chemicals
9:     Cell Function
10:    ECM Function
11:    Update Attributes      ▷ Cell, ECM, Patch and Chemical Attributes
12:  return
```

---

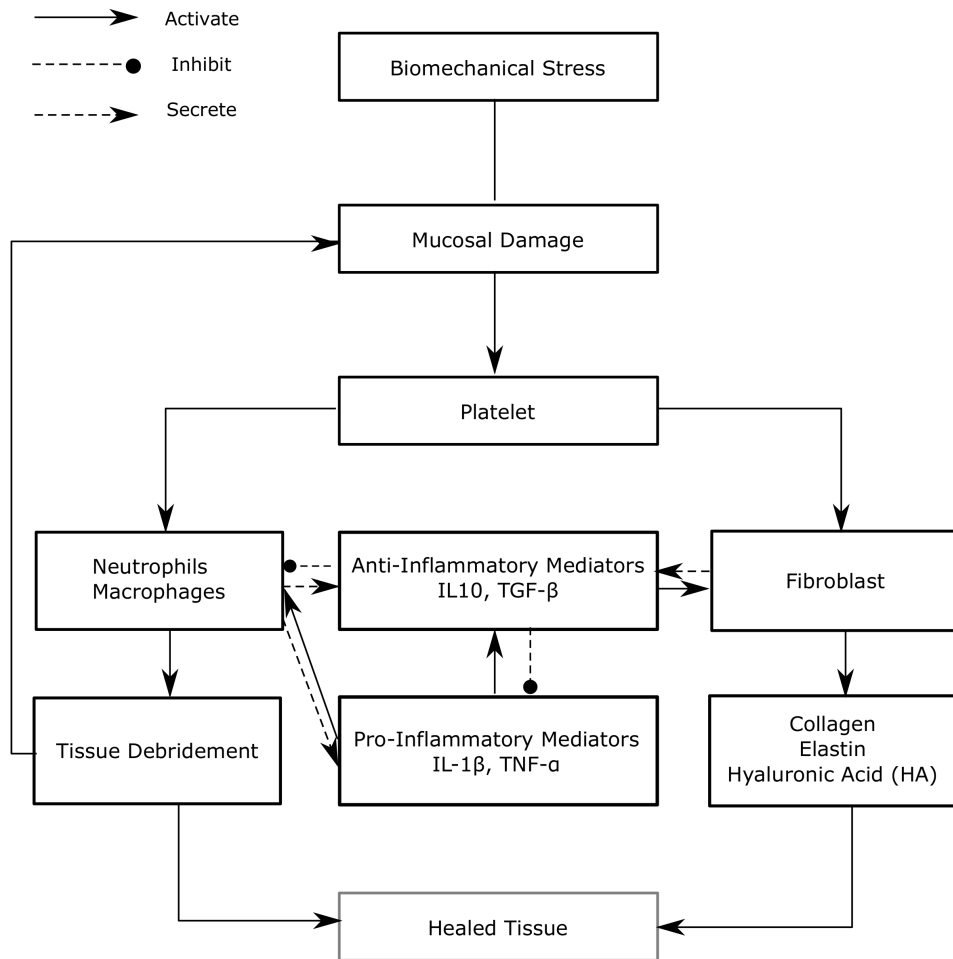


**Figure 2.2:** Flowchart of Vocal Fold Agent Based Model.

Modified from [102].

**Table 2–2** Vocal Fold and HA-Gtn ABM agent sensing abilities.

		Agent Class				
		World	Patch	Chemical	ECM	Cell
	<i>State Variables</i>					
<b>World</b>	Length	x				x
	Width	x				x
	Height	x				x
	Clock	x				x
	Treatment (Voice Rest, Resonant Voice, Spontaneous Speech)	x				x
<b>Patch</b>	Health		x		x	x
	Type (Tissue, Epithelium, Capillary)		x	x	x	x
	Spatial Coordinates		x	x	x	x
	Occupancy (None, Fibroblast, Macrophage, Neutrophil, Platelet)		x			x
	Damage	x	x		x	x
	Composition(PEGDA, HA, Gtn conc)		x			
	Elastic Modulus		x			x
	Crosslink Density		x			
	Swelling Ratio		x	x		
	Mass Loss		x			
	Pore Width		x			x
	<b>Chemical</b>	Chemical concentration(TNF, TGF, FGF, MMP8, IL1 $\beta$ , IL6, IL8, IL10)	x		x	
Chemical Diffusion coefficient				x		x
Fibroblast chemogradient (TGF)				x		x
Macrophage chemogradient (IL1 $\beta$ , TNF, TGF, FGF, IL6, IL8, frag. collagen)				x		x
Neutrophil chemogradient (IL1 $\beta$ , TNF, TGF, FGF, frag. elastin)				x		x
<b>ECM</b>	tropocollagen content	x			x	
	Collagen content	x			x	
	Frag. collagen content	x			x	x
	tropoelastin content	x			x	
	Elastin content	x			x	
	Frag. elastin content	x			x	x
	HA content	x			x	x
	Frag. HA content	x			x	x
<b>Cell</b>	Age					x
	Type (Fibroblast, Macrophage, Neutrophil, Platelet)	x	x			x
	Location		x			x
	Activation State	x				x
	Origins (Blood or tissue)					x
	Migration Speed					x

'x' represents state variables of local agents each agent class can perceive and consider in decisions.

**Table 2–3** Vocal Fold ABM and HA-Gtn ABM initialization.

Parameter	Vocal Fold ABM		HA-Gtn ABM	
	<i>Default Value</i>	<i>Units</i>	<i>Default Value</i>	<i>Units</i>
<b>Time Scale</b>				
Time Step	0.5	Hours	0.5	Hours
Time Horizon	24	Hours	216	Hours
<b>World Dimensions</b>				
Length	24.9	mm	3	mm
Width	1.6	mm	3	mm
Height	17.4	mm	3	mm
<b>Lamina Propria Morphology</b>				
LP Wet Weight	1	g ww		
Epithelium Thickness	0.05	mm		
Capillary Radius	0.045	mm		
SLP width	13	% of width		
ILP width	51	% of width		
DLP width	36	% of width		
<b>Cellularity</b>				
Fibroblast	16.4	10 <sup>6</sup> per g ww	1	10 <sup>6</sup> cells/mL
Macrophage	1.3	10 <sup>6</sup> per g ww		
Myofibroblast	3.1	10 <sup>6</sup> per g ww		
Neutrophil	2.3	10 <sup>6</sup> per g ww		
<b>Behavioral Therapy Treatment</b>				
Voice Rest Vibratory Stress (VRVS)	0	AU		
Voice Rest Impact Stress (VRIS)	0	AU		
Resonant Voice Vibratory Stress (RVVS)	5	AU		
Resonant Voice Impact Stress (RVIS)	10	AU		
Spontaneous Speech Vibratory Stress (SSVS)	10	AU		
Spontaneous Speech Impact Stress (SSIS)	10	AU		

**Table 2–4** Overview of chemical agent rules.

Chemical Agent	Cell Agent Source		Function in ABM
	VFABM	HGABM	
TGF- $\beta$ 1	Fibroblasts Macrophages Neutrophils	Fibroblasts	Inhibit expression of TNF- $\alpha$ in fibroblasts Activate resting fibroblasts Mitogenic to fibroblasts (proliferation) Chemotactic to fibroblasts
bFGF	Fibroblasts Macrophages	Fibroblasts	Mitogenic to fibroblasts (proliferation) Stimulate fibroblast migration
TNF- $\alpha$	Fibroblasts Macrophages Neutrophils	Fibroblasts	Stimulate fibroblast expression of TGF- $\beta$ Mitogenic to fibroblasts (proliferation) Stimulate fibroblast expression of IL-6 Induce tissue damage
IL-1 $\beta$	Macrophages Platelets		Mitogenic to fibroblasts (proliferation)
IL-6	Fibroblasts Macrophages	Fibroblasts	Stimulate collagen synthesis in fibroblasts
IL-8	Fibroblasts Macrophages	Fibroblasts	Inhibit collagen synthesis in fibroblasts
IL-10	Macrophages		Inhibit expression of TNF- $\alpha$ in fibroblasts Inhibit expression of IL-6 and IL-8 in fibroblasts Stimulate fibroblast expression of TGF- $\beta$ Inhibit activation of neutrophils and macrophages
MMP-8	Platelets Neutrophils		Degrades collagen to produce collagen fragments
Collagen	Fibroblasts	Fibroblasts	Repair tissue damage
Elastin	Fibroblasts	Fibroblasts	Repair tissue damage
HA	Fibroblasts	Fibroblasts	Repair tissue damage Inhibit expression of TNF- $\alpha$ and IL-8 in fibroblasts Fragments are mitogenic to fibroblasts (proliferation)

Adapted from [102]. Refer to Appendix A Figure A1 for full list of agent rules.

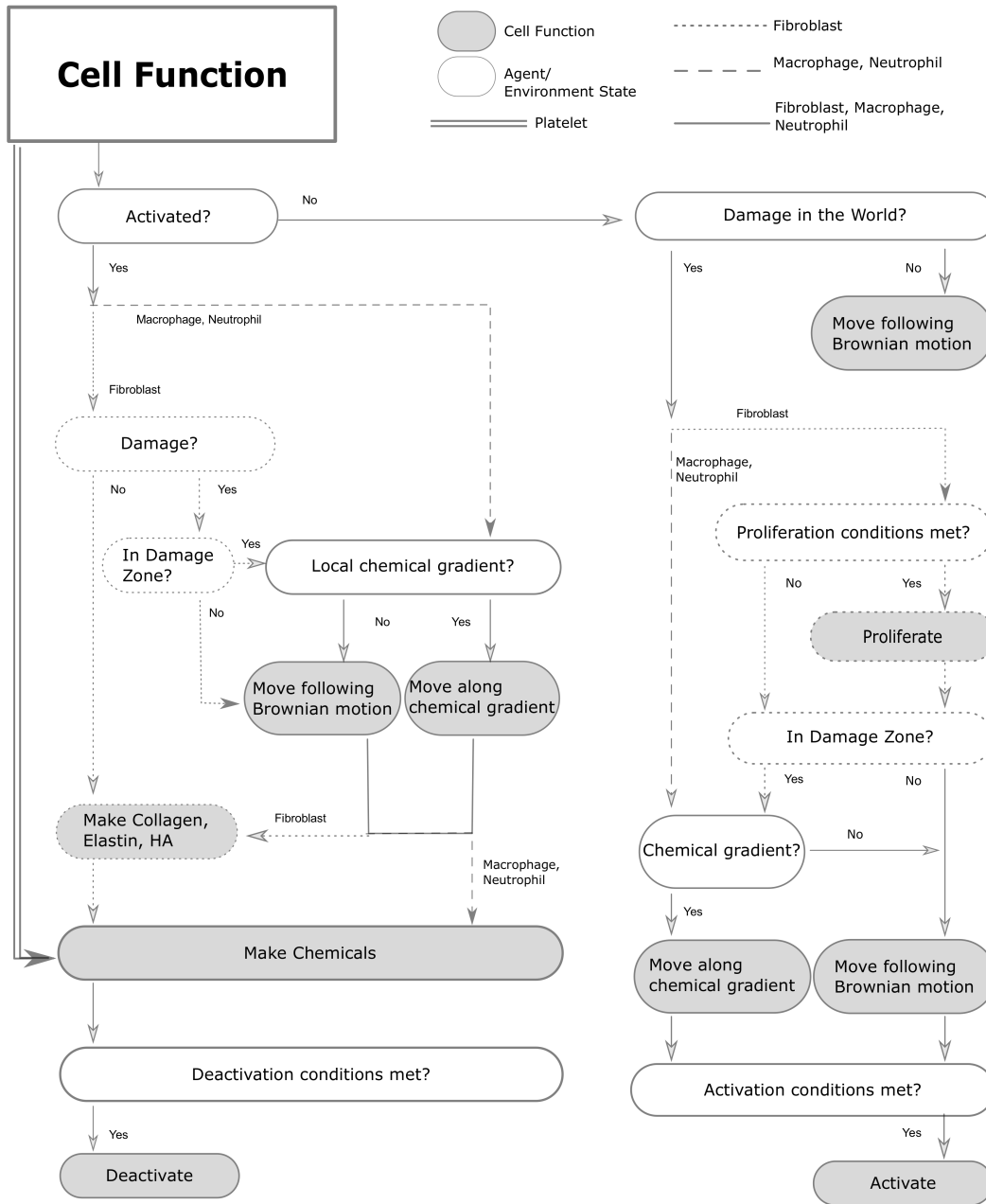


**Figure 2.3:** Flowchart of cell function.

**Table 2–5** Overview of HA-Gtn Agent Based Model agent rules.

Design Parameter	Scaffold Properties	Function in ABM
↑ Total Protein (% w/v) ↑ HA (% w/w) ↑ PEGDA (% w/w)	↑ Elastic Modulus (Pa)	Decreases Vocal Fold Fibroblast migration speed Increases fibroblast synthesis rate of collagen, elastin and HA
↓ Thiol:Double Bond	↑ Crosslinking density (mmol/mL)	Increase in shear modulus
↑ HA (% w/w) ↑ Time (Hours)	↑ Swelling Ratio (w/w)	Increased retention of water and diffusion of oxygen and nutrients
↑ HA (% w/w) ↑ Time (weeks)	↑ Mass Loss Fraction (%)	Instable hydrogel degrades, replaced with cell-synthesized ECM proteins
↓ HA (% w/w)	↑ Pore Size ( $\mu\text{m}$ )	Decreases fibroblast synthesis rate of collagen, elastin and HA

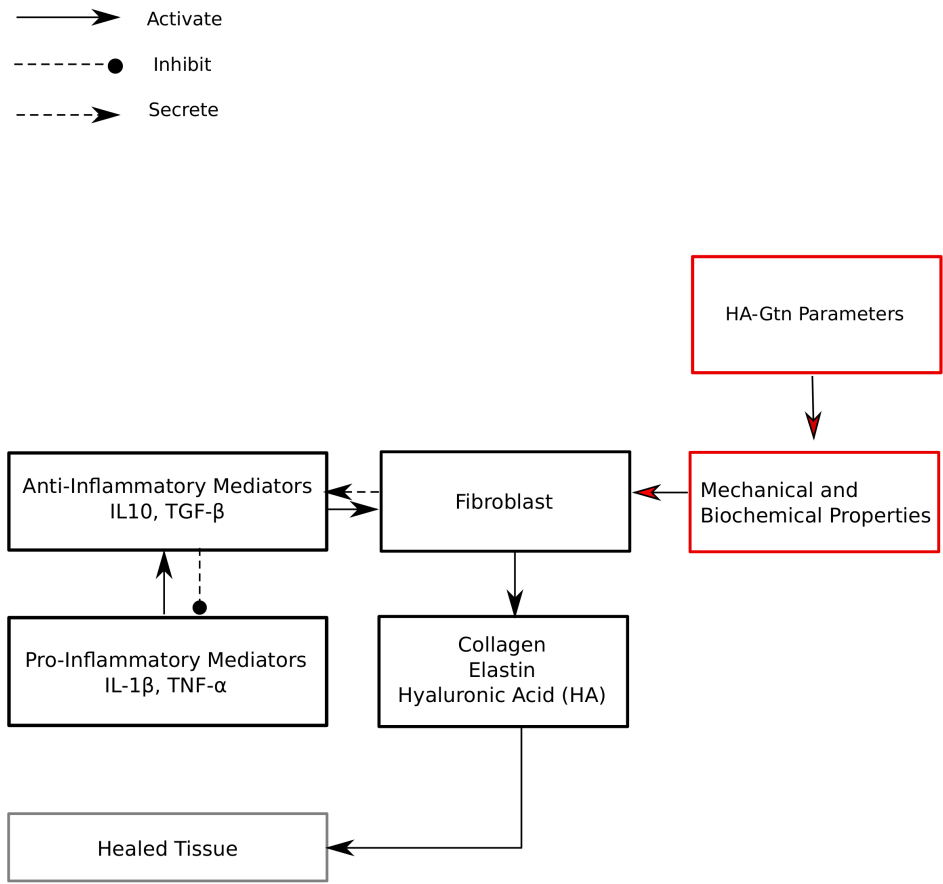


**Figure 2.4:** Flowchart of HA-Gtn Agent Based Model.

Modified from [102].

### 2.3 Agent Based Model Analysis for Verification and Validation

The above proposed VFABM (Section 2.1) has 213 model parameters to be considered for model calibration (Table 2–6). Given the time and labour intensive nature, manual or human-guided exploration of parameter and solution space is infeasible. Systematic, automated and unbiased approaches can greatly simplify this exploration strategy [97]. Sensitivity analysis (SA) refers one type of systematic input-output space exploration to identify parameters for which small variations most impact model output. This can then be used to perform factor fixing or reduction of insensitive parameters to numerical constants is often used to reduce model dimensionality allowing for improved model accuracy, reduction of output variance and model simplification. There exist different SA methods, best suited according to model complexity, simulation time and range of parameter space to be explored (Figure 2.5). A few sophisticated sensitivity analysis methods for solution-space exploration have been applied to ABMs [77]. These include one-parameter-at-a-time (OAT), standardized regression coefficients and variance-based decomposition [153, 77]. Each of these methods are best suited to different SA aims as outlined in Table 2–7.

Variance-based methods are advantageous in cases of non-linear, non-monotonic models with interaction among factors that require full range of factor variation. However its major disadvantage is computational load from requirement of a large number of model evaluations (Table 2–8, Figure 2.5). Consequentially for high dimensional and non-linear models, OAT and variance-decomposition methods are commonly used in combination for comprehensive quantitative analysis with reduced

computational load. In the current study, OAT-based Morris and variance-based Sobol sensitivity analyses were used for solution-space exploration of the ABM, with the purpose of identifying of insensitive parameters for factor fixing and model simplification prior to model calibration.

### 2.3.1 Morris Parameter Screening

The Morris method is a randomized OAT SA method. It is both an efficient and robust technique for identifying and ranking important variables. The Morris method can be used to classify variables into one of three groups: inputs with negligible effects, inputs with large linear effects and inputs with large non-linear and/or interaction effects. The assumption of the Morris method is that for small changes in variable values, variables that yield the largest variation in the model output are the most important. This is evaluated by modifying each variable individually, changing the variable value incrementally between pairs of model simulations. Experiments and variation direction in the input space are chosen at random. These form sampling trajectories through space where several trajectories are chosen to adequately span the parameter and solution space. From the repeated sampling, elementary effects for each input can be estimated from which sensitivity indices are derived.

For a generalized model

$$y = f(X) \tag{2.10}$$

where  $X = (x_1, x_2, \dots, x_k)$  is an array of input factors under consideration. Varying the input factors across  $n$  selected levels,  $Y$  is the corresponding model output time series or objective function. The elementary effect of its  $i$ -th parameter can be estimated by changing the  $i$ -th parameter with step  $\Delta$  while keeping all other

parameters unchanged.  $E_i(X^j)$  is the elementary effect of the  $i$ -th variable at the  $j$ -th repetition, defined by

$$E_i(X^j) = \frac{Y(x_1, \dots, x_i + \Delta, \dots, x_k) - Y(x_1, \dots, x_i, \dots, x_k)}{\Delta}, \quad (2.11)$$

where  $\Delta$  is the magnitude of step and multiple of  $\frac{1}{n-1}$ ,  $n$  is the number of levels,  $(x_1, \dots, x_i + \Delta, \dots, x_k)$  and  $(x_1, \dots, x_i, \dots, x_k)$  are random sample sets within the defined  $n$  dimensional hypercube space. There are three major sensitivity metrics from the elementary effects: mean of the absolute value ( $\mu_i^*$ ), mean ( $\mu_i$ ) and standard deviation ( $\sigma_i$ ). These are given by

$$\mu_i^* = \frac{1}{r} \sum_{j=1}^r |E_i(X^j)|, \quad i = 1, \dots, k, \quad (2.12)$$

$$\mu_i = \frac{1}{r} \sum_{j=1}^r E_i(X^j), \quad i = 1, \dots, k, \quad (2.13)$$

and

$$\sigma_i = \frac{1}{r} \sum_{j=1}^r V(E_i(X^j)), \quad i = 1, \dots, k \quad (2.14)$$

where  $k$  is the number of input factors,  $r$  is the number of randomly sampled trajectories (between 4 and 10 [134]),  $\mu_i$  is a measure of the average direction of dependence of model output on the  $i$ -th feature. A positive  $\mu_i$  value reflects positive correlations between feature and output while negative values reflect negative correlations. In the case where the distribution contains negative elements, the mean may not be very useful because of self-cancellation. Thus when ranking overall factor influence on the output, the mean of the absolute value ( $\mu_i^*$ ) must be considered. For  $\mu_i^*$  equal

to zero, represents zero dependence of output on the  $i$ -th feature is suggested. Additionally, if  $\mu_i^*$  and  $\mu_i$  are equal, the output is understood to have a linearly monotonic dependency on the  $i$ -th feature. The  $\sigma_i$  reflects any non-linear interaction effects of the  $i$ -th feature with other factors. For zero value  $\sigma_i$ , a feature is said to have a linearly dependency while a magnitude equal to  $\mu_i^*$  or coefficient of variance ( $\sigma_i/\mu_i^*$ ) reflect high non-linearity.

### 2.3.2 Sobol Sensitivity Analysis

Sobol is a Monte Carlo variance-based sensitivity analysis method which assigns Sobol sequences such that successive points are chosen with prior knowledge of previously sampled points. It uses a Sobol quasi-random sequence generator to produce a uniformly distributed set of points in the N-dimensional unit cube [75]. This method outperforms crude Monte Carlo sampling methods in the case of multi-dimensional exploration, especially in the case of ABM [92].

Sobol sensitivity measures are based on the decomposition of variance ( $V$ ) of model output,  $y$ . For a generalized model (Equation 2.10), the Hoeffding decomposition [7] can be used for functional decomposition into constituent components using

$$f = f_0 \sum_i f_i + \sum_i \sum_{j>i} f_{ij} + \dots + f_{12\dots k} \quad (2.15)$$

where  $f_i = f_i(X_i)$ ,  $f_{ij} = f_{ij}(X_i, X_j)$  for a total of  $2^k$  terms. The constituent components are obtained from

$$\begin{aligned} f_0 &= E(Y), \\ f_i &= E_{X_i}(Y|X_i) - E(Y), \\ f_{ij} &= E_{X_{ij}}(Y|X_i, X_j) - f_i - f_j - E(Y). \end{aligned} \tag{2.16}$$

The Sobol method postulates the variance of model output  $y$  can be decomposed using

$$V = \sum_i V_i + \sum_i \sum_{j>i} V_{ij} + \dots + V_{1,2,\dots,k}, \tag{2.17}$$

where

$$V_i = V_{X_i}[E_{X_i}(Y|X_i)], \tag{2.18}$$

$$V_{ij} = V_{X_i, X_j}(E_{X_{ij}}(Y|X_i, X_j) - V_i - V_j) \tag{2.19}$$

Here  $V(\cdot)$  is variance,  $E(\cdot)$  is expectation,  $V_{X_i}[E_{X_i}(Y|X_i)]$  is the expected reduction in variance for fixed  $X_i$  and  $V_{X_i, X_j}(E_{X_{ij}}(Y|X_i, X_j) - V_i - V_j)$  is the expected reduction in variance for fixed  $X_i$  and  $X_j$ . Normalizing equation 2.17 by the unconditional output variance  $V$  yields

$$1 = \sum_i S_i + \sum_i \sum_{j>i} S_{ij} + \dots + S_{1,2,\dots,k}. \tag{2.20}$$

The sensitivity metrics can be defined as

$$S_i = \frac{V_i}{V}, 1 \leq i \leq k, \tag{2.21}$$

and

$$S_{ij} = \frac{V_{ij}}{V}, 1 \leq i \leq k, \quad (2.22)$$

and similarly for higher orders. These can be used to determine two common sensitivity indices: the first order index or main effect ( $S_i$ ) and the total sensitivity index or total effect ( $S_{Ti}$ )

$$S_{Ti} = S_i + \sum_j S_{ij} + \sum_j \sum_k S_{ijk} + \dots \quad (2.23)$$

where  $S_i$  represents the average output variance reduction achieved when  $X_i$  is fixed and  $S_{Ti}$  represents the output variance for unknown  $X_i$  or total contribution of  $X_i$  to output variance [152]. The difference between  $S_{Ti}$  and  $S_i$  indicates the strength of variable interaction between the i-th and other factors.

While first order effects are weakly dependent on  $k$  and computationally economical, estimating higher order effects is strictly  $k$ -dependent and is very expensive (Table 2-8). Approaches such as using meta-modeling, emulators or sample-based have been used to estimate total sensitivity indices. The best estimator has been reported to be the Sobol Jansen estimator [132] (Table 2-9). Therefore it is the one used in the current study.

### 2.3.3 Sensitivity Index for Correlated Factors

In the Sobol sensitivity analysis method, inputs are assumed to be independent. As such, there exists a unique decomposition scheme, given by equation 2.15. In the case of dependent or correlated factors, the response variance for a given factor may be influenced by its dependence on other inputs. Consequently, it is misleading and difficult to interpret classical Sobol sensitivity indices for dependent variables.

Although it has been reported that the factor priority setting,  $V_j$ , constitutes a proper metric whatever the correlation and interaction structure of the model [133], it ignores possible emergent interaction effects. Alternatively, Saltelli and Tarantola [133] proposed an adjusted sensitivity index or figure of merit ( $M_j$ ) given by

$$M_j = S(R_j)(1 - \max_{j \in u} |c_{ij}|)(1 + \frac{VT_{NC}^j - V_{NC}^j}{V_{NC}})^2, \quad (2.24)$$

where  $R_j$  is the rank of candidate factor from sensitivity index  $S_j$ ,  $S(R_j)$  is a Savage score [137],  $c_{ij}$  is the correlation coefficient of factors  $X_i$  and  $X_j$ ,  $VT_i$  refers to the partial total order variance the  $i$ -th factor,  $V_i$  refers to the first order partial variance of the  $i$ -th factor,  $V$  refers to the unconditional variance of the output  $y$ ,  $NC$  refers to sensitivity indices for the the non-correlated case. The  $M_j$  coefficients act as a relative sensitivity metric adjusted for correlated parameters. It can be used in identification of smallest number of factors to fix to achieve a target reduction in output variance. This is achieved by penalizing a candidate factor proportional to the degree of correlation or prized depending on its interaction effects with other factors. The  $M_j$  have empirically been shown to be most effective when prize for interaction is squared [133]. The method proposed by Saltelli and Tarantola [133] of using  $M_j$  to quantitatively identify significant parameters for the correlated factor case involves the following four steps:

1. "Rank factors in order of importance using  $V_i$  to obtain a sequence  $V_{R1}, V_{R2}, \dots, V_{Rk}$  where  $V_{R1} > V_{R2} > \dots > V_{Rk}$ . If  $V_{R1} > V - V_{tar}$  where  $V_{tar}$  is the target reduction in variance,  $X_{R1}$  is identified as the only sensitive parameter. If not, continue to step 2

2. Compute the reduction in variance if  $X_{R1}$  and  $X_j$  are fixed ( $V_{R1j}$ ), where  $X_j$  is the factor that exhibits the highest figure of merit. If  $V_{R1j} > V - V_{tar}$ , then fixing factors  $(X_{R1}, X_j)$  would reduce the variance of  $Y$  to equal or smaller than the target variance. Otherwise go to step 3
3. Compute the reduction in variance if  $X_{R1}, X_j, X_m$  are fixed ( $V_{R1jm}$ ), where  $X_m$  is the factor that exhibits the next highest figure of merit. If  $V_{R1jm} > V - V_{tar}$ , then  $(X_{R1}, X_j, X_m)$  are the most significant parameters enabling  $V_{tar}$  reduction in unconditional variance.
4. Continue fixing additional factors in order of highest figure of merit until target reduction in variance is achieved.”

## 2.4 Model Calibration and Validation

All models are abstracted representations of real systems. While they the abstracted model and the real system are fundamentally different, abstracted models can still useful in their approximation of these real systems. It is important to define conditions under which these approximations are accurate and useful. This is accomplished through different model verification and validation methods. Model verification refers to if the model is implemented correctly while model validation refers to the accuracy and consistency in which a computerized model represents the system of study within its intended application.

### 2.4.1 Multivariate Calibration

One objective of this research project is to develop a model to predict patient-specific biomarker population dynamics and population response. Consequently, it should have the capacity to predict biomarker profiles that reflect both events of

real system inflammation and wound healing processes as well as inter-patient variability. Inter-patient variability may arise due to differences in vocal fold geometry, behavioral therapy compliance, variability in phonatory stress susceptibility and accumulation of acute inflammatory response. These factors contribute to the system and agent heterogeneity necessitating model calibration for accurate predictions.

Calibration is the systematic adjustment of model parameter estimates such that model outputs more accurately reflect real system benchmark biomarkers. The calibration steps include: 1) identify inputs, 2) identify calibration targets and 3) define goodness of fit. Top ranked parameters following sensitivity analysis (Section 2.3.1, 2.3.2 and 2.3.3) will be included in the calibration parameter set with the rest being fixed as constants. The calibration targets are cytokine measures from human patients following phonatory loading matching that of our treatment groups [1]. We define a goodness of fit to be minimizing the weighted mean percentage deviation ( $w$ ) between model and real system measures given by

$$w = \sum_{i=1}^n w_i \frac{y_i - y_i^*}{y_i^*} \quad (2.25)$$

where  $w_i$  is the weight assigned to the  $i$ -th endpoint,  $n$  is the number of endpoints,  $y_i$  is the model-based estimate of the  $i$ -th endpoint and  $y_i^*$  is the data-based target value of the  $i$ -th endpoint. For our purposes, we have three time points at 1, 4 and 24 hours with all time points weighted equally. The approach of minimizing deviations was chosen due to its ease of implementation as well as capture magnitude deviation.

### 2.4.2 Predictive Validation

Model validation is an essential step to ensure the clinical relevance of the model. Validation ensures that the model is sufficiently accurate. There exists various types of validation: data, white box, visual check and black box. In this study, black box validation methods were used where for a model under the same conditions (inputs) as the real world system, outputs should be sufficiently similar assuming there is accurate real world data. Although this approach does not guarantee absolute confidence for the currently limited data, it is a good first approximation. In the ABM, validation can be accomplished at three levels: the level of individual response (individual dynamic), the level of the behavior of a population with respect to intrinsic variables (population dynamic), and finally the behavior of the population with respect to an intervention (population response). In this study, we are interested in the population response as those are measurable behavior in voice clinical and our current benchwork.

Our verification and validation of the VFABM focused on predictive and simulation potential of model to simulating population dynamics and comparing results to trends in literature. Predictive capacity of the calibrated HGABM focused on population dynamics of collagen, fibroblast and total protein as well as response of these population to changes in initial conditions defined by HA-Gtn composition.

**Table 2–6** Overview of Vocal Fold Agent Based Model parameters.

Parameter	Nom.	Value	Range	Units
<b>behavioral Therapy Treatment</b>				
Resonant Voice vibratory stress	RVVS	5	[0.5, 50]	AU
Resonant Voice impact stress	RVIS	10	[1, 100]	AU
Spontaneous Speech vibratory stress	SSVS	10	[1, 100]	AU
Spontaneous Speech impact stress	SSIS	10	[1,100]	AU
<b>Acute Phonotrauma Processes</b>				
Platelet recruitment to tissue	$r_{tiss}^P$	20	[2, 200]	Cells
Neutrophil recruitment to capillaries	$r_{cap}^N$	1	[0.1, 10]	Cells
<b>Inflammation Cascade Initiation</b>				
High TNF threshold	$t_{TNF}$	10	[1, 100]	AU
High MMP8 threshold	$t_{MMP8}$	10	[1, 100]	AU
<b>Inflammation Processes</b>				
Neutrophil recruitment interval	$i_{cap}^N$	2	[0.2, 20]	Hours
Neutrophil recruitment	$r_{cap}^N$	8	[0.8, 80]	Cells
Damage-regulation neutrophil recruitment	$r^N$	0.01	[0.001, 0.1]	AU
Macrophage recruitment to capillary interval	$i_{cap}^M$	4	[0.4, 40]	Hours
Macrophage recruitment to capillary	$r_{cap}^M$	1	[0.1, 10]	Cells
Damage-regulated macrophage recruitment	$r^M$	0.01	[0.001, 0.1]	AU
Macrophage recruitment tissue interval	$i_{tiss}^M$	6	[0.6, 60]	Hours
Macrophage recruitment to tissue	$r_{tiss}^M$	1	[0.1, 10]	Cells
Fibroblast recruitment interval	$i_{tiss}^F$	12	[1.2, 120]	Hours
Fibroblast recruitment	$r_{tiss}^F$	1	[0.1, 10]	Cells
Damage-regulated fibroblast recruitment	$r^F$	0.01	[0.0001, 0.1]	AU
<b>Macrophage Inflammation and Wound Healing Processes</b>				
Probability of TNF-mediated activation	$a_{TNF}^{M+}$	100	[10, 1000]	%
Probability of deactivation	$a^{M-}$	3	[0.3, 30]	%
<b>Neutrophil Inflammation and Wound Healing Processes</b>				
Probability of TNF-mediated activation	$a_{TNF}^{N+}$	25	[2.5, 250]	%
Probability of deactivation	$a^{N-}$	0.01	[0.001, 0.1]	%
IL10 inhibition of viability	$d_{IL10}^N$	0.01	[0.001, 0.1]	AU
Probability of death	$d^N$	10	[1, 100]	%
<b>Fibroblast Wound Healing Processes</b>				
TGF stimulated proliferation	$p_{TGF}^F$	1	[0.1, 10]	AU
Probability of proliferation	$p_{\pm}^F$	25	[2.5, 250]	%
Probability of TGF-mediated activation	$a_{TGF}^{F+}$	50	[5, 500]	%
Probability of deactivation	$a^{F-}$	25	[2.5, 250]	%
Collagen synthesis interval	$e_{+}^{col}$	12	[1.2, 120]	Hours
Elastin synthesis interval	$e_{+}^{ela}$	12	[1.2, 120]	Hours
HA synthesis interval	$e_{+}^{HA}$	1	[0.1, 10]	Hours

Refer to Appendix B for list of chemical agent parameters.

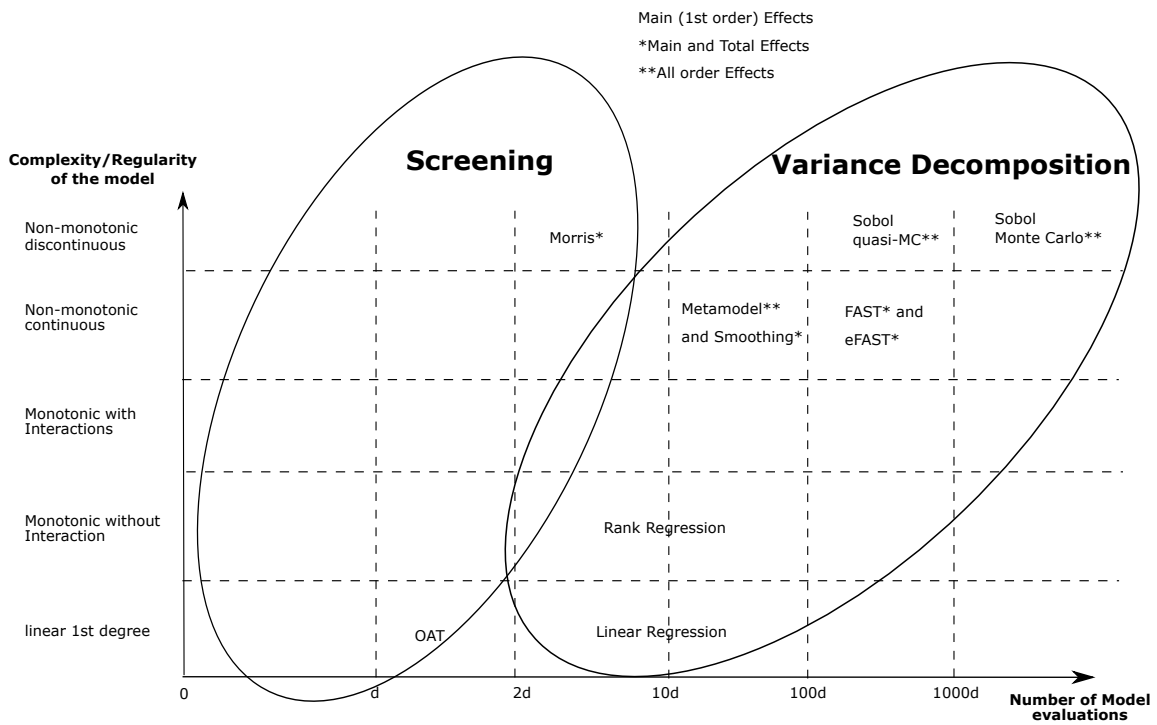


**Figure 2.5:** Complexity and applicability of sensitivity analysis methods.

Modified from [77].

**Table 2–7** Evaluation of sensitivity analysis methods with respect to analysis aims.

SA Type	Sensitivity Analysis Aim	Rating	Evaluation
OAT	Examine Patterns	+	Qualify effect of individual parameter changes on emergent patterns giving insight into model monotonicity, nonlinearities, tipping points.
	Examine Robustness	+/-	Display robustness of patterns to individual changes. Does not include interaction effects.
	Quantify Output Variability	-	Does not consider interaction effects and consequentially variability.
Regression-Based	Examine Patterns	+/-	Descriptive relationships of model output, providing insight into model behavior. Conditional on regression model fit.
	Examine Robustness	+/-	Descriptive relationships provide insight into robustness accounting for interaction effects. Conditional on if good fit is found.
	Quantify Output Variability	+/-	Output variance decomposed attributed to (combination of) parameters. Conditional on fact good fit is found.
Variance-Based	Examine Patterns	-	Averaged effect of parameter over parameter space. Does not explore patterns within space.
	Examine Robustness	-	Does not describe robustness of output, but instead the effects.
	Quantify Output Variability	+	Decompose output variance attributable to (combination of) parameters

+ = Well suited, - = Poorly suited for SA Aim. Modified from [153].

---

**Table 2–8** Morris and Sobol sensitivity analysis applicability.

---

<b>Sensitivity Analysis Method</b>	<b>Morris</b>	<b>Sobol</b>
<b>SA Type</b>	OAT	Variance-based
<b>Sampling Strategy</b>	Monte-Carlo	Sobol quasi-random
<b>Computational Requirement</b>	$n(k+1)$	$n(2k + 2)$
	Cheap	Expensive
<b>Sensitivity Measure</b>	Screening	Quantitative Variance Decomposition
<b>Global Measure</b>	Yes	Yes
	Qualitative	Quantitative
<b>Applicability</b>	Model-Independent	Model-Independent
<b>Reliability</b>	High	High

Modified from [171].

---

**Table 2–9** First ( $S_i$ ) and Total ( $S_{Ti}$ ) sensitivity index equations for variance-based Sobol methods.

$\mathbf{V}_{\mathbf{X}_i}(\mathbf{E}_{\mathbf{X}_i}(\mathbf{Y} \mathbf{X}_i))$ for $S_i$	Reference
$\frac{1}{N} \sum_{j=1}^N f(A)_j f(B_A^{(i)})_j - f_0^2$	Sobol [151]
$V(Y) - \frac{1}{2N} \sum_{j=1}^N (f(B)_j - F(A_B^{(i)})_j)^2$	Sobol Jansen [80]
$\mathbf{E}_{\mathbf{X}_i}(\mathbf{V}_{\mathbf{X}_i}(\mathbf{Y} \mathbf{X}_i))$ for $S_{Ti}$	Reference
$\frac{1}{N} f(A)_j (f(A)_j - f(A_B^{(i)})_j)$	Sobol [151]
$\frac{1}{2N} (f(A)_j - f(A_B^{(i)})_j)^2$	Sobol Jansen [80]

Modified from [132]. Sampling matrices  $\mathbf{A}$  and  $\mathbf{B}$  with generic elements  $a_{ji}$  and  $b_{ji}$ ,  $1 \leq i \leq k$  and  $1 \leq j \leq N$  where  $k$  is the number of factors and  $N$  is the number of simulations. Matrix  $A_B^{(i)}$  ( $B_A^{(i)}$ ) where all columns are from  $\mathbf{A}$  ( $\mathbf{B}$ ) except column  $i$  from  $\mathbf{B}$  ( $\mathbf{A}$ ).

## CHAPTER 3

### Experimental Methods

Training and testing data is required to calibrate the proposed ABM prior to model validation and verification. *In vitro* experimental methods are advantageous when generating training and testing data because of the ease of culture, relatively inexpensive as well as high throughput and high reproducibility. For this study, the HGABM models remodeling processes in a PEGDA crosslinked thiol-modified HA-Gtn hydrogel. As such, *in vitro* methods were used to quantify cellular behavior in HA-Gtn hydrogels with a wide range of biomechanical and chemical properties to train and test the HGABM. Quantitative empirical results regarding collagen, fibroblast and total protein concentration in fibroblast seeded HA-Gtn constructs was required for the calibration and validation of the HGABM (Section 2.2 and 2.4). This chapter outlines the experimental methods taken to synthesize PEGDA crosslinked HA-Gtn hydrogels from components in variable concentration and characterize cellular response *in vitro*.

#### 3.1 Materials

Thiolated HA (Glycosil or CMHA-S, MN = 200 kDa, 40 % thiolation), thiolated Gtn (Gelin-S or Gtn-DTPH, MN = 25 kDa, 40 % thiolation) and poly(ethylene glycol) diacrylate crosslinker (PEGDA MW 3400 g · mol<sup>-1</sup>) were purchased from ESBio (Alameda, CA, USA). Dulbecco Modified Eagles Medium (DMEM), MEM Non-essential Amino acid Solution (NEAA), Fetal Bovine Serum (FBS), sodium pyruvate

(SP), Penicillin/Streptomycin Solution (P/S), 0.25 % Trypsin EDTA solution, Dulbeccos Phosphate Buffered Saline (PBS) were purchased from Sigma Aldrich (St Louis, USA).

### **3.2 Human Vocal Fold Fibroblast Cell Culture**

Immortalized human vocal fold fibroblast (ihVFF) were grown in DMEM cell culture medium with 5 % (v/v) FBS, 1 % (v/v) 1X NEAA, 1 % (v/v) SP, 1 % (v/v) P/S at 37 °C in a humidified atmosphere with 5 % CO<sub>2</sub> and 95 % air. Fresh media was replaced every 3 days. Immortalized cells were used because they are a reproducible, characterized [156], and easily obtainable source of human vocal fold fibroblasts (hVFF) relative to primary human vocal fold fibroblasts.

### **3.3 HA-Gtn Fabrication and and Cell Encapsulation**

A semisynthetic ECM hydrogel based on cross-linked CMHA-S and Gtn-DTPH was prepared as per the recommended manufacturer's protocol [44]. In short, firstly CMHA-S and Gtn-DTPH were allowed to reach room temperature. Under aseptic conditions, 1 mL of degassed, deionized water (DG) water was added to each vial using a syringe and needle. The vials were inverted and gently vortexed to fully dissolve. A solution containing CMHA-S and Gtn-DTPH was prepared by mixing 1 % (w/v) CMHA-S and 1 % (w/v) Gtn-DTPH in volumetric ratios of 2:1, 5:1 and 10:1 (referred to as GH2, GH5, GH10 respectively). Cells were added to the HA-Gtn mixture for a final concentration of  $1 \times 10^6$  cells/mL. A crosslinker, PEGDA, was added to the HA-Gtn-cell solution for a final crosslinker concentration 0.25 % (w/v) and prepared for homogeneity. Cell-gel constructs were grown in ihVFF cell culture

medium described in Section 3.2 with added 1% (v/v) ascorbic acid and changed every 3 days.

### **3.4 Biochemical Analyses**

#### **3.4.1 Total Protein Assay**

The total protein concentration in the culture medium was measured using a Bradford Protein Assay following the manufacturer's protocol (Quickstart, Bio-rad). Unknown samples were mixed with Bradford working reagent followed by incubation for 5 min at room temperature. The total protein concentration was quantified by reading the absorbance of the unknown sample along with standard curve from known protein standards.

#### **3.4.2 Soluble Collagen Assay**

The amount of deposited collagen at specified time intervals was quantified using the Sircol Collagen Dye Binding Assay kit (Biocolor Assays). The recommended manufacturers protocol was followed [14]. Briefly, at the time of sacrifice hydrogel samples were transferred to screw top vials, weighed, flash frozen in liquid nitrogen and stored at  $-80^{\circ}\text{C}$ . For acid-pepsin extraction, samples underwent incubation in 1 mL acid-pepsin solution (0.1 mg/mL 0.5 M acetic acid pepsin) at  $-80^{\circ}\text{C}$  for 24 h. Following incubation, samples were sonicated for 30 min followed by centrifugation at 14 500 rpm for 15 min after which the acid extract were passed through a  $0.4\ \mu\text{m}$  filter. Acid Neutralizing Reagent (TRIS-HCl, NaOH) and cold Isolation and Concentration Reagent (Polyethylene glycol in TRIS-HCl, pH 7.6) were added to 0.5 mL acid extracts. Tubes were mixed by inversion then incubated in an ice-water mix at  $4^{\circ}\text{C}$  for 48 h. Samples were centrifuged at 12 000 rpm for 10 min and supernatant was

slowly removed to precipitate collagen from the acid extract solution. Afterwards, 0.5 mL of Sircol Dye (Sirius Red in picric acid) was added to each sample tube and mixed in a mechanical shaker for 30 min. The collagen-dye pellet was precipitated by centrifugation at 12 000 rpm for 10 min and dissolved in alkali releasing reagent (0.5 M NaOH). The absorbance of the sample was measured at 540 nm using a microplate reader (Molecular Devices Spectramax M5) at 502/523 nm. The absorbance of the sample against a known standard curve were used to determine the amount of collagen.

### **3.4.3 Cell Proliferation Assay**

To evaluate cell proliferation, quantification of DNA was performed using the PicoGreen double-stranded-DNA quantification kit (Invitrogen). At time interval of interest, the 3D cell-hydrogel construct was suspended in an extraction buffer (1 N NH<sub>4</sub>OH, 0.2% (v/v) Triton x-100) and treated with a tissue disrupter to release DNA. The extract was used for the PicoGreen assay following the manufacturers instructions [76]. In short, TE buffer (10 mM Tris-HCl, 1 mM EDTA, pH 7.5) was diluted 20 fold with sterile distilled water. Quant-iT PicoGreen reagent was diluted 200 fold with the TE buffer. The experimental DNA solution was added in equal volumes to the aqueous working solution of Quant-iT PicoGreen reagent. The samples were then incubated at room temperature for 2 min to 5 min , protected from light. The sample fluorescence was measured using a microplate reader. A standard curve generated from a cell suspension of known density was used to determine the number of cells.

#### 3.4.4 Viability Assay

Cell viability was determined using a two-probe fluorescence LIVE/DEAD Viability/Cytotoxicity Assay kit (Molecular Probes) for mammalian cells. The two probes Calcein AM and Ethidium homodimer-1 (EthD-1) measure intracellular esterase activity and plasma membrane integrity and as such are used to identify live and dead cells respectively. Cell viability was measured following the manufacturer's protocol [126]. In short, samples were washed in D-PBS for three times for 5 min to remove serum esterase activity in serum supplemented growth media. A working solution (2  $\mu$ M calcein AM and 4  $\mu$ M EthD -1 in tissue culture grade D-PBS) was added to cover the 3D cell-hydrogel construct samples. Samples were incubated for 30 min at room temperature in covered petri dishes. Following incubation, samples were washed in D-PBS three times for 5 min. The labeled cells were viewed under a fluorescence microscope (Zeiss LSM710) at 525(33) nm and 664(77) nm for calcein and EthD-1 respectively.

## CHAPTER 4

### Results

#### 4.1 Vocal Fold Agent Based Model

##### 4.1.1 Morris Screening Plots

The VFABM had 24 measurable model outputs; 8 collective chemical populations (TNF, TGF, FGF, MMP8, IL-1, IL-6, IL-8, IL-10) for 3 treatments groups (voice rest, resonant voice and spontaneous speech). The Morris screening analysis assigned each of the 213 model parameters a qualitative sensitivity metrics corresponding to each of these model outputs. Figure 4.1 is a graphical representation of sensitivity metrics of all parameters for one of the measurable model outputs; TNF population levels for the voice rest case. Each parameter is represented on the plot by a point with the coordinate  $(\mu_i^*, \sigma_i)$  defined in Section 2.3.1. Parameters with  $\mu_i^* > 0$  were classified as important and influential on the output. A large coefficient of variance ( $\sigma_i / \mu_i^*$ ) implies that there are interaction effects between input  $i$  and the other inputs. All influential parameters display a coefficient of variance  $0 \leq \sigma_i / \mu_i^* \leq 1$ , suggesting significant non-linear effects. Many of the top influential parameters ranked by  $\mu_i^*$  values in Figure 4.1 were related to macrophage, fibroblast and platelet cytokine synthesis. Less influential parameters with lower  $\mu_i^*$  display higher non-linear behavior.

### 4.1.2 System Dynamics for Model Outputs across Treatment Groups

Averages of absolute mean ( $\mu_i^*$ ) and coefficient of variation ( $\sigma_i / \mu_i^*$ ) metrics were compared for different collective chemical populations and treatment groups (Figure 4.2). Chemical populations were classified as representing proinflammatory (Figure 4.2:A, C) and anti-inflammatory system response (Figure 4.2:B, D).

The absolute mean reflects the dependence of the model output on model parameters, where higher values reflect higher dependence. The average absolute mean varied greatly across treatment groups for both anti- and pro-inflammatory markers (Figure 4.2:A, B). Average values were significantly greater than the threshold  $\mu_i^* = 0.05$ , suggesting all chemical populations for all treatment groups are greatly dependent on parameter estimation. Pro-inflammatory biomarkers TNF, IL8, as well as anti-inflammatory biomarkers TGF, MMP8 and IL6 had significantly higher mean  $\mu_i^*$  values for the voice rest case. Pro-inflammatory FGF and IL-1beta as well as anti-inflammatory IL-10 output biomarkers demonstrated similar mean  $\mu_i^*$  values for all treatment groups.

The coefficient of variation reflects the linearity of output dependency on model factors. The model outputs across all treatment groups demonstrated non-linear dependency (Figure 4.2C, D). Voice rest treatment had the highest degree of non-linearity, for both pro-inflammatory markers (TNF, IL-1beta) and anti-inflammatory markers (TGF, MMP8 and IL6). FGF, IL8 and IL10 has similar degree of linearity across treatment groups.

The relative mean ( $\mu_i/\mu_i^*$ ) reflects both positive/negative correlation as well as monotonicity of the system, where  $\mu_i/\mu_i^* = 1$  represent a linearly monotonic dependency. None of the model outputs suggested linearly monotonic dependency. There was no strong positive or negative correlation for any model output or treatment group.

Three major types sensitivity analysis methods are available (Table 2-7, 2-8). Information regarding system dynamics from the Morris sensitivity analysis can aid in choosing an appropriate sensitivity analysis method with the smallest computational complexity. Given the non-linear and non-monotonic behavior of system, it would be the best to use variance-based sensitivity analysis methods owing to their ability of quantifying non-linear responses and full exploration of input space. Variance-based method parameters was chosen allowing for consideration of non-uniform factor probability distribution as well as minimization of number of model evaluations and computational time.

#### **4.1.3 Parameter Classification**

The Morris method is not quantitative and therefore cannot be used reliably for factor prioritization. It can however be used to fix non-influential factors within their range of uncertainty without any effects on model output variance allowing for significant reductions in model complexity as well as computation cost for subsequent sensitivity analysis and model calibration. Each of 213 model parameters (Table 2-6) was classified as either influential or non-influential with respect to 8 chemical populations for 3 different treatment groups (Figure 4.3). A threshold of  $\mu_i^* \leq 0.05$  was used to classify non-influential factors. Although this cutoff value is not

distinctly defined in literature, 0.05 is frequently accepted for this type of analysis in distinguishing unimportant parameters in complex models [174]. Many parameters related to cell activation, high chemical related damage threshold, chemical half-life and cytokine synthesis were classified as non-influential across the three treatment groups. Parameters related to cell recruitment, ECM synthesis and platelet cytokine synthesis were classified as influential. The influence of stress and cell cytokine secretion related parameters were identified as highly treatment dependent. This is as expected given that agent-rules governing agent behavior varies between treatment groups.

#### 4.1.4 Sobol Sensitivity Analysis

The Morris method can only identify qualitatively important parameters with respect to the responses of interest. The Sobol variance-based sensitivity method was used subsequently to quantify the variance contribution of influential parameters to model outputs. Sobol sensitivity analysis yields two sensitivity metrics for each parameter: 1) first order ( $S_i$ ), and 2) total order ( $ST_i$ ). The first order sensitivity metric  $S_i = V_i/V(y)$  is widely regarded as a proper measure of sensitivity to rank input factors in order of importance for non-additive models with correlated input factors [133]. The total effects sensitivity metric provides information on non-additive contributions of factors to model dynamics. For a purely additive model we anticipate  $\sum_{i=1}^k S_i = 1$  whereas for non-additive models with the difference between  $ST_i$  and  $S_i$  reflecting non-additive contributions.

Figure 4.4 is a graphical representation of first and total sensitivity indices of influential parameters for one of the measurable model outputs; TNF population

levels for the voice rest case. All  $S_{T_i}$  are significantly greater than  $S_i$  indicating the strong non-additive effects of parameters on model output. The  $S_i$  do have negative values due to their high variance relative to unconditional output variance. Additionally, the sum of all first order indices yields  $\sum_{i=1}^k S_i > 1$ . This is mathematically inaccurate and suggest correlation between various parameters. The assumption of independent parameters is violated and the Sobol metrics are no longer an accurate quantitative metric of parameter sensitivity.

#### 4.1.5 Figure of Merit as Sensitivity metric

Figure 4.5A shows the  $S_{T_i}$  for model factors ranked in descending order. Bootstrap replicates were used to approximate confidence intervals. There are fairly large variations in total order indices with non-statistically significant differences in indices for consecutively ranked parameters. This further highlights the fact that Sobol total order indices alone are not an adequate measure of factor ranking. Figure 4.5B shows the total order sensitivity indices ranking in descending order and the figure of merit ( $M_i$ ). The adjustment by the figure of merit as a sensitivity metric takes into consideration factor correlation and interaction. The relative importance of factor changes greatly, suggesting great correlative and interactive effects and the importance of considering them when performing sensitivity analysis.

A Figure of Merit was used as the sensitivity measure for model parameters (Table 4-1). Pro-inflammatory response reflected by TNF, FGF, IL-1 $\beta$  and IL8 model outputs were greatly sensitive to cell chemical synthesis, specifically fibroblast TGF, IL8, IL6 synthesis and neutrophil MMP8 synthesis. Additionally, neutrophil and macrophage recruitment as well as collagen synthesis, elastin synthesis and high

TNF damage were the most significant parameters. Anti-inflammatory response given by TGF, MMP8, IL8 and IL10 model outputs were most sensitive to fibroblast TNF, TGF and IL8 synthesis, neutrophil MMP8, macrophage TNF, IL10 and platelet TNF synthesis. In addition, neutrophil and macrophage recruitment were among the most significant events modulating anti-inflammatory response. The identification of these key factors allow for model simplification and reduction in number of parameters requiring calibration prior to validation.

## **4.2 HA-Gtn Scaffold Agent Based Model**

### **4.2.1 Overview**

The HA-Gtn Scaffold ABM (HGABM) is an extension of the existing VFABM. The HGABM maintains all cell and ECM related agent rules within VFABM while integrating mechanical and biochemical characteristics created by crosslinked thiolated HA-Gtn hydrogels and cellular response. Manual adjustment of top ranked sensitive parameters from Sobol analysis were used to conduct comparative calibration minimizing deviations against experimental data. Under the hypothesis that a model is validated when for the same input conditions the real system and simulation will have sufficiently similar outputs, first pass attempts at black box predictive validation were conducted against the real system *in vitro* experimental data.

### **4.2.2 Event Validation**

Various validation techniques are available for model verification and validation. Prior to the integration of the mechanical, viscoelastic and biochemical cues pertinent to the biomaterials, event validation was conducted as an initial validation

of *in vivo* VFABM against general inflammation response dynamics. Event validation uses occurrences of benchmark events in simulation model and compare to those of the real system to determine if they are similar. Predominant cell types present at various stages of inflammation are well documented in literature. In general, neutrophils predominate the first several days following injury after which they disintegrate and disappear 24 - 48 hours following migration. They are then replaced by monocytes through chemotactic factors from vasculature. Monocyte migration continues for days or weeks following injury, whereupon they differentiate into macrophage cell types. It is important to note that the intensity and time variables of cell recruitment are highly dependent on tissue type as well as on the severity of injury. A comparison between VFABM and reports in the wound repair literature (Fig 4.6 and 1.3) show that there are notable similarities in cell populations over time. Namely, the VFABM captures the dynamics in the recruitment of platelets, neutrophils, macrophages followed by fibroblasts in a sequential fashion as reported in wound repair literature.

### **4.2.3 Face Verification**

Time-varying HA-Gtn hydrogel properties and consequential biomechanical cues such as elastic modulus, swelling ratio and mass loss in the HGABM were benchmarked against those found in literature. The HA-Gtn hydrogels follow rules of mixture, where gelatin acts to dilute HA concentration. As such for decreasing Gtn:HA volumetric ratios there is a lower elastic modulus (Fig 4.7). The mechanical properties follow that of literature, namely the swelling ratio follows a logarithmic

change over time, reaches within 90% of swelling equilibrium within 24 hours. Additionally, mass loss reflects that reported in literature, degrading up to 60% by 14 days (Figure 4.7).

#### 4.2.4 Model Calibration

The HGABM used the experimental conditions as input factors into the model (HA concentration, Gtn concentration, PEGDA concentration) and baseline output biomarkers (collagen content, cell population, total protein). The top ranked parameters from the sensitivity analysis as well as new parameters from additional rules related to biomaterial micro-environment properties were manually calibrated iteratively to minimize deviation between model simulation and experimental results for collagen content, fibroblast population and total protein at time points 2 (72 hours) and 3 (144 hours) (Fig 4.8). Comparison between calibration model profile, the HGABM was not sufficient to accurately capture all cell population dynamics. In Figure 4.8A, despite similarities in trends, the magnitude and rate of cell population dynamics are notably different. In Figure 4.8A following calibration, the model failed to reflect an initial synthesis phenotypic stage of the cells at 72 hours. It is unclear whether this is due to shortcomings of the model or flaws in the calibration.

The predictive power of the calibrated HGABM was tested for different initial hydrogel compositions. Experimental and simulation data for relative concentrations of HA:Gtn for 2:1, 5:1 and 10:1 case were compared (Figure 4.9). The deviation from experimental bench marks were greater for all output biomarkers for lower higher HA:Gtn concentrations. The HGABM was able to more accurately predict population profiles for hydrogels with a higher proportion of HA.

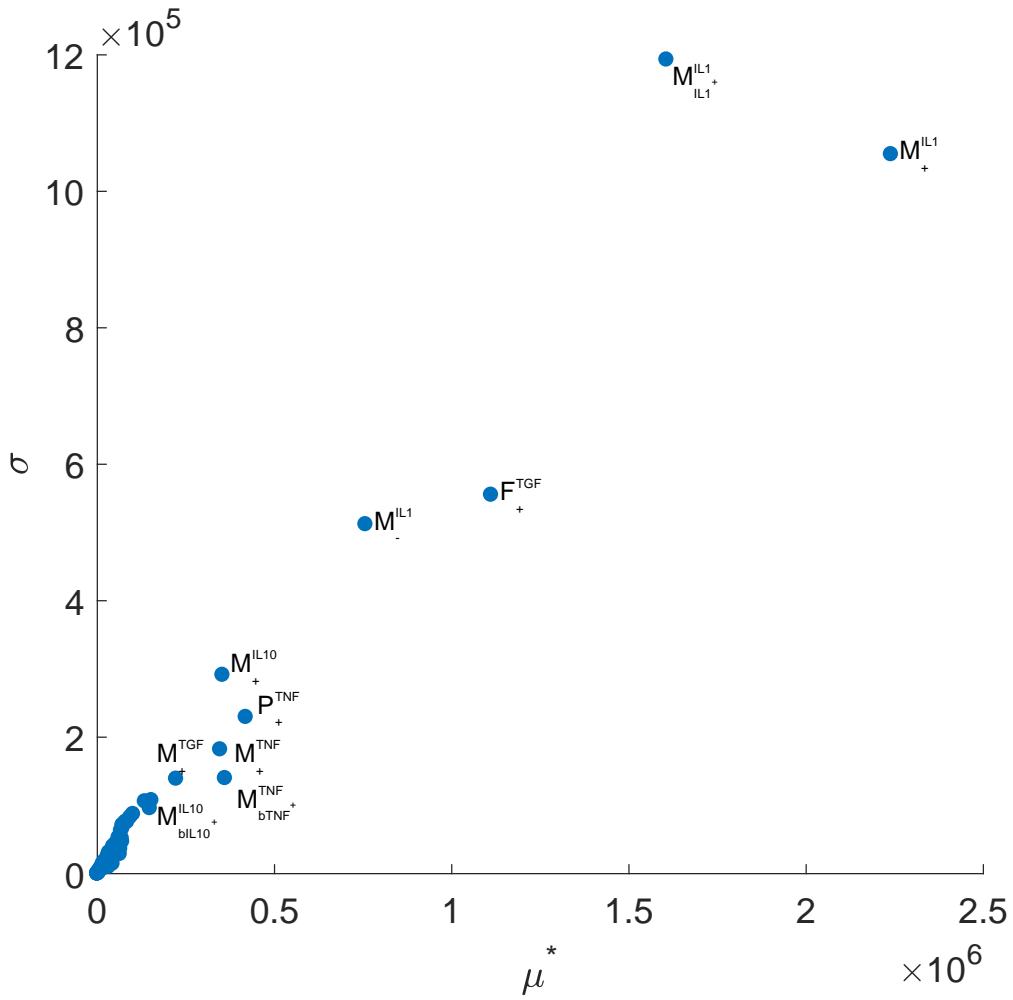


**Figure 4.1:** Vocal Fold Agent Based Model parameters sensitivity indices for TNF model output in the voice rest case.

Complete Morris Screening Results for all model outputs in three treatment cases in Appendix D.

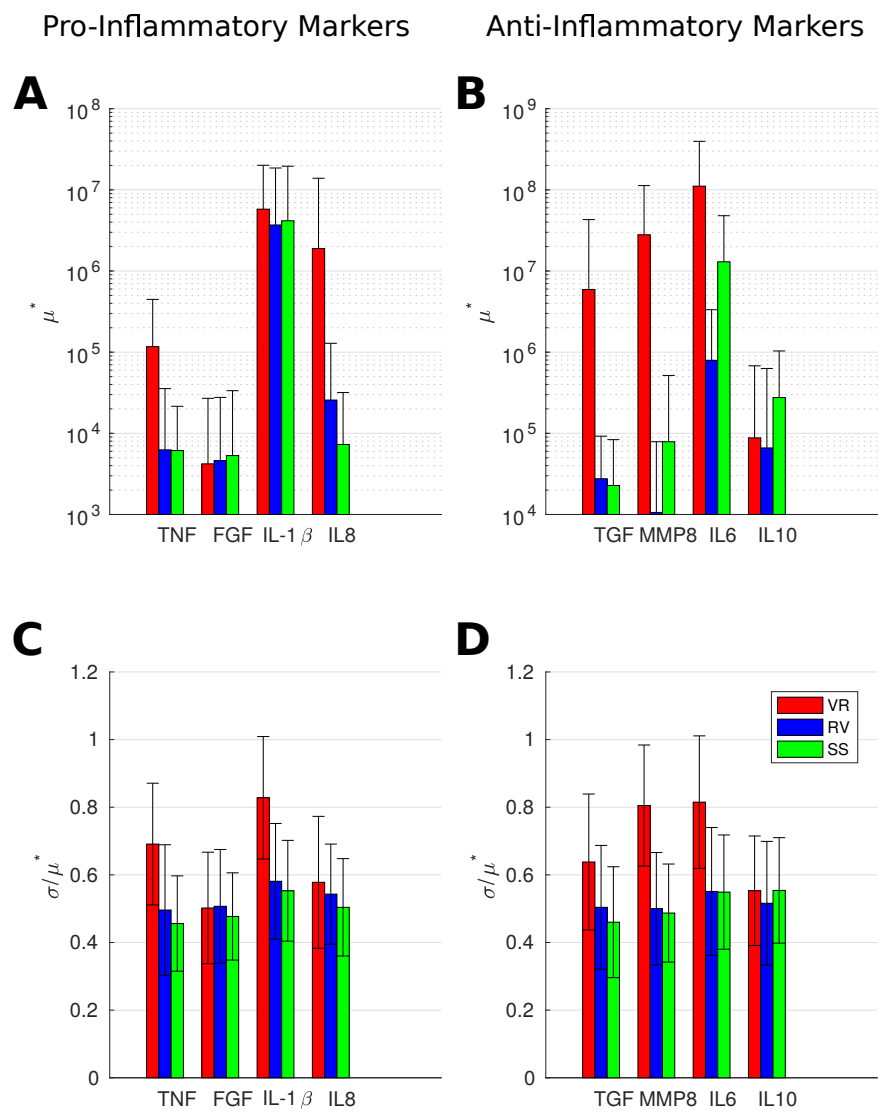


**Figure 4.2:** Average Morris sensitivity indices (A-B) absolute mean and (C-D) coefficient of variation for pro- and anti-inflammatory chemical populations.

Bar values represent average sensitivity index; Error bars represent standard deviation.

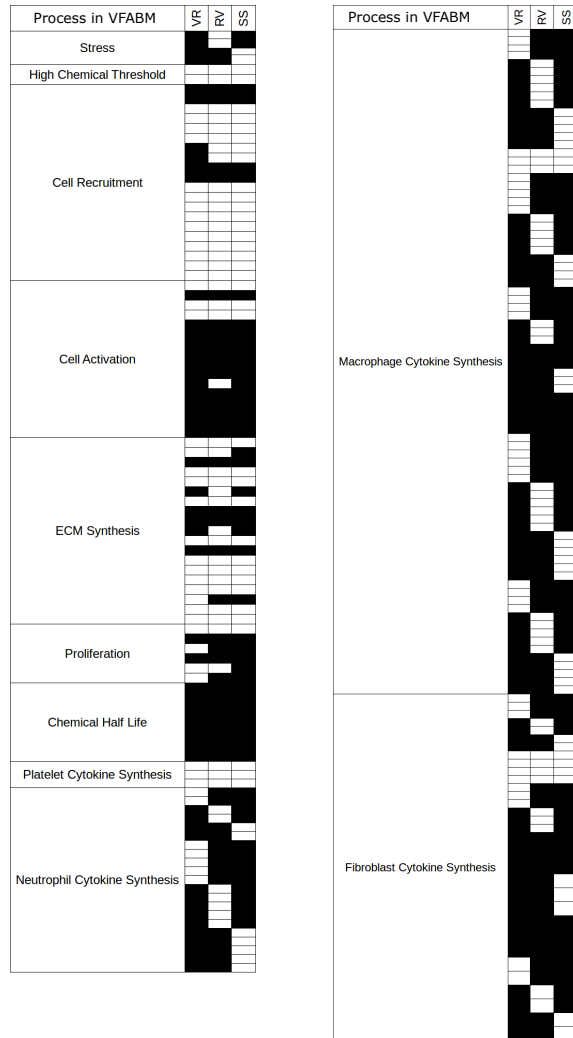


**Figure 4.3:** Identification of influential parameters for voice rest (VR), resonant voice (RV) and spontaneous speech (SS) using Morris screening methods.

Each row represents a model parameter, related to a event or process in the VFABM. Black represents parameters with  $\mu_i^* \geq 0.05$  for all outputs indicating significant influence on the model output.

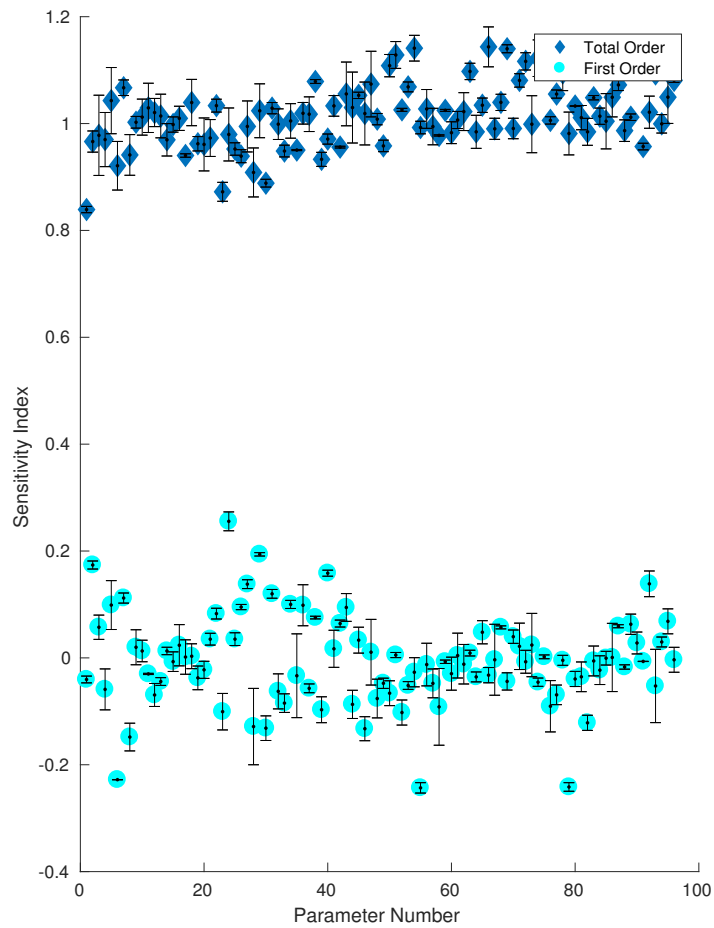


**Figure 4.4:** Sobol-Jansen first and total order sensitivity indices for TNF model output for the voice rest case.

Each data point represents the average sensitivity index and error bar represents standard error for 100 bootstrap replicates for a given model parameter. A full list of model parameters can be found in Appendix B.

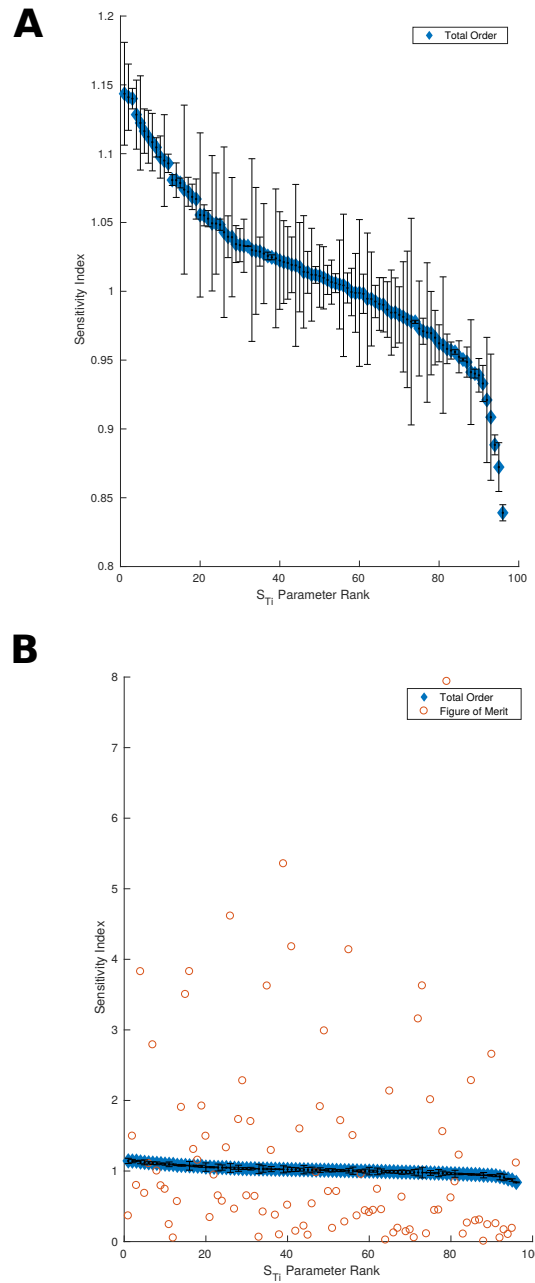


**Figure 4.5:** Sobol-Jansen total order sensitivity indices (A) ranked in descending order (B) compared to Figure of Merit sensitivity indices.

**Table 4-1** Top ranked influential parameters according to Figure of Merit.

M Ranking	Model Output							
	TNF	TGF	FGF	MMP8	IL1	IL6	IL8	IL10
1	$i_{cap}^M$	$r_{cap}^N$	$F_{IL10}^{TNF-}$	$t_{TNF}$	$t_{TNF}$	$N_{TGF-}^{MMP8}$	$r_{cap}^N$	$N_{TGF-}^{MMP8}$
2	$F_{+}^{IL8}$	$i_{tiss}^M$	$p_{+}^F$	$i_{cap}^M$	$i_{tiss}^F$	$t_{TNF}$	$i_{tiss}^M$	$M_{IL1+}^{IL8}$
3	$F_{-}^{IL6}$	$F_{+}^{TGF}$	$r_{tiss}^F$	$i_{tiss}^M$	$N_{TGF-}^{MMP8}$	$M_{tTNF+}^{TNF}$	$e_{+}^{col}$	$F_{IL10-}^{TNF}$
4	$F_{+}^{IL6}$	$e_{+}^{col}$	$F_{+}^{TGF}$	$N_{TGF-}^{MMP8}$	$i_{cap}^M$	$i_{tiss}^M$	$F_{+}^{TGF}$	$r_{tiss}^F$
5	$e_{+}^{ela}$	$N_{TGF-}^{MMP8}$	$N_{+}^{TNF}$	$F_{+}^{IL8}$	$N_{+}^{MMP8}$	$M_{IL10+}^{IL10}$	$r_{tiss}^M$	$P_{+}^{TNF}$

**Table 4–2** Comparison of Sobol Jansen and Figure of Merit sensitivity rankings for pro-inflammatory model output.

TNF			FGF		
Factor	M (Ranking)	$S_{Ti}$ (Ranking)	Factor	M (Ranking)	$S_{Ti}$ (Ranking)
$i_{cap}^M$	56.2 (1)	0.69 (1)	$F_{IL10}^{TNF-}$	14.2 (1)	0.88 (48)
$F_{+}^{IL8}$	11.9 (2)	0.71 (8)	$p_{+}^F$	12.4 (2)	0.65 (16)
$F_{-}^{IL6}$	9.7 (3)	0.73 (12)	$r_{tiss}^F$	10 (3)	0.68 (44)
$F_{+}^{IL6}$	8.9 (4)	0.73 (14)	$F_{+}^{TGF}$	9.9 (4)	0.8 (53)
$e_{+}^{ela}$	8.1 (5)	0.67 (3)	$N_{+}^{TNF}$	8.3 (5)	1.34 (50)

IL-1 $\beta$			IL8		
Factor	M (Ranking)	$S_{Ti}$ (Ranking)	Factor	M (Ranking)	$S_{Ti}$ (Ranking)
$t_{TNF}$	260.2 (1)	0.69 (31)	$r_{cap}^N$	7.84e+06 (1)	0.68 (43)
$i_{tiss}^F$	82.3 (2)	0.68 (41)	$i_{tiss}^M$	2820 (2)	0.69 (23)
$N_{TGF-}^{MMP8}$	32 (3)	1.33 (45)	$e_{+}^{col}$	448.5 (3)	0.67 (22)
$i_{cap}^M$	20.3 (4)	0.69 (1)	$F_{+}^{TGF}$	91.1 (4)	0.83 (64)
$N_{+}^{MMP8}$	18.1 (5)	1.34 (47)	$r_{tiss}^M$	27.1 (5)	0.68 (26)

**Table 4–3** Comparison of Sobol Jansen and Figure of Merit sensitivity rankings for anti-inflammatory model output.

TGF			MMP8		
Factor	M (Ranking)	$S_{Ti}$ (Ranking)	Factor	M (Ranking)	$S_{Ti}$ (Ranking)
$r_{cap}^N$	1.58e+09 (1)	0.68 (43)	$t_{TNF}$	212.2 (1)	0.69 (31)
$i_{tiss}^M$	1690.2 (2)	0.69 (23)	$i_{cap}^M$	25.4 (2)	0.69 (1)
$F_+^{TGF}$	205.4 (3)	0.83 (64)	$i_{tiss}^M$	13.3 (3)	0.69 (23)
$e_+^{col}$	195.5 (4)	0.67 (22)	$N_{TGF-}^{MMP8}$	11.7 (4)	1.33 (45)
$N_{TGF-}^{MMP8}$	46.1 (5)	1.33 (45)	$F_+^{IL8}$	11.3 (5)	0.71 (8)

IL6			IL10		
Factor	M (Ranking)	$S_{Ti}$ (Ranking)	Factor	M (Ranking)	$S_{Ti}$ (Ranking)
$N_{TGF-}^{MMP8}$	1213.9 (1)	1.33 (45)	$N_{TGF-}^{MMP8}$	17.4 (1)	1.33 (45)
$t_{TNF}$	78.5 (2)	0.69 (31)	$M_{IL1+}^{IL8}$	12.1 (2)	1.03 (51)
$M_{bTNF+}^{TNF}$	11.9 (3)	1.33 (79)	$F_{IL10-}^{TNF}$	11.4 (3)	0.88 (48)
$i_{tiss}^M$	11.5 (4)	0.69 (23)	$r_{tiss}^F$	10.6 (4)	0.68 (44)
$M_{IL10+}^{IL10}$	11 (5)	0.93 (49)	$P_+^{TNF}$	7.6 (5)	2.2 (61)

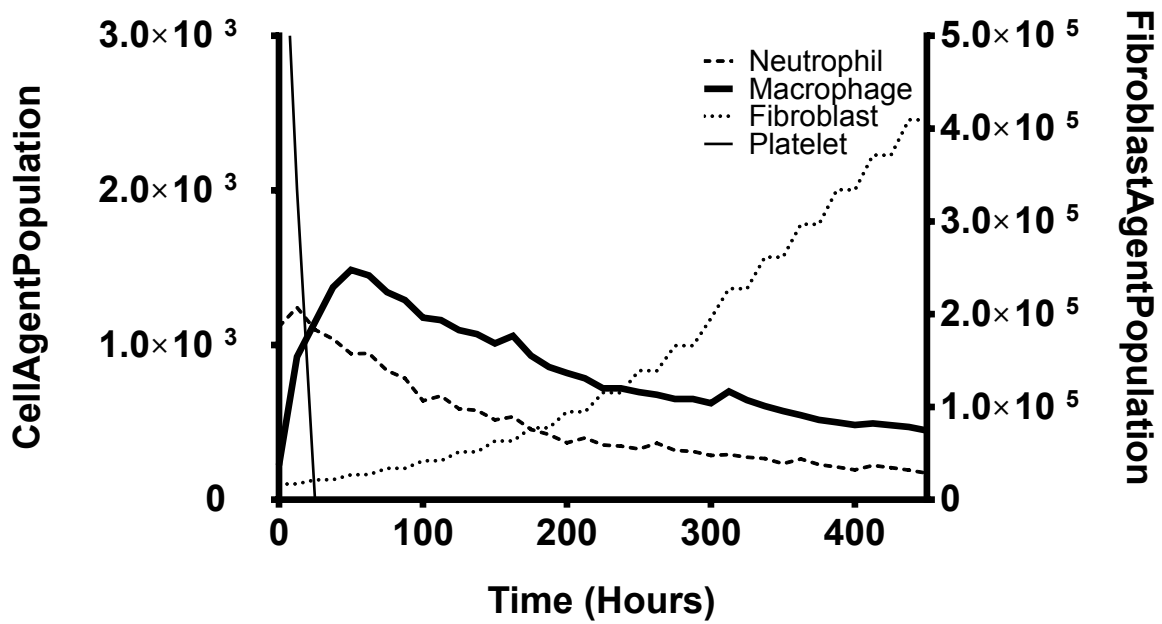
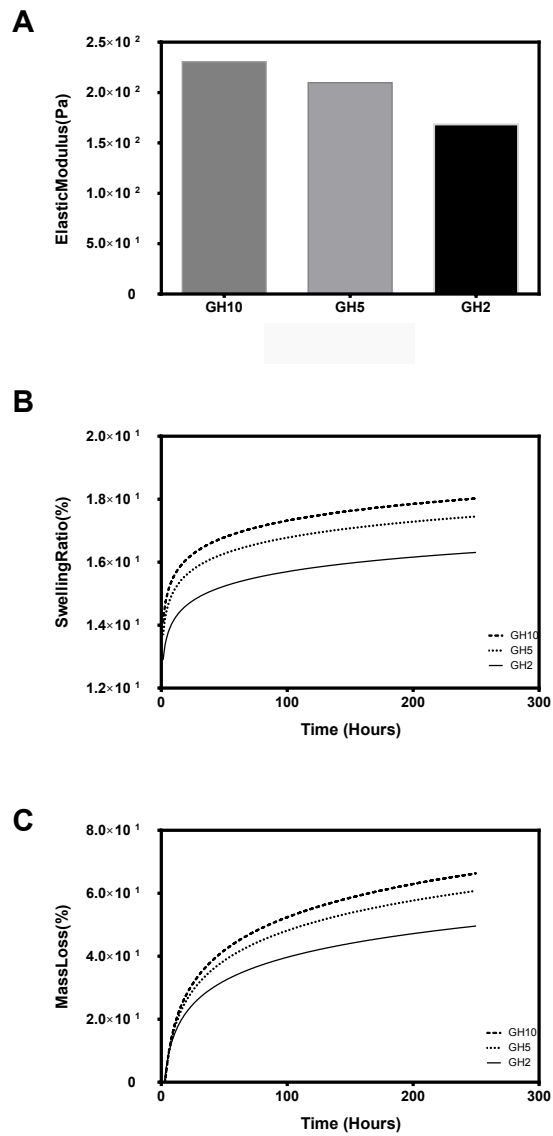
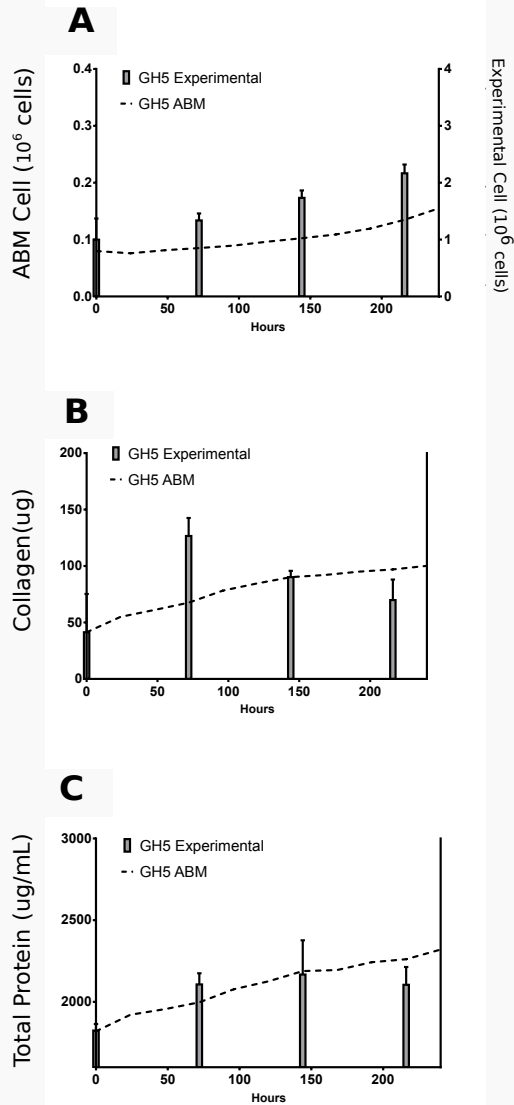


Figure 4.6: Vocal Fold Agent Based Model cell population profiles.



**Figure 4.7:** Hyaluronic-Acid Gelatin Agent Based Model time-varying mechanical properties (A) elastic modulus, (B) swelling ratio, (C) mass loss for different scaffold compositions.

## HA:Gtn 5:1



**Figure 4.8:** Black box validation of calibrated Hyaluronic Acid-Gelatin Agent Based Model outputs (A) fibroblast, (B) collagen, (C) total protein.

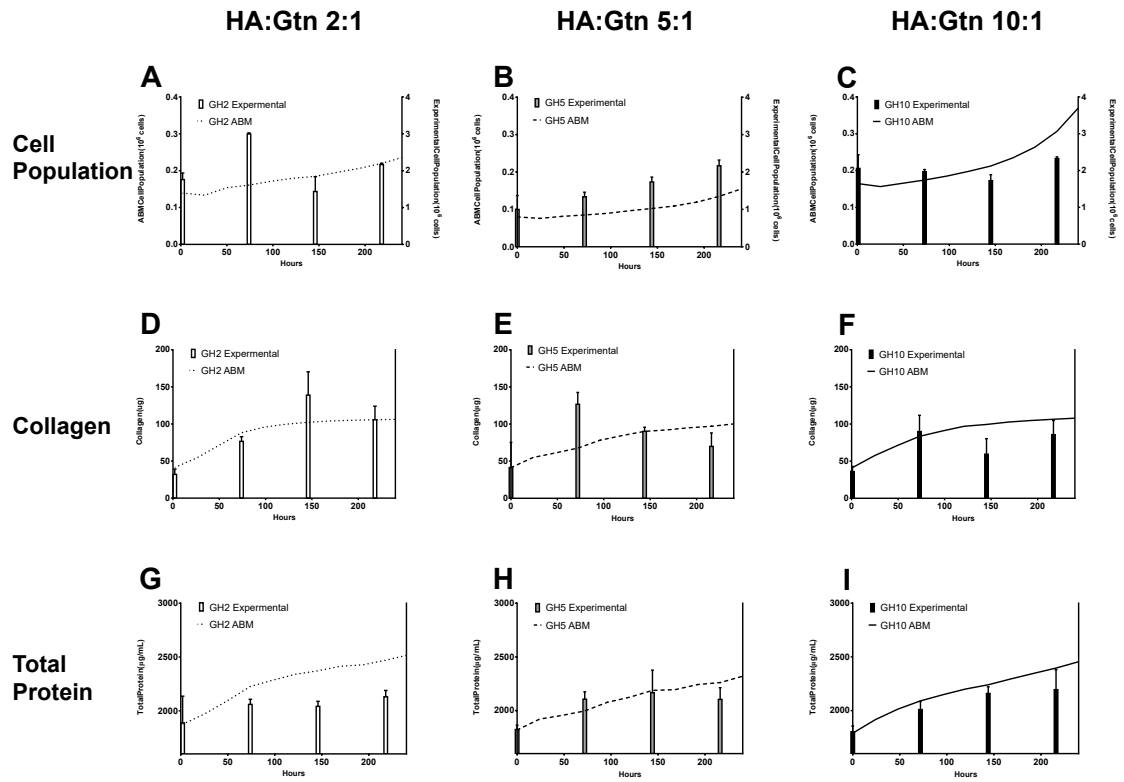


**Figure 4.9:** Calibrated Hyaluronic Acid-Gelatin Agent Based Model population response prediction.

## CHAPTER 5 Discussion

### 5.1 Vocal Fold ABM

#### 5.1.1 Sensitivity Analysis

In complex models, most factors exhibit non-linear, non-monotonic relationship with output responses. However, most practices only explore simple main effects, evaluating the effect of one factor at fixed values of the other factors. This pooling of high-level interactions in standard ANOVA or Bayesian ANOVA methods do not sufficiently encompass the complexity of the system. Despite criticism analysis of simple effects, it remains the most frequent practice due to limitations in software packages which do not enable isolation of interaction effects. Interaction effects between factors exist when changes in one factor have different effects on the response variable, depending on the value of the other factor [39]. Adding interaction terms to a regression model can greatly expand understanding of the relationships among the variables in the model and allows more hypotheses to be tested. Global sensitivity analysis methods that consider higher order statistics to understand intricacies of complex systems.

In the case of ABMs, two main motivations for extensive sensitivity analysis are to explore uncertainties in actual values of model parameters and model non-linearity. There are three components that introduce uncertainties to a model: (1) variations in noise level and random seed, (2) variations parameter values, (3) variations in the

model. In this study, we focus on the first two; the effects of intrinsic variation due to the stochastic nature of the model and external variations of model parameters. The aim is to search parameter space for stable and inactive states where model is insensitive to parameter changes and tipping points where there are dramatic changes in system behaviors.

Global variance-based analysis was used to sample the entire parameter space to obtain information about external variations from parameter values. The sum of first-order sensitivity indices shows that the ABM was not additive and had significant interaction effects. Based on total effect indices, we can observe factor interactivity, stability in relative significance of inputs. Significant correlations between input parameters in the sample were evident. As such, unique decomposition was impossible to fully separate and quantify contributions of those parameters to the output. Consequently Figure of Merit metric was used to quantify interaction and correlation effects.

### 5.1.2 Figure of Merit

Figure of Merit (M) considers both factor interaction and correlation effects between factors while classical Sobol Jansen total effect indices ( $S_{Ti}$ ) only consider interaction effects. Comparing factor rankings according these two methods highlight differences in parameterization (Table 4-2, 4-3). Many top ranked parameters according to figure of merit were ranked poorly according to Sobol. This highlights the importance of considering parameter correlations when performing sensitivity analysis.

Importance assessments for correlated inputs require significantly more evaluations of the model than the non-correlated case. The Figure of Merit used to analyse variance-based sensitivity metrics for the correlated case. The procedure followed to estimate conditional variances was on the order of  $k$ . Better results can be obtained by computing all possible conditional variances, although these procedures are significantly more expensive [114]. A few groups have proposed different alternative schemes [169, 100, 117, 15, 16]. However none of the work proposed an exact and unambiguous definition of functional ANOVA for correlated inputs. However these required different sampling methods which were infeasible for this research project given time restraints.

### 5.1.3 Model Limitations

The VFABM is a 3D representation of an average adult human vocal fold. Given constraints in computational complexity, the *world* structure was limited to a 2D domain x-y plane. This introduces limitations of a physiologically relevant and predictive model as it greatly reduces the world size, number of agents, movement is limited to a single plane and consequentially frequency of agent interactions. Additionally boundary effects on chemical diffusion are greater, exaggerating intra-cellular signaling.

This 2D assumption is analogous to 2D monolayer and 3D cell cultures. Although 2D models are easier to control, observe, measure and manipulate relative to 3D models there are limitations in ability to accurately represent *in vivo* systems. However higher degree of structural complexity and greater tendency to retain homeostasis make 3D models physiologically relevant and predictive as biomimetic models.

Integration of flow and barrier tissues allow for more accurate cell signaling and interactions which inspire differentiation and metabolic adaptation. Understanding these limitations and uncertainty they introduce to predictive capability is important in applying the model to complex 3D tissue systems.

#### **5.1.4 Model Significance**

The long term aim of the present work is to predict cellular and ECM protein trajectories using agent based modeling to simplify behavioral clinical treatment and injectable biomaterial optimization for vocal fold augmentation. The obtained results serve greatly to better understand cellular cytokine synthesis as dominant processes driving the model. Additionally identification of key parameters allow for prioritization and consequentially simplification of number of calibration parameters. These greatly reduce computational complexity and time, a major barrier to the adoption of such a technology in a clinical setting.

### **5.2 HA-Gtn Scaffold Agent Based Model**

#### **5.2.1 Validation and Verification**

The model did not closely predict fairly simple linear system dynamics of cell-scaffold behavior. This is presumable because of the small size of the simulation as well as the simplicity of the rules. The agent rules integrated relating cell phenotype and hydrogel properties can be simply represented mathematically. Agent based models are better suited for cases where rules are difficult to integrate and require a degree of abstraction. In its current state, biomaterial modeling is better suited for less computationally intensive methods, such as ODE or population-based methods.

However as the rules grow in complexity and as the need to integrate and abstract rules from different time and spatial ABM scales may be more useful.

### 5.2.2 Model Limitations

There exist major differences between simulation and experimental systems which may account for poor predictive capability. One such difference is that experimental methods required changing of medium every 3 days to ensure cell viability. This removes cumulative signaling molecules significantly changing the interaction of cells and the surrounding microenvironment. Thus the assumption that the real world data is accurate and sufficiently similar is not met for black box validation. Another major difference is the integration of rules related to biomechanical signaling. Most research regarding HA-Gtn hydrogels has been focused on viscoelastic and mechanical properties. However biochemical properties have a significant role in determining cell phenotype. Although the model could better approximate population response for high HA:Gtn volumetric ratio, it was unable to predict synthesis or proliferative phases in hydrogels with higher concentrations of Gtn. As explained in section 1.4.3, Gtn has significant role in modulating cellular attachment and consequentially cell growth and differentiation. Expansions of model agent rules related to hydrogel-cell adhesion and consequential impact on cell phenotype should be integrated.

Another source of uncertainty may be in the calibration method. Manual calibration was labor intensive, inefficient and likely inaccurate given highly non-linear and non-monotonic behavior and high parameter interaction effects of the system. As such, it is recommended that a more robust calibration method is needed. Given

the model dynamics, derivative or genetic algorithm optimization algorithms can aid greatly in the efficacy of parameter calibration and predictive capacity of the model.

Finally, there were limitations in size of simulation given the large computational load. Work has been done to optimize and parallelize the model. Speedups on the order of 10x have been achieved through parallelization and streamlining pipeline workflow on multi-processor platforms using OpenMP, CUDA-C for model enabling larger simulations and real time visualization [140, 141, 139]. This reduced memory requirement allowed for computational speed ups which in the future would allow for tissue-level representative simulation environments. Additionally, development of real time *in situ* visualization for animation of model operational behavior would aid in better simulating spatial events for users

### 5.2.3 Model Significance

The HA-Gtn Scaffold Agent Based Model was developed to model tissue remodeling processes by vocal fold fibroblast cells in HA-Gtn hydrogel. This study served to identify and integrate current understanding from literature the relationship between tunable hydrogel composition, biomechanical and chemical properties with cellular response. Quantitative empirical results regarding collagen, fibroblast and total protein concentration in fibroblast seeded HA-Gtn constructs was collected to train and test the current model. Following calibration of the top influential parameters against experimental data, the model was not able predict biomarker profiles accurately across the range of test conditions. However, this shortcomings of the ABM indicated the need of integrating additional agent-rules of cell-biochemical interactions in the model.

## CHAPTER 6

### Conclusions

Agent based models are a flexible bottom-up modeling method that is being used increasingly to model complex biological systems. Its modular design and flexibility in integrating abstract features at various time and spatial scales is advantageous over traditional mechanistic models. Additionally, emergent system properties not obvious from encoded interactions enable it to predict behaviors outside of training conditions and time points. This is advantageous in personalized medicine and behavioral therapy for vocal fold lesions as well as biomaterial design. In this project we extend previous acute phonotrauma ABM modeling cellular-level inflammation, wound healing and remodeling processes in vocal folds to predict healing and new tissue generation *in vivo* as well as *in vitro*. Model validation against clinical and experimental data necessitated model calibration. Prior to model calibration model parameters were screened and sensitivity analysis was conducted to identify and rank high order effects of parameters on model outputs. For the *in vivo case*, initial results suggested strong therapy-dependent sensitivity to model parameters. Model parameter were shown to have greater influence on anti-inflammatory model biomarkers with parameter displaying high non-linear effects with respect to both pro- and anti-inflammatory markers. Sensitivity analysis methods indicated high influence of cell chemsynthesis-related parameter on both pro- and anti-inflammatory markers. The

choice of sensitivity analysis method and sensitivity metric was important in adjusting correlated parameters for accurate factor priority setting. Identification of key parameters from sensitivity analysis allowed for simplification and speed up of event calibration. Initial black box validation against clinical and experimental data for the *in vivo* VFABM and *in vitro* HGABM was performed following calibration of key parameters. There were many limitations of the current work that should be addressed in the future.

### **6.1 Future Work**

Speed ups from heterogenous platform programming are currently being explored [140]. Real time visualization as well as full scale simulation enabled by these speed ups may be key tools for face verification in the future. Sensitivity analysis was applied to the VFABM. We can assume the subsequent results are sufficiently accurate for the model's intended purpose over the domain of the model's intended applicability. However, results ranking key influential parameters were used to calibrate the HGABM. Additional rules and new parameters may change the order of effects of a parameter. Ideally sensitivity analysis is applied to the HGABM separately in the future. Currently manual iterative calibration methods are slow and inefficient. In the future, optimization algorithms such as the genetic algorithm may reduce calibration time as well as increase predictive accuracy.

## Appendix A: Vocal Fold Agent Based Model Agent Rules

Substances	Cell Sources	Functions in Wound Healing Used in the ABM
<b>TGF-<math>\beta</math>1</b>	Fibroblasts Macrophages Platelets	Chemotactic to neutrophils, macrophages and fibroblasts
		Inhibit expression of TNF- $\alpha$ in neutrophils, macrophages, and fibroblasts
<b>bFGF</b>	Fibroblasts Macrophages	Inhibit expression of MMP-8 in neutrophils
		Inhibit expression of IL-1 $\beta$ in macrophages (minimal effect)
<b>TNF-<math>\alpha</math></b>	Fibroblasts Macrophages Neutrophils	Activate resting fibroblasts
		Mitogenic to fibroblasts (proliferation)
<b>IL-1<math>\beta</math></b>	Macrophages Platelets	Stimulate collagen, elastin and hyaluronan synthesis in fibroblasts
		Chemotactic to neutrophils and macrophages
<b>IL-6</b>	Macrophages Fibroblasts	Mitogenic to fibroblasts (proliferation)
		Stimulate fibroblast migration
<b>IL-8</b>	Macrophages Fibroblasts	Inhibit collagen and elastin synthesis in fibroblasts
		Stimulate hyaluronan synthesis in fibroblasts
<b>IL-10</b>	Macrophages	Chemotactic to neutrophils and macrophages
		Activate neutrophils and macrophages
<b>Collagen</b>	Fibroblasts	Stimulate expression of MMP-8 in neutrophils
		Stimulate expressions of TNF- $\alpha$ , IL-1 $\beta$ , IL-6, and IL-8 in macrophages
<b>Elastin</b>	Fibroblasts	Stimulate expression of TGF- $\beta$ in macrophages and fibroblasts
		Mitogenic to fibroblasts (proliferation)
<b>HA</b>	Fibroblasts	Stimulate expression of IL-6 in fibroblasts
		Inhibit elastin synthesis in fibroblasts
<b>MMP-8</b>	Neutrophils Platelets	Stimulate hyaluronan synthesis in fibroblasts
		Induce tissue damage
<b>IL-6</b>	Macrophages Fibroblasts	Chemotactic to neutrophils
		Stimulate collagen synthesis in fibroblasts
<b>IL-8</b>	Macrophages Fibroblasts	Chemotactic to neutrophils
		Stimulate collagen synthesis in fibroblasts
<b>IL-10</b>	Macrophages	Inhibit expression of TNF- $\alpha$ in neutrophils, macrophages, fibroblasts
		Inhibit expression of IL-1 $\beta$ in macrophages
<b>HA</b>	Fibroblasts	Inhibit expression of IL-6 and IL-8 in macrophages and fibroblasts
		Stimulate expression of TGF- $\beta$ in macrophages and fibroblasts
<b>Collagen</b>	Fibroblasts	Stimulate expression of IL-10 in macrophages
		Inhibit activated neutrophil lifespan
<b>Elastin</b>	Fibroblasts	Inhibit activation of neutrophils and macrophages
		Degrades collagen to produce collagen fragments
<b>HA</b>	Fibroblasts	Collagen repairs tissue damage
		Collagen fragments are chemotactic to neutrophils and macrophages
<b>HA</b>	Fibroblasts	Elastin repairs tissue damage
		Elastin fragments are chemotactic to macrophages
<b>HA</b>	Fibroblasts	HA repairs tissue damage
		HA inhibits expression of TNF- $\alpha$ , IL-8 and collagen synthesis in fibroblasts
<b>HA</b>	Fibroblasts	HA fragments stimulate expressions of TNF- $\alpha$ , IL-1 $\beta$ and IL-8 in macrophage
		HA fragments are mitogenic to fibroblasts (proliferation)
<b>HA</b>	Fibroblasts	HA fragments stimulate collagen synthesis in fibroblasts

ABM = agent-based model; TGF = transforming growth factor; TNF = tumor necrosis factor; MMP = matrix metalloproteinase; IL = interleukin; bFGF = basic fibroblast growth factor; HA = hyaluronan.

**Figure A1:** Vocal Fold Agent Based Model agent rules.

## Appendix B: Vocal Fold Agent Based Model Chemsynthesis Agent Rules and Parameters

Cytokine	Treatment	Fibroblast	Neutrophil	Macrophage	Platelet
<b>TNF</b>	VR	$\frac{F_0}{F_1 + pTGF + pIL10 + nHA}$	$\frac{M0}{M1 + pTGF + pIL10}$	$\frac{M2 + pTNF + pIL1 + fHA}{M3 + pTGF + pIL10}$	
	RV	$\frac{F3}{F4 + pTGF + pIL6 + pIL10 + nHA}$	$\frac{N2}{N3 + pTGF + pIL10}$	$\frac{M6 + pTNF + pIL1 + fHA + RVIS + M7}{M8 + pTGF + pIL6 + M9 + pIL10}$	
	SS	$\frac{F5}{F6 + pTGF + pIL6 + pIL10 + nHA}$	$\frac{N4}{N5 + pTGF + pIL10}$	$\frac{M11 + pTNF + pIL1 + M12 + fHA + SSIS + M13}{M14 + pTGF + pIL6 + pIL10}$	
	VR				
<b>TGF</b>	RV	$F7 + F8 + (F9 + pTNF + pIL10)$		$M15 + (M16 + pTNF + pIL10)$	P0
	SS				
	VR				
<b>FGF</b>	RV	$F10$		$M17$	
	SS				
	VR			$\frac{M20 + pTNF + pIL1 + M21 + fHA}{M22 + pTGF + pIL10}$	
<b>IL1</b>	RV			$\frac{M25 + pTNF + M26 + pIL1 + fHA + RVIS}{M27 + pTGF + pIL6 + pIL10}$	$P1 + bIL1$
	SS			$\frac{M30 + pTNF + pIL1 + fHA + SSIS}{M31 + pTGF + pIL6 + pIL10}$	
	VR	$\frac{F11 + \frac{F12 + pTNF}{F13 + pIL10}}{F14 + (F15 + RVIS + F16)}$		$\frac{M34 + pTNF + pIL1}{M35 + pIL10}$	
<b>IL6</b>	RV	$\frac{F17 + \frac{F18 + pTNF}{F19 + pIL10}}{F14 + (F15 + RVIS + F16)}$		$M36 + (M37 + RVIS + M38)$	
	SS			$\frac{M40 + pTNF + pIL1}{M41 + pIL10}$	

<b>IL6</b>	<=7d	$F_{20} * (F_{21} + SSVS * F_{22})$	$M42 * (M43 + SSVS * M44)$
	SS		
	>7d	$\frac{F_{24} + pTNF}{F_{23} * F_{25} + pIL10}$	$\frac{M46 + pTNF + pIL1 * M47}{M48 + pIL10 * M49}$
<b>IL8</b>	VR	$\frac{F_{26}}{F_{27} + pIL10 + nHA}$	$\frac{M52 + pTNF * M53 + pIL1 * M54 + FHA}{M55 + pIL10}$
	RV	$\frac{F_{28}}{F_{29} + pIL10 + nHA}$	$\frac{M57 + pTNF + pIL1 * M58 + FHA + RVS * M59}{M60 + pIL10 * M61}$
	SS	$\frac{F_{30}}{F_{31} + pIL10 + nHA}$	$\frac{M63 + pTNF + pIL1 * M64 + FHA + SSVS * M65}{M66 + pIL10 * M67}$
<b>IL10</b>	VR		$bIL10 * M68 + M69 * (M70 + pIL10 * M71)$
	RV		$bIL10 * M72 + M73 * (M74 + pIL6 * M75 + pIL10 * M76)$
	SS		$bIL10 * M77 + M78 * (M79 + pIL6 * M80 + pIL10 * M81)$
<b>MMP8</b>	VR	$N6 * \frac{N7 + pTNF * N8}{N9 + pTGF * N10}$	
	RV	$N11 * \frac{N12 + pTNF * N13}{N14 + pTGF * N15}$	$P2 * bMMP8$
	SS	$N16 * \frac{N17 + pTNF * N18}{N19 + pTGF * N20}$	

VR = Voice Rest; RV = Resonant Voice; SS = Spontaneous Speech  
 TNF = tumor necrosis factor; TGF = Transforming Growth Factor; FGF = FibroblastGrowth Factor; MMP8 = Matrix Metalloproteinase 8; IL-1B = interleukin 1 beta; IL6 = interleukin 6; IL8 = interleukin 8; IL10 = interleukin 10

FH = Fibroblast chemsynthesis parameter; MH = Macrophage chemsynthesis parameter; NH = Neutrophil chemsynthesis parameter; PH = Platelet chemsynthesis parameter where # = 1, 2, 3, ...  
 bX = initial baseline X concentration; pX = patch X concentration where X = TNF, TGF, FGF, MMP8, IL-1B, IL6, IL8, IL10  
 nY = number of newly synthesized Y; FY = number of fragmented Y on patch where Y = hyaluronan(HA)  
 RVS = Resonant Voice Vibratory Stress; RVS = Resonant Voice Impact Stress; SSVS = Spontaneous Speech Vibratory Stress; SSVS = Spontaneous Speech Impact Stress

**Figure B1:** Vocal Fold Agent Based Model chemical synthesis agent rules.

**Table 6–1** Vocal Fold Agent Based Model parameters nomenclature and default value.

Parameter Number	Treatment	Nomenclature	Chemsynthesis Nomenclature	Default Value	Range
1	VR,RV,SS	$P^{TNF}$	P0	0.1	0.01 to 1
2	VR,RV,SS	$P^{LL+}$	P1	0.1	0.01 to 1
3	VR,RV,SS	$P^{MMPs+}$	P2	0.5	0.05 to 5
4	VR	$N^{+}$	N0	1	0.1 to 10
5	VR	$N^{TNF}$	N1	1	0.1 to 10
6	RV	$N^{TNF}$	N2	20	2 to 200
7	RV	$N^{TNF}$	N3	1	0.1 to 10
8	SS	$N^{TNF}$	N4	1	0.1 to 10
9	SS	$N^{TNF}$	N5	1	0.1 to 10
10	VR	$N^{MMPs}$	N6	1	0.1 to 10
11	VR	$N^{MMPs}$	N7	250	25 to 2500
12	VR	$N^{MMPs}$	N8	1	0.1 to 10
13	VR	$N^{MMPs}$	N9	1	0.1 to 10
14	VR	$N^{MMPs}$	N10	1	0.1 to 10
15	RV	$N^{MMPs}$	N11	1	0.1 to 10
16	RV	$N^{MMPs}$	N12	10	1 to 100
17	RV	$N^{MMPs}$	N13	2	0.2 to 20
18	RV	$N^{MMPs}$	N14	1	0.1 to 10
19	RV	$N^{MMPs}$	N15	0.5	0.05 to 5
20	SS	$N^{MMPs}$	N16	15	1.5 to 150
21	SS	$N^{MMPs}$	N17	100	10 to 1000
22	SS	$N^{MMPs}$	N18	3	0.3 to 30
23	SS	$N^{MMPs}$	N19	1	0.1 to 10
24	SS	$N^{MMPs}$	N20	1	0.1 to 10
25	VR	$M^{TNF+}$	M0	0.5	0.05 to 5
26	VR	$M^{TNF}$	M1	1	0.1 to 10
27	VR	$M^{TNF}$	M2	1	0.1 to 10
28	VR	$M^{TNF}$	M3	1	0.1 to 10
29	RV	$M^{TNF+}$	M4	0.5	0.05 to 5
30	RV	$M^{TNF}$	M5	2	0.2 to 20
31	RV	$M^{TNF}$	M6	1	0.1 to 10
32	RV	$M^{TNF}$	M7	0.1	0.01 to 1
33	RV	$M^{TNF}$	M8	1	0.1 to 10
34	RV	$M^{TNF}$	M9	0.1	0.01 to 1
35	SS	$M^{TNF}$	M10	1	0.1 to 10
36	SS	$M^{TNF}$	M11	1	0.1 to 10
37	SS	$M^{TNF}$	M12	5	0.5 to 50
38	SS	$M^{TNF}$	M13	0.1	0.01 to 1
39	SS	$M^{TNF}$	M14	1	0.1 to 10
40	VR,RV,SS	$M^{TGF}$	M15	1	0.1 to 10
41	VR,RV,SS	$M^{TGF}$	M16	1	0.1 to 10
42	VR,RV,SS	$M^{EGF}$	M17	1	0.1 to 10
43	VR	$M^{LL+}$	M18	2	0.2 to 20
44	VR	$M^{LL+}$	M19	1	0.1 to 10
45	VR	$M^{LL+}$	M20	15	1.5 to 150
46	VR	$M^{LL+}$	M21	15	1.5 to 150
47	VR	$M^{LL+}$	M22	1	0.1 to 10
48	RV	$M^{LL+}$	M23	0.5	0.05 to 5
49	RV	$M^{LL+}$	M24	1	0.1 to 10
50	RV	$M^{LL+}$	M25	1	0.1 to 10
51	RV	$M^{LL+}$	M26	0.5	0.05 to 5
52	RV	$M^{LL+}$	M27	1	0.1 to 10
53	SS	$M^{LL+}$	M28	13	1.3 to 130
54	SS	$M^{LL+}$	M29	1	0.1 to 10
55	SS	$M^{LL+}$	M30	1	0.1 to 10
56	SS	$M^{LL+}$	M31	1	0.1 to 10
57	VR	$M^{LL6+}$	M32	0.01	0.001 to 0.1
58	VR	$M^{LL6+}$	M33	1	0.1 to 10
59	VR	$M^{LL6+}$	M34	1	0.1 to 10
60	VR	$M^{LL6+}$	M35	1	0.1 to 10
61	RV	$M^{LL6+}$	M36	0.5	0.05 to 5
62	RV	$M^{LL6+}$	M37	1	0.1 to 10
63	RV	$M^{LL6+}$	M38	10	1 to 100
64	RV	$M^{LL6+}$	M39	0.5	0.05 to 5
65	RV	$M^{LL6+}$	M40	1	0.1 to 10
66	RV	$M^{LL6+}$	M41	1	0.1 to 10
67	SS	$M^{LL6+}$	M42	1	0.1 to 10
68	SS	$M^{LL6+}$	M43	1	0.1 to 10
69	SS	$M^{LL6+}$	M44	10	1 to 100
70	SS	$M^{LL6+}$	M45	1	0.1 to 10
71	SS	$M^{LL6+}$	M46	1	0.1 to 10
72	SS	$M^{LL6+}$	M47	4	0.4 to 40
73	SS	$M^{LL6+}$	M48	1	0.1 to 10
74	SS	$M^{LL6+}$	M49	0.5	0.05 to 5
75	VR	$M^{LL6+}$	M50	2	0.2 to 20

Parameter Number	Treatment	Nomenclature	Chemsynthesis Nomenclature	Default Value	Range
76	VR	$M_{+}^{ILS}$	M51	1	0.1 to 10
77	VR	$M_{+}^{ILS}$	M52	10	1 to 100
78	VR	$M_{TNF+}^{ILS}$	M53	5	0.5 to 50
79	VR	$M_{+}^{ILS}$	M54	5	0.5 to 50
80	VR	$M_{+}^{ILS}$	M55	1	0.1 to 10
81	RV	$M_{+}^{ILS}$	M56	1	0.1 to 10
82	RV	$M_{+}^{ILS}$	M57	100	10 to 1000
83	RV	$M_{L1+}^{ILS}$	M58	100	10 to 1000
84	RV	$M_{RVIS+}^{ILS}$	M59	0.1	0.01 to 1
85	RV	$M_{+}^{ILS}$	M60	1	0.1 to 10
86	RV	$M_{IL10-}^{ILS}$	M61	0.5	0.05 to 5
87	SS	$M_{+}^{ILS}$	M62	10	1 to 100
88	SS	$M_{+}^{ILS}$	M63	1	0.1 to 10
89	SS	$M_{L1+}^{ILS}$	M64	7	0.7 to 70
90	SS	$M_{SSIS+}^{ILS}$	M65	0.1	0.01 to 1
91	SS	$M_{+}^{ILS}$	M66	1	0.1 to 10
92	SS	$M_{+}^{ILS}$	M67	0.5	0.05 to 5
93	VR	$M_{IL10-}^{IL10+}$	M68	0.01	0.001 to 0.1
94	VR	$M_{IL10+}^{IL10+}$	M69	1	0.1 to 10
95	VR	$M_{+}^{IL10}$	M70	1	0.1 to 10
96	VR	$M_{IL10+}^{IL10+}$	M71	0.1	0.01 to 1
97	RV	$M_{IL10+}^{IL10+}$	M72	0.01	0.001 to 0.1
98	RV	$M_{+}^{IL10}$	M73	1	0.1 to 10
99	RV	$M_{+}^{IL10}$	M74	4	0.4 to 40
100	RV	$M_{IL6+}^{IL10}$	M75	0.001	0.0001 to 0.01
101	RV	$M_{IL10+}^{IL10+}$	M76	0.001	0.0001 to 0.01
102	SS	$M_{+}^{IL10}$	M77	0.05	0.005 to 0.5
103	SS	$M_{+}^{IL10}$	M78	1	0.1 to 10
104	SS	$M_{+}^{IL10}$	M79	1	0.1 to 10
105	SS	$M_{IL6+}^{IL10}$	M80	0.0005	0.00005 to 0.005
106	SS	$M_{IL10+}^{IL10+}$	M81	0.0005	0.00005 to 0.005
107	VR	$F_{+}^{TNF}$		10	1 to 100
108	VR	$F_{+}^{TNF}$		1	0.1 to 10
109	VR	$F_{IL10-}^{TNF}$		2	0.2 to 20
110	RV	$F_{+}^{TNF}$		20	2 to 200
111	RV	$F_{+}^{TNF}$		1	0.1 to 10
112	SS	$F_{+}^{TNF}$		1	0.1 to 10
113	SS	$F_{+}^{TNF}$		1	0.1 to 10
114	VR,RV,SS	$F_{+}^{TGF}$		10	1 to 100
115	VR,RV,SS	$F_{+}^{TGF}$		0.5	0.05 to 5
116	VR,RV,SS	$F_{+}^{TGF}$		1	0.1 to 10
117	VR,RV,SS	$F_{+}^{TGF}$		5	0.5 to 50
118	VR	$F_{+}^{IL6}$		0.01	0.001 to 0.1
119	VR	$F_{+}^{IL6}$		1	0.1 to 10
120	VR	$F_{+}^{IL6}$		1	0.1 to 10
121	RV	$F_{+}^{IL6}$		1	0.1 to 10
122	RV	$F_{+}^{IL6}$		1	0.1 to 10
123	RV	$F_{RVVS+}^{IL6}$		10	1 to 100
124	RV	$F_{+}^{IL6}$		0.5	0.05 to 5
125	RV	$F_{+}^{IL6}$		1	0.1 to 10
126	RV	$F_{+}^{IL6}$		1	0.1 to 10
127	SS	$F_{+}^{IL6}$		1	0.1 to 10
128	SS	$F_{+}^{IL6}$		1	0.1 to 10
129	SS	$F_{SSVS+}^{IL6}$		10	1 to 100
130	SS	$F_{+}^{IL6}$		10	1 to 100
131	SS	$F_{+}^{IL6}$		1	0.1 to 10
132	SS	$F_{+}^{IL6}$		1	0.1 to 10
133	VR	$F_{+}^{ILS}$		1	0.1 to 10
134	VR	$F_{+}^{ILS}$		1	0.1 to 10
135	RV	$F_{+}^{ILS}$		0.05	0.005 to 0.5
136	RV	$F_{+}^{ILS}$		1	0.1 to 10
137	SS	$F_{+}^{ILS}$		5	0.5 to 50
138	SS	$F_{+}^{ILS}$		1	0.1 to 10
139	RV	$RVIS$		5	0.5 to 50
140	RV	$RVVS$		10	1 to 100
141	SS	$SSIS$		10	1 to 100
142	SS	$SSVS$		10	1 to 100
143	VR,RV,SS	$t_{TNF}$		10	1 to 100
144	VR,RV,SS	$t_{MMP8}$		10	1 to 100
145	VR,RV,SS	$i_{cap}^N$		2	
146	VR,RV,SS	$i_{cap}^M$		4	
147	VR,RV,SS	$i_{cap}^N$		2	
148	VR,RV,SS	$i_{cap}^M$		4	
149	VR,RV,SS	$i_{tiss}^M$		6	
150	VR,RV,SS	$i_{tiss}^F$		12	

Parameter Number	Treatment	Nomenclature	Chemsynthesis Nomenclature	Default Value	Range
151	RV,SS	$r_{fiss}^P$		20	2 to 200
152	RV,SS	$r_{cgp}^N$		1	0.1 to 10
153	VR,RV,SS	$r_{cgp}^N$		8	0.8 to 80
154	VR,RV,SS	$r_{cgp}^M$		1	0.1 to 10
155	VR,RV,SS	$r_{cgp}^N$		8	0.8 to 80
156	VR,RV,SS	$r_{cgp}^M$		0.01	0.001 to 0.1
157	VR,RV,SS	$r_{cgp}^M$		1	0.1 to 10
158	VR,RV,SS	$r_{cgp}^M$		0.01	0.001 to 0.1
159	VR,RV,SS	$r_{fiss}^M$		1	0.1 to 10
160	VR,RV,SS	$r_{fiss}^M$		0.01	0.001 to 0.1
161	VR,RV,SS	$r_{fiss}^M$		1	0.1 to 10
162	VR,RV,SS	$r_{fiss}^F$		1	0.1 to 10
163	VR,RV,SS	$r_{fiss}^F$		0.01	0.001 to 0.1
164	VR,RV,SS	$r_{fiss}^F$		1	0.1 to 10
165	VR,RV,SS	$a_{TCF}^+$		10	1 to 100
166	VR,RV,SS	$a_{TCF}^+$		50	5 to 100
167	VR,RV,SS	$a_{TCF}^+$		0	0.1 to 10
168	VR,RV,SS	$a_{TCF}^+$		25	2.5 to 100
169	VR,RV,SS	$a_{TCF}^-$		2.5	0.25 to 25
170	VR,RV,SS	$a_{LL10}^{M_+}$		0.1	0.01 to 1
171	VR,RV,SS	$a_{LL10}^{M_+}$		0	0.1 to 10
172	VR,RV,SS	$a_{LL10}^{M_+}$		25	2.5 to 100
173	VR,RV,SS	$a_{LL10}^{M_+}$		10	1 to 100
174	VR,RV,SS	$a_{LL10}^{M_+}$		3	0.3 to 30
175	VR,RV,SS	$a_{LL10}^{N_+}$		0.1	0.01 to 1
176	VR,RV,SS	$a_{LL10}^{N_+}$		0	0.1 to 10
177	VR,RV,SS	$a_{LL10}^{N_+}$		25	2.5 to 100
178	VR,RV,SS	$a_{LL10}^{N_+}$		10	1 to 100
179	VR,RV,SS	$d_{LL10}^N$		10	1 to 100
180	VR,RV,SS	$d_{LL10}^N$		0.01	0.001 to 0.1
181	VR,RV,SS	$e_{+}^{col}$		1	0.1 to 10
182	VR,RV,SS	$e_{+}^{col}$		0	0.1 to 10
183	VR,RV,SS	$e_{+}^{col}$		0.01	0.001 to 0.1
184	VR,RV,SS	$e_{+}^{col}$		50	5 to 100
185	VR,RV,SS	$e_{+}^{col}$		25	2.5 to 100
186	VR,RV,SS	$e_{+}^{col}$		2	0.2 to 20
187	VR,RV,SS	$e_{+}^{col}$		10	1 to 100
188	VR,RV,SS	$e_{+}^{col}$		5	0.5 to 50
189	VR,RV,SS	$e_{+}^{ela}$		1	0.1 to 10
190	VR,RV,SS	$e_{+}^{ela}$		0	0.1 to 10
191	VR,RV,SS	$e_{+}^{ela}$		25	2.5 to 100
192	VR,RV,SS	$e_{+}^{ela}$		2	0.2 to 20
193	VR,RV,SS	$e_{+}^{HA}$		1	0.1 to 10
194	VR,RV,SS	$e_{+}^{HA}$		0	0.1 to 10
195	VR,RV,SS	$e_{+}^{HA}$		50	5 to 100
196	VR,RV,SS	$e_{+}^{HA}$		5	0.5 to 50
197	VR,RV,SS	$e_{+}^{HA}$		10	1 to 100
198	VR,RV,SS	$e_{+}^{col}$		12	1.2 to 120
199	VR,RV,SS	$e_{+}^{HA}$		1	0.1 to 10
200	VR,RV,SS	$p_{+}^F$		24	2.4 to 120
201	VR,RV,SS	$p_{+}^{TCF}$		10	1 to 100
202	VR,RV,SS	$p_{+}^F$		1	0.1 to 10
203	VR,RV,SS	$p_{+}^F$		0	0.1 to 10
204	VR,RV,SS	$p_{+}^F$		25	2.5 to 100
205	VR,RV,SS	$p_{-}^F$		3	0.3 to 30
206	VR,RV,SS	$h_{TNF}$		0.2	0.01 to 60
207	VR,RV,SS	$h_{TCF}$		0.2	0.01 to 60
208	VR,RV,SS	$h_{EGF}$		0.2	0.01 to 60
209	VR,RV,SS	$h_{MMP8}$		0.2	0.01 to 60
210	VR,RV,SS	$h_{IL1}$		0.2	0.01 to 60
211	VR,RV,SS	$h_{IL6}$		0.2	0.01 to 60
212	VR,RV,SS	$h_{IL8}$		0.2	0.01 to 60
213	VR,RV,SS	$h_{IL10}$		0.5	0.01 to 60

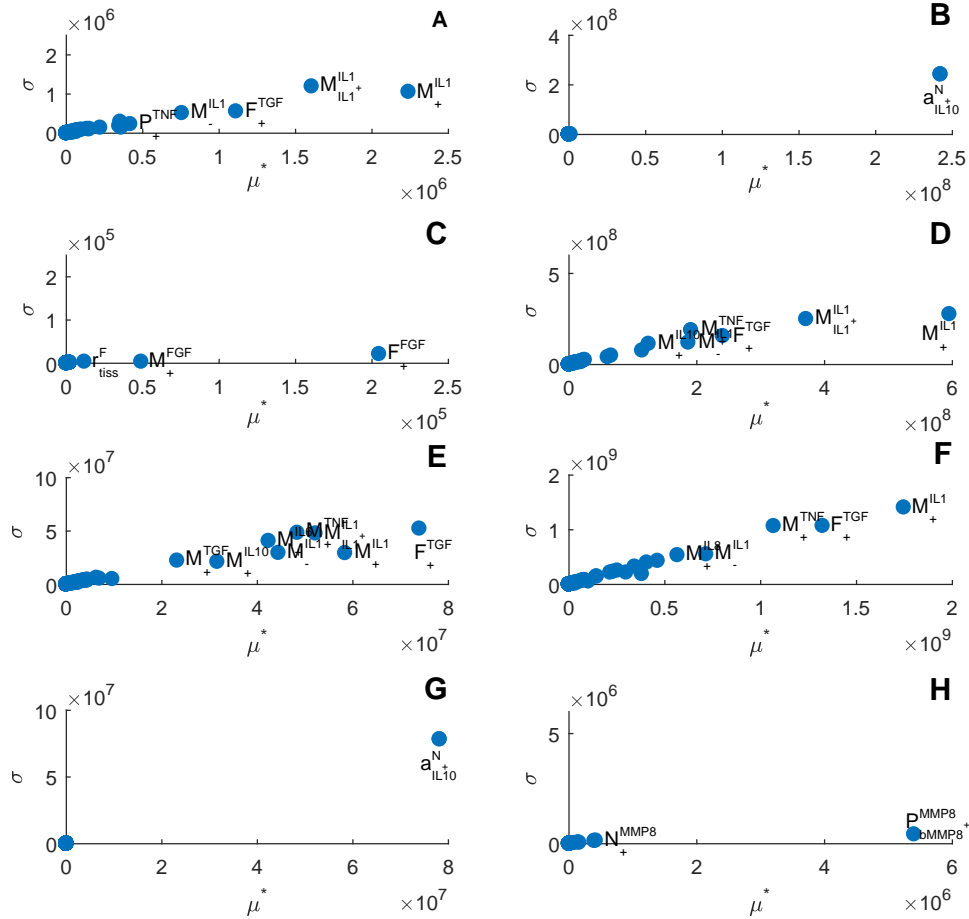
## Appendix C: Hyaluronic Acid-Gelatin Agent Based Model Agent Rules

Reference	Gel Property	Scaffold ABM Rule (relating Gel Parameter and Property)	Constraints
Vanderhoff 2009	Elastic Modulus (Pa)	$E = 0.002 \cdot ((70.8 \cdot TP_{WP} + 18.8) \cdot HA_{WP} + 319.8 \cdot TP_{WP}) + 1.2 \cdot ((1111 \cdot HA_{WP} + 6.8) \cdot XL_{WP})$	$0 < HA_{WP} < 1.6$ $0.1 < PEGDA_{WP} < 0.8$
Shu 2004	Crosslinking Density (mmol/ml)	$P_{XL} = -2.3 \cdot T_{MR} + 10.1$	$1 < MR_{Tg} < 3$
Zheng 2011	Swelling Ratio (w/w)	$Q = (0.4 \cdot HA_{WP} + 0.4) \cdot \ln(t_{min}) + (3 \cdot HA_{WP} + 7.9)$ $Q = (0.4 \cdot HA_{WP} + 0.4) \cdot \ln(1400) + (3 \cdot HA_{WP} + 7.9)$	$0 < t_{min} < 1400$ $t_{min} > 1400$
Zheng 2011	Mass Loss (%)	$W_{loss} = (17.7 \cdot HA_{WP} - 0.9) \cdot t_{weeks} + (71.3 \cdot HA_{WP} + 5.2)$	$0 < HA_{WP} < 1$ $1 < t_{week} < 4$
Vanderhoff 2009	Pore Size (µm)	$p = -345.2 \cdot HA_{WP}^2 + 309.9 \cdot HA_{WP} + 138.1$	$0 < HA_{WP} < 1$

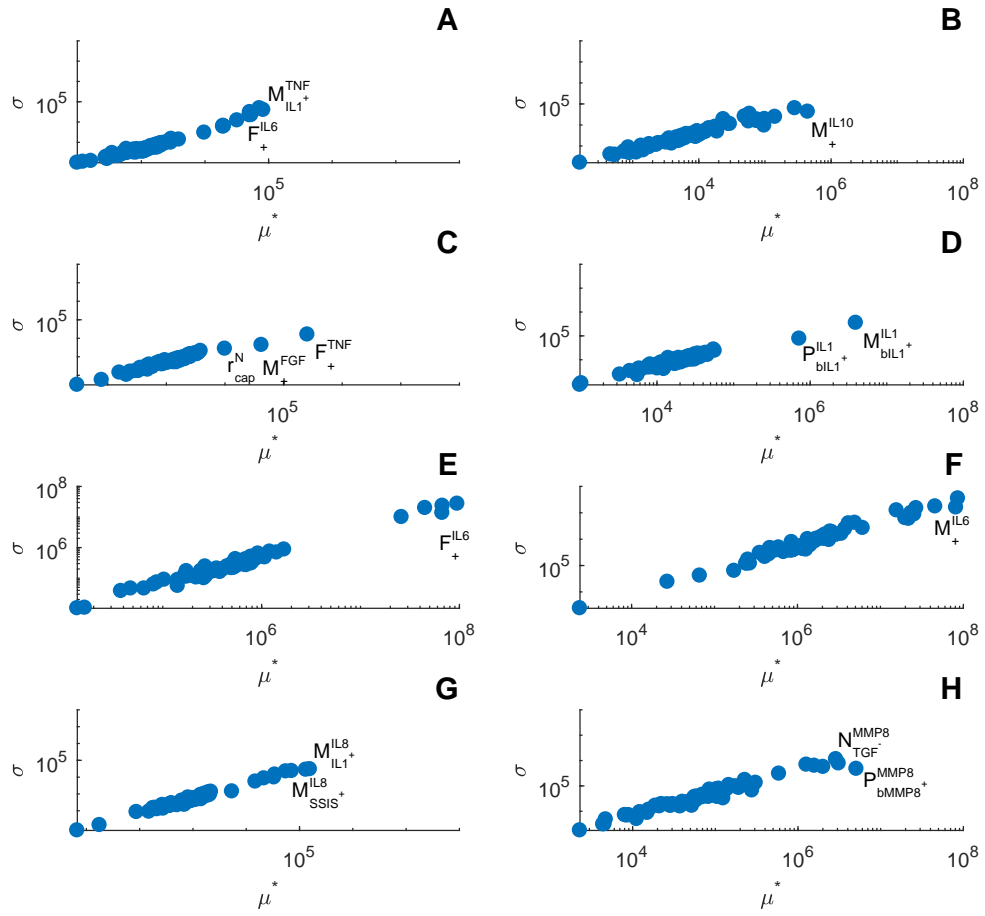
Reference	Cell Behavior	Scaffold ABM Rule (Relating Gel Parameter/Property and Cell Behavior)	Constraint
Ghosh 2007	Migration Speed (um/min)	$v = -0.11 \cdot \ln(E) + 1.3$	$95Pa < E < 4270Pa$
Liao 2008	Collagen per cell ( $10^4$ ug), 30 days	$COL = 2.8 \cdot 10^{-3} \cdot (14.7 \cdot E + 26.2) + (-0.18 \cdot p + 6)$	$30kPa < E < 100kPa$
Chen 2008	Immortalized Fibroblast Collagen Production	$COL_i = 1.45 \cdot COL$	
Liao 2008	Elastin per cell ( $10^4$ ug), 30 days	$ELN = 6 \cdot 10^{-5} \cdot (71.4 \cdot E + 40.2) + 10^{-3} \cdot (-0.02 \cdot p + 0.66)$	$30kPa < E < 100kPa$
Chen 2008	Immortalized Fibroblast Elastin Production	$ELN_i = 7.69 \cdot ELN$	
Liao 2008	sGAG per cell ( $10^4$ ug), 30 days	$sGAG = 1.2 \cdot (0.01 \cdot E - 0.2) + 0.54 \cdot (-0.02 \cdot p + 0.54)$	$30kPa < E < 100kPa$
Liu 2004	Cell Population (% of initial population)	$c = (-12 \cdot HA_{w/w} + 11.9) \cdot \ln(t_{hour}) + (21.5 \cdot HA_{w/w} \cdot -20)$	$0.25 < HA_{w/w} < 1$
Chen 2010	Viability Rate (%)	$vT = 0.75 \cdot \ln(t_{day}) + 61.7$	$0 < t_{day} < 7$

Figure C1: HA-Gtn Agent Based Model agent rules.

## Appendix D: Vocal Fold Agent Based Model Morris Screening Results



**Figure D1:** Morris parameter screening with respect to output (A) TNF, (B) TGF, (C) FGF, (D) MMP8, (E) IL1, (F) IL6, (G) IL8, (H) IL10 for voice rest case.



**Figure D2:** Morris parameter screening with respect to output (A) TNF, (B) TGF, (C) FGF, (D) MMP8, (E) IL1, (F) IL6, (G) IL8, (H) IL10 for spontaneous speech case.

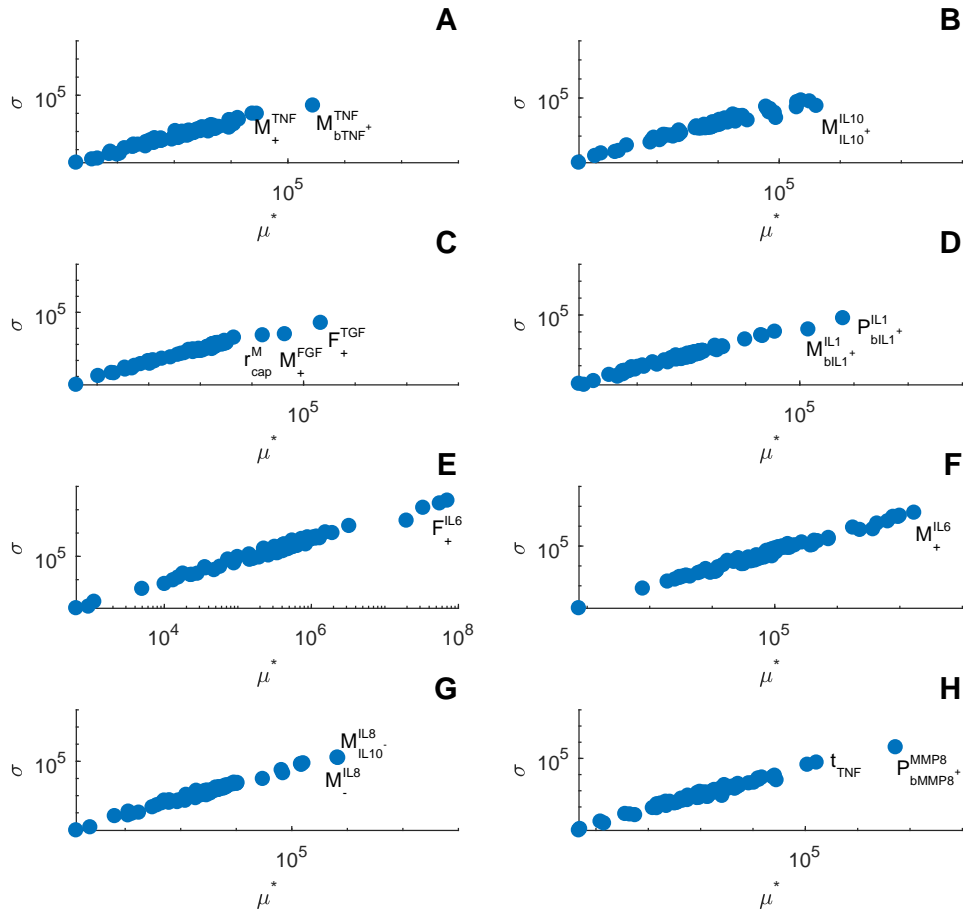


**Figure D3:** Morris parameter screening with respect to output (A) TNF, (B) TGF, (C) FGF, (D) MMP8, (E) IL1, (F) IL6, (G) IL8, (H) IL10 for resonant voice case.

## References

- [1] Katherine Verdolini Abbott, Nicole Y. K. Li, Ryan C. Branski, Clark A. Rosen, Elizabeth Grillo, Kimberly Steinhauer, and Patricia A. Hebda. Vocal exercise may attenuate acute vocal fold inflammation. *Journal of Voice*, 26(6):814–e1, 2012.
- [2] Ulla M. Agren, Markku Tammi, Markku Ryyanen, and Raija Tammi. Developmentally programmed expression of hyaluronan in human skin and its appendages. *Journal of investigative dermatology*, 109(2):219–224, 1997.
- [3] B. Alberts, D. Bray, J. Lewis, M. Raff, K. Roberts, and J. D. Watson. *Molecular biology of the cell, 3rd edn.* Garland Science, 1994.
- [4] Gary An. In silico experiments of existing and hypothetical cytokine-directed clinical trials using agent-based modeling. *Critical care medicine*, 32(10):2050–2060, 2004.
- [5] James M. Anderson. Biological responses to materials. *Annual Review of Materials Research*, 31(1):81–110, 2001.
- [6] Peter Angele, Rainer Muller, Detlef Schumann, Carsten Englert, Johannes Zellner, and Brian Johnstone Jung Yoo et al. Characterization of esterified hyaluronan-gelatin polymer composites suitable for chondrogenic differentiation of mesenchymal stem cells. *Journal of Biomedical Materials Research Part A* 91, 2:416–427, 2009.
- [7] G. E. B. Archer, A. Saltelli, and I. M. Sobol. Sensitivity measures, anova-like techniques and the use of bootstrap. *Journal of Statistical Computation and Simulation*, 58(2):99–120, 1997.
- [8] A. D. Augst, H. K. Kong, and D. J. Mooney. Alginate hydrogels as biomaterials. *Macromolecular Bioscience*, 6:623–33, 2006.

- [9] Marco Baggiolini, A. Walz, and S. L. Kunkel. Neutrophil-activating peptide-1/interleukin 8, a novel cytokine that activates neutrophils. *Journal of Clinical Investigation*, 84(4):1045, 1989.
- [10] Philip A. Band. Hyaluronan derivatives: chemistry and clinical applications. *ChemInform*, 29:46, 1998.
- [11] Rebecca S. Bartlett, Susan L. Thibeault, and Glenn D. Prestwich. Therapeutic potential of gel-based injectables for vocal fold regeneration. *Biomedical Materials*, 7:2, 2012.
- [12] Michael S. Benninger, David Alessi, Sanford Archer, Robert Bastian, Charles Ford, James Koufman, Robert T. Sataloff, Joseph R. Spiegel, and Peak Woo. Vocal fold scarring: current concepts and management. *Otolaryngology-Head and Neck Surgery*, 115(5):474–482, 1996.
- [13] D. Berry, K. Verdolini, D. Montequin, M. Hess, R. Chan, and I. Titze. A quantitative output-cost ratio in voice production. *J Speech Lang Hear Res*, 44:29–37, 2001.
- [14] Biocolor. Biocolor sircol soluble collagen assay. Accessed: 2016-07-07.
- [15] Emanuele Borgonovo. A new uncertainty importance measure. *Reliability Engineering & System Safety*, 92(6):771–784, 2007.
- [16] Emanuele Borgonovo, William Castaings, and Stefano Tarantola. Moment independent importance measures: new results and analytical test cases. *Risk Analysis*, 31(3):404–428, 2011.
- [17] R. C. Branski, K. Verdolini, V. Sandulache, C. A. Rosen, and P. A. Hebda. Vocal fold wound healing: A review for clinicians. *Journal of Voice*, 20(3):432–42, 2006.
- [18] Paul Bulpitt and Daniel Aeschlimann. New strategy for chemical modification of hyaluronic acid: preparation of functionalized derivatives and their use in the formation of novel biocompatible hydrogels. *Journal of biomedical materials research*, 47(2):152–169, 1999.
- [19] Davide Campoccia, Patrick Doherty, Marco Radice, Paola Brun, Giovanni Abatangelo, and David F. Williams. Semisynthetic resorbable materials from hyaluronan esterification. *Biomaterials*, 19(23):2101–2127, 1998.

- [20] Janina K. Casper and Rebecca Leonard. *Understanding voice problems: A physiological perspective for diagnosis and treatment*. Lippincott Williams & Wilkins, 2006.
- [21] Michael Catten, Steven D. Gray, Thomas H. Hammond, Ruixia Zhou, and Elizabeth Hammond. Analysis of cellular location and concentration in vocal fold lamina propria. *Otolaryngology-Head and Neck Surgery*, 118(5):663–667, 1998.
- [22] J. Cedervall, L. Ahrlund-Richter, B. Svensson, K. Forsgren, F. H. Haurer, D. Vidovska, and S. Hertegard. Injection of embryonic stem cells into scarred rabbit vocal folds enhances healing and improves viscoelasticity: Short-term results. *Laryngoscope*, 117:2075–81, 2007.
- [23] Roger W. Chan, Steven D. Gray, and Ingo R. Titze. The importance of hyaluronic acid in vocal fold biomechanics. *Otolaryngology-Head and Neck Surgery*, 124(6):607–614, 2001.
- [24] Chih-Hung Chang, Hwa-Chang Liu, Chien-Cheng Lin, Cheng-Hung Chou, and Feng-Huei Lin. Gelatin chondroitin hyaluronan tri-copolymer scaffold for cartilage tissue engineering. *Biomaterials*, 24(26):4853–4858, 2003.
- [25] W. Y. John Chen and Giovanni Abatangelo. Functions of hyaluronan in wound repair. *Wound Repair and Regeneration*, 7(2):79–89, 1999.
- [26] X. Chen and S. L. Thibeault. Biocompatibility of a synthetic extracellular matrix on immortalized vocal fold fibroblasts in 3d culture. *Acta Biomater*, 6(8):2940–48, 2011.
- [27] W-f. Cheung, T. F. Cruz, and E. A. Turley. Receptor for hyaluronan-mediated motility (rhamm), a hyaladherin that regulates cell responses to growth factors. *Biochemical Society Transactions*, 27(2):135–141, 1999.
- [28] D. D. K. Chhetri. Lamina propria replacement therapy with cultured autologous fibroblasts for vocal fold scars. *Otolaryngology Head and Neck Surgery*, 131:864–70, 2004.
- [29] Dinesh K. Chhetri, Christian Head, Elena Revazova, Stephen Hart, Sunita Bhuta, and Gerald S. Berke. Lamina propria replacement therapy with cultured autologous fibroblasts for vocal fold scars. *Otolaryngology-Head and Neck Surgery*, 131(6):864–870, 2004.

- [30] Dinesh K. Chhetri and Abie H. Mendelsohn. Hyaluronic acid for the treatment of vocal fold scars. *Current opinion in otolaryngology & head and neck surgery*, 18(6):498–502, 2010.
- [31] E. J. Chong, T. T. Phan, I. J. Lim, Y. Z. Zhang, B. H. Bay, S. Ramakrishna, and C. T. Lim. Evaluation of electrospun pcl/gelatin nanofibrous scaffold for wound healing and layered dermal reconstitution. *Acta biomaterialia*, 3(3):321–330, 2007.
- [32] R. Clark. "Wound repair. Overview and general considerations" in *The Molecular and Cellular Biology of Wound Repair*. Plenum Press, New York, 1998.
- [33] Andrea Classen, Jorge Lloberas, and Antonio Celada. Macrophage activation: classical vs. alternative. *Macrophages and Dendritic Cells: Methods and Protocols* ., pages 29–43, 2009.
- [34] Joel H. Collier, James P. Camp, Terry W. Hudson, and Christine E. Schmidt. Synthesis and characterization of polypyrrole-hyaluronic acid composite biomaterials for tissue engineering applications. *Journal of biomedical materials research*, 50(4):574–584, 2000.
- [35] M. S. Courey, J. A. Shohet, M. A. Scott, and R. H. Ossoff. Immunohistochemical characterization of benign laryngeal lesions. *Otol Rhinol Laryngol*, 105:525–31, 1996.
- [36] I. Darby, O. Skalli, and G. Gabbiani.  $\alpha$ -smooth muscle actin is transiently expressed by myofibroblasts during experimental wound healing. *Lab Invest*, 63(1):21–29, 1990.
- [37] Jeffrey M. Davidson, Ornella Zoia, and Ji-Min Liu. Modulation of transformation growth factor-beta 1 stimulated elastin and collagen production and proliferation in porcine vascular smooth muscle cells and skin fibroblasts by basic fibroblast growth factor, transformation growth factor-alpha, and insulin-like growth factor. *Journal of cellular physiology*, 155(1):149–156, 1993.
- [38] Madruga de Melo, Erich Christiano, Miriam Lemos, Arago Ximenes Filho, Luiz Ubirajara Sennes, Paulo Hilario Nascimento Saldiva, and Domingos Hiroshi Tsuji. Distribution of collagen in the lamina propria of the human vocal fold. *The laryngoscope*, 113(12):2187–2191, 2003.

- [39] Yadolah Dodge. *The concise encyclopedia of statistics*. Springer, Science & Business Media, 2008.
- [40] Gary P. Dowthwaite, Jo C. W. Edwards, and Andrew A. Pitsillides. An essential role for the interaction between hyaluronan and hyaluronan binding proteins during joint development. *Journal of Histochemistry & Cytochemistry*, 46(5):641–651, 1998.
- [41] S. Duffo, S. L. Thibeault, W. Li, X. Z. Shu, and G. D. Prestwich. Vocal fold tissue repair in vivo using a synthetic extracellular matrix. *Tissue Eng*, 12(8):2171–80, 2006.
- [42] Suzy Duffo, Susan L. Thibeault, Wenhua Li, Xiao Zheng Shu, and Glenn Prestwich. Effect of a synthetic extracellular matrix on vocal fold lamina propria gene expression in early wound healing. *Tissue engineering*, 12(11):3201–3207, 2006.
- [43] Joycelyn Entwistle, Christine L. Hall, and Eva A. Turley. Ha receptors: regulators of signalling to the cytoskeleton. *Journal of cellular biochemistry*, 61(4):569–577, 1996.
- [44] ESIBio. ESIBio 3-d cell encapsulation in hydrogels using tc inserts. Accessed: 2016-07-07.
- [45] Gilles Faury. Function-structure relationship of elastic arteries in evolution: from microfibrils to elastin and elastic fibres. *Pathologie Biologie*, 49(4):310–325, 2001.
- [46] C. N. Ford and D. M. Bless. Clinical experience with injectable collagen for vocal fold augmentation. *The Laryngoscope*, 96(8):863–869, 1986.
- [47] J. R. E. Fraser, T. C. Laurent, and U. B. G. Laurent. Hyaluronan: its nature, distribution, functions and turnover. *Journal of internal medicine*, 242(1):27–33, 1997.
- [48] Peter Fratzl. *Collagen: structure and mechanics, an introduction*. Springer, US, 2008.
- [49] Marcos Garcia-Fuentes, Elisabeth Giger, Lorenz Meinel, and Hans P. Merkle. The effect of hyaluronic acid on silk fibroin conformation. *Biomaterials*, 29(6):633–642, 2008.

- [50] Kaustabh Ghosh, Zhi Pan, E. Guan, Shouren Ge, Yajie Liu, Toshio Nakamura, Xiang-Dong Ren, Miriam Rafailovich, and Richard A. F. Clark. Cell adaptation to a physiologically relevant ecm mimic with different viscoelastic properties. *Biomaterials*, 28(4):671–679, 2007.
- [51] Kaustabh Ghosh, Xiang-Dong Ren, Xiao Zheng Shu, Glenn D. Prestwich, and Richard A. F. Clark. Fibronectin functional domains coupled to hyaluronan stimulate adult human dermal fibroblast responses critical for wound healing. *Tissue engineering*, 12(3):601–613, 2006.
- [52] S. D. Gray, E. H. Hammond, and D. Hanson. Benign pathologic response of the larynx. *Ann Otol Rhinol Laryngol*, 104:8–13, 1995.
- [53] Steven D. Gray. Cellular physiology of the vocal folds. *Otolaryngologic Clinics of North America*, 33(4):679–697, 2000.
- [54] Steven D. Gray, Fariborz Alipour, Ingo R. Titze, and Thomas Hale Hammond. Biomechanical and histologic observations of vocal fold fibrous proteins. *Annals of Otolaryngology, Rhinology & Laryngology*, 109(1):77–85, 2000.
- [55] Steven D. Gray, Karen J. Chan, and Bryan Turner. Dissection plane of the human vocal fold lamina propria and elastin fibre concentration. *Acta otolaryngologica*, 120(1):87–91, 2000.
- [56] Steven D. Gray, Minoru Hirano, and Kiminori Sato. Molecular and cellular structure of vocal fold tissue. *Vocal fold physiology: Frontiers in basic science* :, pages 1–36, 1993.
- [57] Steven D. Gray, Shirley S. N. Pignatari, and Penny Harding. Morphologic ultrastructure of anchoring fibers in normal vocal fold basement membrane zone. *Journal of Voice*, 8(1):48–52, 1994.
- [58] Volker Grimm, Uta Berger, Finn Bastiansen, Sigrunn Eliassen, Vincent Ginot, Jarl Giske, John Goss-Custard, Tamara Grand, Simone K Heinz, Geir Huse, Andreas Huth, Jane U Japsen, and Christian Jorgensen et al. A standard protocol for describing individual-based and agent-based models. *Ecological modelling*, 198(1):115–126, 2006.
- [59] Volker Grimm, Uta Berger, Donald L. DeAngelis, J. Gary Polhill, Jarl Giske, and Steven F. Railsback. The odd protocol: a review and first update. *Ecological modelling*, 221(23):2760–2768, 2010.

- [60] H. E. Gunter. Modeling mechanical stresses as a factor in the etiology of benign vocal fold lesions. *J of Biomech*, 37:1119–1224, 2004.
- [61] Emilie Hachet, Hlne Van den Berghe, Eric Bayma, Marc R Block, , and Rachel Auzly-Velty. Design of biomimetic cell-interactive substrates using hyaluronic acid hydrogels with tunable mechanical properties. *Biomacromolecules*, 13(6):1818–1827, 2012.
- [62] Mariah S. Hahn, James B. Kobler, Barry C. Starcher, Steven M. Zeitels, and Robert Langer. Quantitative and comparative studies of the vocal fold extracellular matrix i: elastic fibers and hyaluronic acid. *Annals of Otology, Rhinology & Laryngology*, 115(2):156–164, 2006.
- [63] Mariah S. Hahn, James B. Kobler, Steven M. Zeitels, and Robert Langer. Quantitative and comparative studies of the vocal fold extracellular matrix ii: collagen. *Annals of Otology, Rhinology & Laryngology*, 115(3):225–232, 2006.
- [64] T. H. Hammond, R. Zhou, E. H. Hammond, A. Pawlak, and S. D. Gray. The intermediate layer: A morphologic study of elastin and hyaluronic acid constituents of normal human vocal folds. *Journal of Voice*, 11(1):59–66, 1997.
- [65] Thomas H. Hammond, Steven D. Gray, John Butler, Ruixia Zhou, and Elizabeth Hammond. Age-and gender-related elastin distribution changes in human vocal folds. *Otolaryngology–Head and Neck Surgery*, 119(4):314–322, 1998.
- [66] Thomas Hale Hammond, Steven D. Gray, and John E. Butler. Age-and gender-related collagen distribution in human vocal folds. *Annals of Otology, Rhinology & Laryngology*, 109(10):913–920, 2000.
- [67] Minoru Hirano. Morphological structure of the vocal cord as a vibrator and its variations. *Folia phoniatica et logopaedica*, 26(2):89–94, 1974.
- [68] Minoru Hirano, Kiminori Sato, and Tadashi Nakashima. Fibroblasts in human vocal fold mucosa. *Acta oto-laryngologica*, 119(2):271–276, 1999.
- [69] S. Hirano. Growth factor therapy for vocal fold scarring in a canine model. *Annals of Otology, Rhinology and Laryngology*, 113, 2004.
- [70] S. Hirano. Prevention of vocal fold scarring by topical injection of hepatocyte growth factor in a rabbit model. *Laryngoscope*, 114:548–56, 2004.

- [71] S. Hirano. Current treatment of vocal fold scarring. *Current Opinion in Otolaryngology and Head and Neck Surgery*, 113:143–47, 2005.
- [72] Shigeru Hirano, Diane Bless, Dennis Heisey, and Charles Ford. Roles of hepatocyte growth factor and transformation growth factor b1 in production of extracellular matrix by canine vocal fold fibroblasts. *The Laryngoscope*, 113(1):144–148, 2003.
- [73] E. B. Holberg, R. E. Hillman, B. Hammarberg, M. Sodersten, and P. Doyle. Efficacy of behaviorally based voice therapy protocol for vocal nodules. *Journal of Voice*, 15(3):395–412, 2001.
- [74] Sung Ran Hong, Moo Sang Chong, Sang Bong Lee, Young Moo Lee, Kang Won Song, Moon Hyang Park, and Sung Hwa Hong. Biocompatibility and biodegradation of cross-linked gelatin/hyaluronic acid sponge in rat subcutaneous tissue. *Journal of Biomaterials Science, Polymer Edition*, 15(2):201–214, 2004.
- [75] Sobol Im, V. I. Turchaninov, Yu L. Levitan, and B. V. Shukhman. *Quasirandom sequence generators*, Keldysh Inst. Appl. Maths RAS Acad. Sci, 1992.
- [76] Invitrogen. Invitrogen quant-it picogreen dsdna reagent and kits. Accessed: 2016-07-07.
- [77] Bertrand Iooss and Paul Lematre. A review on global sensitivity analysis methods. In *Uncertainty Management in Simulation-Optimization of Complex Systems*, . US, pages 101–122. 2015.
- [78] Kosuke Ishii, Masumi Akita, Kotaro Yamashita, and Hajime Hirose. Age-related development of the arrangement of connective tissue fibers in the lamina propria of the human vocal fold. *Annals of Otology, Rhinology & Laryngology*, 109(11):1055–1064, 2000.
- [79] Kevin A. Janes and Michael B. Yaffe. Data-driven modelling of signal-transduction networks. *Nature Reviews Molecular Cell Biology*, 7(11):820–828, 2006.
- [80] Michiel Jw. Jansen. Analysis of variance designs for model output. *Computer Physics Communications*, 117(1):35–43, 1999.

- [81] Xinqiao Jia, Jason A. Burdick, James Kobler, Rodney J. Clifton, John J. Rosowski, Steven M. Zeitels, and Robert Langer. Synthesis and characterization of in situ cross-linkable hyaluronic acid-based hydrogels with potential application for vocal fold regeneration. *Macromolecules*, 37(9):3239–3248, 2004.
- [82] Iecun Johanes, Elaine Mihelc, Mahalakshmi Sivasankar, and Albena Ivanisevic. Morphological properties of collagen fibers in porcine lamina propria. *Journal of Voice*, 25(2):254–257, 2011.
- [83] M. M. Johns. Update on the etiology, diagnosis and treatment of vocal fold nodules, polyps and cysts. *Current Opinion in Otolaryngology and Head and Neck Surgery*, pp., pages 456–61, 2003.
- [84] S. Kanemaru, T. Nakamura, K. Omori, H. Kojima, A. Magruffov, Y. Hiratsuka, S. Hirano, J. Ito, and Y. Shimizu. Regeneration of the vocal fold using autologous mesenchymal stem cells. *Annals of Otolaryngology, Rhinology and Laryngology*, 112, 2003.
- [85] Shin-Ichi Kanemaru, Hisayoshi Kojima, Shigeru Hirano, Tatsuo Nakamura, Akhmar Magruffov, Juichi Ito, Koichi Omori, Yasuyuki Hiratsuka, and Yasuhiko Shimizu. Regeneration of the vocal fold using autologous mesenchymal stem cells. *Annals of Otolaryngology, Rhinology & Laryngology*, 112(11):915–920, 2003.
- [86] R. D. Kent. *The MIT Encyclopedia of Communication Disorder*. MIT Press, 2004.
- [87] Cay M. Kielty, Michael J. Sherratt, and C. Adrian Shuttleworth. Elastic fibres. *Journal of cell science*, 115(14):2817–2828, 2002.
- [88] Taek Gyoung Kim, Hyun Jung Chung, and Tae Gwan Park. Macroporous and nanofibrous hyaluronic acid/collagen hybrid scaffold fabricated by concurrent electrospinning and deposition/leaching of salt particles. *Acta biomaterialia*, 4(6):1611–1619, 2008.
- [89] Suzanne N. King, Fei Chen, Marie E. Jett, and Susan L. Thibeault. Vocal fold fibroblasts immunoregulate activated macrophage phenotype. *Cytokine*, 61(1):228–236, 2013.
- [90] Cheryl B. Knudson and Warren Knudson. Cartilage proteoglycans. *In Seminars in cell & developmental biology*, 12(2):69–78, 2001.

- [91] M. N. Kotby, A. M. Nassar, E. I. Seif, E. H. Helal, and M. M. Saleh. Ultrastructural features of vocal fold nodules and polyps. *Acta Otolaryngol*, 105:477–82, 1988.
- [92] S. S. Kucherenko. On global sensitivity analysis of quasi-monte carlo algorithms. *Monte Carlo Methods and Applications mcma*, 11(1):83–92, 2005.
- [93] J. K. Kutty and K. Webb. Tissue engineering therapies for the vocal fold lamina propria. *Tissue Engineering*, 15:249–62, 2009.
- [94] Jui-Yang Lai and Ya-Ting Li. Functional assessment of cross-linked porous gelatin hydrogels for bioengineered cell sheet carriers. *Biomacromolecules*, 11(5):1387–1397, 2010.
- [95] Torvard C. Laurent and J. R. Fraser. Hyaluronan. *The FASEB Journal*, 6(7):2397–2404, 1992.
- [96] J. Lee, M. J. Cuddihy, and N. A. Kotov. Three-dimensional cell culture matrices: State of the art. *Tissue Engineering: Part B*, 14:61–86, 2008.
- [97] Ju-Sung Lee, Tatiana Filatova, Arika Ligmann-Zielinska, Behrooz Hassani-Mahmooei, Forrest Stonedahl, Iris Lorscheid, Alexey Voinov, J. Gary Polhill, Zhanli Sun, and Dawn C. Parker. The complexities of agent-based modeling output analysis. *Journal of Artificial Societies and Social Simulation*, 18:4, 2015.
- [98] Sang Bong Lee, Hyun Wook Jeon, Young Woo Lee, Seong Kwan Cho, Young Moo Lee, Kang Won Song, Moon Hyang Park, and Sung Hwa Hong. Artificial dermis composed of gelatin, hyaluronic acid and (1-3)(1-6)-glucan. *Macromolecular Research*, 11(5):368–374, 2003.
- [99] Su Jin Lee, So Yeon Kim, and Young Moo Lee. Preparation of porous collagen/hyaluronic acid hybrid scaffolds for biomimetic functionalization through biochemical binding affinity. *Journal of Biomedical Materials Research Part B: Applied Biomaterials*, 82(2):506–518, 2007.
- [100] Genyuan Li, Herschel Rabitz, Paul E. Yelvington, Oluwayemisi O. Oluwole, Fred Bacon, Charles E. Kolb, and Jacqueline Schoendorf. Global sensitivity analysis for systems with independent and/or correlated inputs. *The Journal of Physical Chemistry A*, 114(19):6022–6032, 2010.

- [101] N. Y. K. Li, K. Verdolini, G. Clermont, Q. Mi, E. N. Rubinstein, P. A. Hebda, and Y. Vodovotz. A patient-specific in silico model of inflammation and healing tested in acute vocal fold injury. *PLoS ONE*, 3:7, 2008.
- [102] N. Y. K. Li, Y. Vodovotz, P. A. Hebda, and K. Verdolini Abbott. Biosimulation of inflammation and healing in surgically injured vocal folds. *Ann Otol Rhinol Laryngol*, 119(6):412–23, 2010.
- [103] Nicole Y. K. Li, Yoram Vodovotz, Kevin H. Kim, Qi Mi, Patricia A. Hebda, and Katherine Verdolini Abbott. Biosimulation of acute phonotrauma: an extended model. *The Laryngoscope*, 121(11):2418–2428, 2011.
- [104] Sio-Mei Lien, Liang-Yu Ko, and Ta-Jen Huang. Effect of pore size on ecm secretion and cell growth in gelatin scaffold for articular cartilage tissue engineering. *Acta Biomaterialia*, 5(2):670–679, 2009.
- [105] Changying Ling, Masaru Yamashita, Emily A. Waselchuk, Jennifer L. Raasch, Diane M. Bless, and Nathan V. Welham. Alteration in cellular morphology, density and distribution in rat vocal fold mucosa following injury. *Wound repair and regeneration*, 18(1):89–97, 2010.
- [106] Xiaohua Liu and Peter X. Ma. Phase separation, pore structure, and properties of nanofibrous gelatin scaffolds. *Biomaterials*, 30(25):4094–4103, 2009.
- [107] Y. Liu, X. Z. Shu, S. D. Gray, and Prestwich Gd. Disulfide-crosslinked hyaluronan-gelatin sponge: growth of fibrous tissue in vivo. *J Biomed Mater Res A*, 68:142–9, 2004.
- [108] Y. Luo, K. R. Kirker, and G. D. Prestwich. *Modification of natural polymers: hyaluronic acid*. In *Atal A, Langer R, eds. Methods of tissue engineering*. Academic Press, San Diego, Calif, 2002.
- [109] Yi Luo, Kelly R. Kirker, and Glenn D. Prestwich. Cross-linked hyaluronic acid hydrogel films: new biomaterials for drug delivery. *Journal of controlled release*, 69(1):169–184, 2000.
- [110] Ying Luo, James B. Kobler, Steven M. Zeitels, and Robert Langer. Effects of growth factors on extracellular matrix production by vocal fold fibroblasts in 3-dimensional culture. *Tissue Engineering*, 12(12):3365–3374, 2006.

- [111] Ralph. Mac Nally. Regression and model-building in conservation biology biogeography and ecology: the distinction between - and reconciliation of - 'predictive' and 'explanatory' models. *Biodiversity & Conservation*, 9(5):655–671, 2000.
- [112] P. S. Mallur and C. A. Rosen. Vocal fold injection: Review of indications, techniques, and materials for augmentation. *Clinical and Experimental Otolaryngology*, 3(4):177–182, 2010.
- [113] M. Martins-Green. The dynamics of cell-ecm interactions with implications for tissue engineering. In *In Lanza, R. and Langer, R. and Chick, W. Principles of Tissue Engineering*. R. G. Landes Company, New York, 1997.
- [114] Michael D. McKay, John D. Morrison, and Stephen C. Upton. Evaluating prediction uncertainty in simulation models. *Computer Physics Communications*, 117(1):44–51, 1999.
- [115] Qi Mi, Beatrice Rivière, Gilles Clermont, David L. Steed, and Yoram Vodovotz. Agent-based model of inflammation and wound healing: insights into diabetic foot ulcer pathology and the role of transforming growth factor-b1. *Wound Repair and Regeneration*, 15(5):671–682, 2007.
- [116] Diran O. Mikaelian, Louis D. Lowry, and Robert T. Sataloff. Lipoinjection for unilateral vocal cord paralysis. *The Laryngoscope*, 101(5):465–468, 1991.
- [117] Jaime Moore and Susan Thibeault. Insights into the role of elastin in vocal fold health and disease. *Journal of Voice*, 26(3):269–275, 2012.
- [118] Ibrahim Mossallam, M. Nasser Kotby, A. F. E. A. Ghaly, Alia Mahmoud Nassar, and M. A. Barakah. Histopathological aspects of benign vocal fold lesions associated with dysphonia. *Vocal Fold histopathology: A. symposium*, pages 65–80, 1986.
- [119] Shoji Ohya, Yasuhide Nakayama, and Takehisa Matsuda. Thermoresponsive artificial extracellular matrix for tissue engineering: hyaluronic acid bioconjugated with poly (n-isopropylacrylamide) grafts. *Biomacromolecules*, 2(3):856–863, 2001.
- [120] Yong Doo Park, Nicola Tirelli, and Jeffrey A. Hubbell. Photopolymerized hyaluronic acid-based hydrogels and interpenetrating networks. *Biomaterials*, 24(6):893–900, 2003.

- [121] Agnieszka S. Pawlak, Elizabeth Hammond, Thomas Hammond, and Steven D. Gray. Immunocytochemical study of proteoglycans in vocal folds. *Annals of Otolaryngology, Rhinology & Laryngology*, 105(1):6–11, 1996.
- [122] Tara Pouyani and Glenn D. Prestwich. Functionalized derivatives of hyaluronic acid oligosaccharides: drug carriers and novel biomaterials. *Bioconjugate chemistry*, 5(4):339–347, 1994.
- [123] G. D. Prestwich, Y. Liu, M. Serban, B. Yu, X. Z. Shu, and A. Scott. 3-d culture in synthetic extracellular matrices: New tissue models for drug toxicology and cancer drug discovery, invited. *Adv. Enz. Res*, 2007.
- [124] Glenn D. Prestwich, Dale M. Marecak, James F. Marecek, Koen P. Vercruyse, and Michael R. Ziebell. Controlled chemical modification of hyaluronic acid: synthesis, applications, and biodegradation of hydrazide derivatives. *Journal of Controlled Release*, 53(1):93–103, 1998.
- [125] Glenn D. Prestwich and Koen P. Vercruyse. Profiles therapeutic applications of hyaluronic acid and hyaluronan derivatives. *Pharmaceutical Science & Technology Today*, 1(1):42–43, 1998.
- [126] Molecular Probes. Molecular Probes live/dead viability/cytotoxicity kit for mammalian cells. Accessed: 2016-07-07.
- [127] Anand Ramamurthi and Ivan Vesely. Smooth muscle cell adhesion on crosslinked hyaluronan gels. *Journal of biomedical materials research*, 60(1):195–205, 2002.
- [128] B. D. Ratner, A. S. Hoffman, F. J. Schoen, and J. E. Lemons. *Biomaterials Science: An introduction to Materials in Medicine*. Academic Press, 2 edition, 1997.
- [129] Buddy D. Ratner, Allan S. Hoffman, Frederick J. Schoen, and Jack E. Lemons. *Biomaterials science: an introduction to materials in medicine*. Academic press, 2004.
- [130] C. A. Rosen. *Nodules, Polyps and cysts: Diagnosis and current treatment*. in Paper presented at the Annual Meeting of the American Academy of Otolaryngology - Head and Neck Surgery Foundation, New York, 2004.
- [131] John S. Rubin, Robert T. Sataloff, and Gwen S. Korovin. *Diagnosis and treatment of voice disorders*. Plural Publishing, 2014.

- [132] Andrea Saltelli, Paola Annoni, Ivano Azzini, Francesca Campolongo, Marco Ratto, and Stefano Tarantola. Variance based sensitivity analysis of model output. design and estimator for the total sensitivity index. *Computer Physics Communications*, 181(2):259–270, 2010.
- [133] Andrea Saltelli and Stefano Tarantola. On the relative importance of input factors in mathematical models: safety assessment for nuclear waste disposal. *Journal of the American Statistical Association*, 97(459):702–709, 2002.
- [134] Andrea Saltelli, Stefano Tarantola, Francesca Campolongo, and Marco Ratto. *Sensitivity analysis in practice: a guide to assessing scientific models*. John Wiley & Sons, 2004.
- [135] Kiminori Sato. Reticular fibers in the vocal fold mucosa. *Annals of Otology, Rhinology & Laryngology*, 107(12):1023–1028, 1998.
- [136] Kiminori Sato, Minoru Hirano, and Tadashi Nakashima. Age-related changes of collagenous fibers in the human vocal fold mucosa. *Annals of Otology, Rhinology & Laryngology*, 111(1):15–20, 2002.
- [137] I. Richard Savage. Contributions to the theory of rank order statistics-the two-sample case. *The Annals of Mathematical Statistics*, 27(3):590–615, 1956.
- [138] P. G. Scott, C. M. Dodd, E. E. Tredget, A. Ghahary, and F. Rahemtulla. Immunohistochemical localization of the proteoglycans, decorin, biglycan and versican and transforming growth factor-beta in post-burn hypertrophic and mature scar. *Histopathology*, 26:423–31, 1995.
- [139] N. Seekhao, J. JaJa, L. Mongeau, and N. Y. Li-Jessen. In situ visualization for 3d agent-based vocal fold inflammation and repair simulation. *Supercomputing frontiers and innovations*, 4(3):68, 2017.
- [140] N. Seekhao, C. Shung, J. Jaja, L. Mongeau, and N. Y. K. Li-Jessen. Real-time agent-based modeling simulation with in-situ visualization of complex biological systems a case study on vocal fold inflammation and healing. In *IEEE 15th International Workshop on High Performance Computational Biology*, 2015.
- [141] Nuttiiya Seekhao, Caroline Shung, Joseph JaJa, Luc Mongeau, and Nicole Y. K. Li-Jessen. Real-time agent-based modeling simulation with in-situ visualization of complex biological systems a case study on vocal fold inflammation

and healing. Paper presented at the 15th IEEE International Workshop on High Performance Computational Biology, Chicago, Illinois, USA., 2016.

- [142] S. K. Seidlits, C. T. Drinnan, R. R. Petersen, J. B. Shear, L. J. Suggs, and C. E. Schmidt. Fibronectin-hyaluronic acid composite hydrogels for three-dimensional endothelial cell culture. *Acta Biomaterialia*, 7(6):2401–09, 2011.
- [143] Stephanie K. Seidlits, Zin Z. Khaing, Rebecca R. Petersen, Jonathan D. Nickels, Jennifer E. Vanscoy, Jason B. Shear, and Christine E. Schmidt. The effects of hyaluronic acid hydrogels with tunable mechanical properties on neural progenitor cell differentiation. *Biomaterials*, 31(14):3930–3940, 2010.
- [144] Maisie L. Shindo, Lauren S. Zaretsky, and Dale H. Rice. Autologous fat injection for unilateral vocal fold paralysis. *Annals of Otolaryngology & Laryngology*, 105(8):602–606, 1996.
- [145] X. Z. Shu, S. Ahmad, Y. Liu, and Prestwich Gd. Synthesis and evaluation of injectable in situ crosslinkable synthetic extracellular matrices (secms) for tissue engineering. *J Biomed Mater Res A*, 79A:902–12, 2006.
- [146] Xiao Zheng Shu, Kaustabh Ghosh, Yanchun Liu, Fabio S. Palumbo, Yi Luo, Richard A. Clark, and Glenn D. Prestwich. Attachment and spreading of fibroblasts on an rgd peptide-modified injectable hyaluronan hydrogel. *Journal of biomedical materials research Part A*, 68(2):365–375, 2004.
- [147] Xiao Zheng Shu, Yanchun Liu, Yi Luo, Meredith C. Roberts, and Glenn D. Prestwich. Disulfide cross-linked hyaluronan hydrogels. *Biomacromolecules*, 3(6):1304–1311, 2002.
- [148] Xiao Zheng Shu, Yanchun Liu, Fabio Palumbo, and Glenn D. Prestwich. Disulfide-crosslinked hyaluronan-gelatin hydrogel films: a covalent mimic of the extracellular matrix for in vitro cell growth. *Biomaterials*, 24(21):3825–3834, 2003.
- [149] Xiao Zheng Shu, Yanchun Liu, Fabio S. Palumbo, Yi Luo, and Glenn D. Prestwich. In situ crosslinkable hyaluronan hydrogels for tissue engineering. *Biomaterials*, 25(7):1339–1348, 2004.
- [150] Xiao Zheng Shu and Glenn D. Prestwich. Therapeutic biomaterials from chemically modified hyaluronan. *Chemistry and biology of hyaluronan* :, pages 475–504, 2004.

- [151] Ilya M. Sobol. Global sensitivity indices for nonlinear mathematical models and their monte carlo estimates. *Mathematics and computers in simulation*, 55(1):271–280, 2001.
- [152] S. Tarantola, N. Giglioli, J. Jesinghaus, and A. Saltelli. Can global sensitivity analysis steer the implementation of models for environmental assessments and decision-making? *Stochastic Environmental Research and Risk Assessment*, 16(1):63–76, 2002.
- [153] Guus ten Broeke, George van Voorn, and Arend Ligtenberg. Which sensitivity analysis method should i use for my agent-based model? *Journal of Artificial Societies & Social Simulation*, 19(1), 2016.
- [154] S. L. Thibeault, D. M. Bless, and S. D. Gray. Interstitial protein alterations in rabbit vocal fol with scar. *J Voice*, 17:376–82, 2003.
- [155] S. L. Thibeault, S. D. Gray, D. M. Bless, R. W. Chan, and C. N. Ford. Histologic and rheologic characterization of vocal fold scarring. *J Voice*, 16:96–104, 2002.
- [156] Susan L. Thibeault, Wenhua Li, and Stephanie Bartley. A method for identification of vocal fold lamina propria fibroblasts in culture. *Otolaryngology—Head and Neck Surgery*, 139(6):816–822, 2008.
- [157] I. R. Titze. Mechanical stress in phonation. *Journal of Voice*, 8:99–105, 1994.
- [158] I. R. Titze. The human instrument. *Scientific American*, 298:94–101, 2008.
- [159] I. R. Titze, J. G. Svec, and P. S. Popolo. Vocal dose measures: Quantifying accumulated vibration exposure in vocal fold tissues. *Journal of Speech, Lanugage and Hearing Research*, 46:919–32, 2003.
- [160] Wei Seong Toh, Teck Chuan Lim, Motoichi Kurisawa, and Myron Spector. Modulation of mesenchymal stem cell chondrogenesis in a tunable hyaluronic acid hydrogel microenvironment. *Biomaterials*, 33(15):3835–3845, 2012.
- [161] Janssen L. Vanderhooft, Mataz Alcoutlabi, Jules J. Magda, and Glenn D. Prestwich. Rheological properties of cross-linked hyaluronan-gelatin hydrogels for tissue engineering. *Macromolecular bioscience*, 9(1):20–28, 2009.
- [162] Koen P. Vercruyssen and Glenn D. Prestwich. Hyaluronate derivatives in drug delivery. *Critical Reviews in Therapeutic Drug Carrier Systems*, 15(5), 1998.

- [163] K. Verdolini, C. Rosen, and R. C. Branski. *ASHA classification manual for voice disorders - I*. Erlbaum, Mahwah, NJ, 2006.
- [164] K. Verdolini, C. A. Rosen, R. C. Branski, and P. A. Hebda. Shifts in biochemical markers associated with wound healing in laryngeal secretions following phonotrauma: a preliminary study. *Ann Oto Laryngol*, 112:1021–25, 2003.
- [165] Katherine Verdolini, Ryan C. Branski, Clark A. Rosen, and Patricia A. Hebda. Shifts in biochemical markers associated with wound healing in laryngeal secretions following phonotrauma: a preliminary study. *Annals of Otology, Rhinology & Laryngology*, 112(12):1021–1025, 2003.
- [166] Yoram Vodovotz, Marie Csete, John Bartels, Steven Chang, and Gary An. Translational systems biology of inflammation. *PLoS Comput Biol*, 4:4, 2008.
- [167] U. Wilensky. *NetLogo Heat Diffusion model*. Center for Connected Learning and Computer-Based Modeling, Northwestern University, Evanston, IL, 1998.
- [168] U. Wilensky. *NetLogo*. Center for Connected Learning and Computer-Based Modeling, Northwestern University, Evanston, IL, 1999.
- [169] Chonggang Xu and George Zdzislaw Gertner. Uncertainty and sensitivity analysis for models with correlated parameters. *Reliability Engineering & System Safety*, 93(10):1563–1573, 2008.
- [170] Shintaro Yamane, Norimasa Iwasaki, Tokifumi Majima, Tadao Funakoshi, Tatsuya Masuko, Kazuo Harada, Akio Minami, Kenji Monde, and Shin ichiro Nishimura. Feasibility of chitosan-based hyaluronic acid hybrid biomaterial for a novel scaffold in cartilage tissue engineering. *Biomaterials*, 26(6):611–619, 2005.
- [171] Jing Yang. Convergence and uncertainty analyses in monte-carlo based sensitivity analysis. *Environmental Modelling & Software*, 26(4):444–457, 2011.
- [172] Edwin M. L. Yiu, Karen M. K. Chan, Nicole Y. K. Li, Raymond Tsang, Katherine Verdolini Abbott, Elaine Kwong, Estella P. M. Ma, Fred W. Tse, and Zhixiu Lin. Wound-healing effect of acupuncture for treating phonotraumatic vocal pathologies: A cytokine study. *The Laryngoscope*, 126:1, 2016.
- [173] Fan Zhang, Chuanglong He, Lijun Cao, Wei Feng, Hongsheng Wang, Xiumei Mo, and Jinwu Wang. Fabrication of gelatin-hyaluronic acid hybrid scaffolds

with tunable porous structures for soft tissue engineering. *International journal of biological macromolecules*, 48(3):474–481, 2011.

- [174] Xy. Zhang, M. N. Trame, L. J. Lesko, and S. Schmidt. Sobol sensitivity analysis: a tool to guide the development and evaluation of systems pharmacology models. *CPT: pharmacometrics & systems pharmacology*, 4(2):69–79, 2015.